A calcium-binding protein CAS regulates the CO_2-concentrating mechanism in the green alga *Chlamydomonas reinhardtii*

Wang, Lianyong

Table of Contents

Abstract

Photosynthetic organisms possess a capacity to sense and respond to various environmental stresses, such as light, CO_2, and temperature, to optimize photosynthesis. In particular, aquatic photosynthetic organisms induce a CO_2-concentrating mechanism (CCM) to maintain photosynthesis in CO_2-limiting stress conditions by sensing the availability of CO_2 and light. The components of the CCM, including carbonic anhydrases, membrane proteins for inorganic carbon (Ci) uptake, factors associated with the formation of pyrenoid where ribulose-1,5-bisphosphate carboxylase/oxygenase is enriched for CO_2-fixation, and proteins for recycling of leaked CO_2 from pyrenoid, have been identified in the eukaryotic green alga *Chlamydomonas reinhardtii*. So far, two regulatory factors, CCM1 and LCR1, have also been characterized. CCM1 is a master regulator of the 47 low-CO_2 (LC, 0.04% CO_2)-inducible genes, including *HLA3* encoding a HCO_3^- transporter in the plasma membrane, *LCIA* encoding a possible HCO_3^- channel in the chloroplast envelope, and *LCR1* encoding an LC-inducible DNA-binding transcriptional regulator. However, chloroplast-mediated regulation of the CCM remains to be elucidated.

In order to elucidate the regulatory network of CCM, three CO_2-requiring mutants have been isolated by gene tagging. In one of the three mutants, a *Chlamydomonas* ortholog of *Arabidopsis* chloroplast calcium (Ca^{2+})-binding protein CAS was disrupted, and this mutant was designated as H82. Introducing a wild-type *CAS* gene into H82 rescued the defects in growth rate, photosynthetic Ci affinity, internal Ci accumulation, and accumulation of HLA3 and LCIA in LC conditions. The mRNA levels of *HLA3* and *LCIA* failed to be maintained in H82 at the increased levels seen in wild-type cells and complemented cells in LC conditions. Additionally, *Chlamydomonas* CAS possessed a Ca^{2+}-binding activity *in vitro*, and the accumulation of HLA3 and LCIA was also impaired by the perturbation of intracellular Ca^{2+} homeostasis. These results suggest that CAS could control the expression of LC-induced *HLA3* and *LCIA* by post-transcriptional regulation in Ca^{2+}-dependent manner.

In response to LC stress in light, most of CAS protein changed its localization from dispersed across the thylakoid membrane to being associated with tubule-like structures in the pyrenoid. This relocation of CAS and the accumulation of HLA3 and LCIA were suppressed by inhibitors of photosynthetic electron transport. Considering the facts that the relocation and accumulation of CAS were not affected by the defect of CCM1, and that the accumulation of CCM1 was not affected in the H82 mutant, CCM1 and CAS could individually function in regulating the expression of *HLA3* and *LCIA* in response to CO_2 and light.

These findings suggest that *Chlamydomonas* CAS regulates CCM and the expression of genes including *HLA3* and *LCIA* through a Ca^{2+}-mediated retrograde signal from the thylakoid in the chloroplast to the nucleus in response to CO_2 and light.

Abbreviation

ABC	adenosine triphosphate-binding cassette
ABI4	abscisic acid-insensitive 4
AM	acetoxymethyl
BAPTA	1,2-bis (*o*-aminophenoxy) ethane-N, N, N, N'-tetraacetic acid
Bis-Tris	2,2-bis(hydroxymethyl)-2,2',2''-nitrilotriethanol
$[Ca^{2+}]_{cyt}$	cytosolic calcium concentration
$[Ca^{2+}]_{stro}$	stroma calcium concentration
CA	carbonic anhydrase
CAM	crassulacean acid metabolism
CAS	calcium sensing receptor
CBB	coomassie brilliant blue
CCM	carbon dioxide (CO_2)-concentrating mechanism
CCP	chloroplast carrier protein
CCRE	CO_2/cAMP-responsive element
CEF	cyclic electron flow
Chl	chlorophyll
CHX	cycloheximide
Ci	inorganic carbon
DBMIB	2,5-dibromo-3-methyl-6-isopropylbenzoquinone
DCMU	3-(3,4-dichlorophenyl)-1,1-dimethylurea
DDM	n-dodecyl-*β*-D-maltoside
DIC	differential interference contrast
FCCP	carbonyl cyanide p-trifluoromethoxyphenyl hydrazone
FDR	false discovery rate
FNT	formate-nitrite transporter
FPKM	fragments per kilobase of exon per million mapped fragments
GCA2	growth controlled by abscisic acid 2
HC	high-CO_2, air containing 5% (vol/vol) CO_2
HEPES	4-(2-hydroxyethyl)-1-piperazineethanesulfonic acid
HLA3	high-light activated 3
HSM	high-salt medium supplemented with 20 mM MOPS
HSP70A	heat shock protein 70A
HT1	high temperature 1
hyg	hygromycin
IPTG	isopropyl-*β*-D-thiogalactopyranoside
$K_{0.5}$ (Ci)	inorganic carbon concentration required for half maximal velocity
LC	low-CO_2, ordinary air containing 0.04% (vol/vol) CO_2
LCE	light-dependent CO_2-exchange

LCI	low-CO_2-inducible
LTTR	LysR transcriptional regulator
MAPK	mitogen-activated protein kinase
MATE	multidrug and toxic compound extrusion
MES	2-(N-morpholino)ethanesulfonic acid
MOPS	3-(N-morpholino)propanesulfonic acid
NADPH	nicotinamide adenine dinucleotide phosphate
NDH	nicotinamide adenine dinucleotide dehydrogenase
NIA1	nitrate reductase 1
OST1	protein kinase open stomata 1
par	paromomycin
PBS	phosphate-buffered saline
PEP	phosphoenolpyruvate
PGA	phosphoglyceric acid
PMSF	phenylmethylsulfonyl fluoride
PVDF	polyvinylidene difluoride
qE	energy-dependent quenching
qRT-PCR	quantitative reverse transcription polymerase chain reaction
qT	quenching by state transition
QUAC1	quickly activating anion channel 1
RHC1	resistance to high-CO_2 1
Rubisco	ribulose 1,5-bisphosphate carboxylase/oxygenase
RBCS2	rubisco small subunit 2
RuBP	ribulose-1,5-bisphosphate acid
SIS	sorbitol impermeable space
SLAC1	slow anion channel associated 1
SLC	solute carrier
$t_{1/2}$	half-time
TAP	tris-acetate-phosphate
TAIL-PCR	thermal asymmetric interlaced polymerase chain reaction
UCH	ubiquitin carboxyl-terminal hydrolase
UTR	untranslated region
VLC	very low-CO_2, air containing 0.003% (vol/vol) CO_2
WT	wild-type
W-5	N-(6-aminohexyl)-1-naphthalenesulfonamide hydrochloride
W-7	N-(6-aminohexyl)-5-chloro-1-naphthalenesulfonamide hydrochloride

Introduction

Photosynthetic organisms possess a capacity to sense and respond to changes in their environment, such as light, temperature, and various nutrient availabilities, to optimize photosynthetic activity. Photosynthesis, as a vital biological process that converts light energy into chemical energy, ultimately supports the growth of almost all living organisms. The pivotal pathway in photosynthesis is the Calvin–Benson–Bassham cycle for carbon fixation (Benson and Calvin, 1950), which incorporates inorganic carbon (Ci; carbon dioxide (CO_2) and /or bicarbonate (HCO_3^-)) into organic carbon and stores solar energy in carbohydrates. The first major step of the cycle is the generation of an organic compound, phosphoglyceric acid (3-PGA), from CO_2 catalyzed by the ribulose-1,5-bisphosphate carboxylase/oxygenase (Rubisco). Unlike the ancient environment when Rubisco first evolved, a high oxygen (O_2):CO_2 ratio with 21% O_2 and approximately 0.04% CO_2 in the present atmosphere enhances the oxygenase activity for fixing O_2 in an energetically wasteful cycle named photorespiration (Moroney et al., 1986a) rather than carboxylase activity. The shortage of carbon supply, as one of the major environmental stresses, impacts many physiological aspects of plants, especially photosynthetic efficiency due to the low-CO_2 affinity of Rubisco. Most vascular plants control their CO_2 uptake by controlling the opening and closing of stomata in response to environmental CO_2 concentration (Engineer et al., 2016; Fig. 1). These events are controlled by β-carbonic anhydrase (CA)1 and CA4 (Hu et al., 2009), multidrug and toxic compound extrusion (MATE)-type transporter resistance to high-CO_2 1 (RHC1) (Tian et al., 2015), protein kinase high temperature 1 (HT1) (Hashimoto et al., 2006; Matrosova et al., 2015; Hashimoto-Sugimoto et al., 2016), protein kinase open stomata 1 (OST1) (Xue et al., 2011), growth controlled by abscisic acid 2 (GCA2) (Young et al., 2006), quickly activating anion channel 1 (QUAC1) (Meyer et al., 2010), slow anion channel associated 1 (SLAC1) (Negi et al., 2008; Vahisalu et al., 2008).

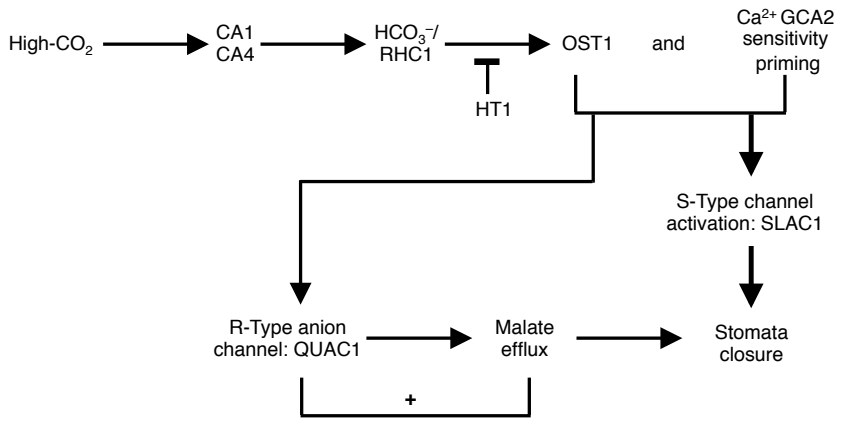

Figure 1. A model illustrating the functions of proteins in guard cells mediating CO_2 control of stomata movements (modified from Engineer et al., 2016). In this model, the HT1 protein kinase functions as a negative regulator. CA1, CA4, OST1, GCA2, QUAC1 and SLAC1 function as positive mediators of high-CO_2-induced stomata closure. Abbreviations: CA, carbonic anhydrase; HT1, high temperature 1; RHC1, resistance to high-CO_2 1; OST1, open stomata 1; GCA2, growth controlled by abscisic acid 2; QUAC1, quickly activating anion channel 1; SLAC1, slow anion channel associated 1. '+' indicates that the extracellular malate can increase the activity of QUAC1.

Another adaptive strategy, named the CO_2-concentrating mechanism (CCM), has also developed to efficiently maintain photosynthetic activity by raising the available CO_2 concentration around the catalytic site of Rubisco. As a biochemical CCM in C_4 or Crassulacean acid metabolism (CAM) plants, CO_2 is first converted into HCO_3^-, which is the substrate for phosphoenolpyruvate (PEP) carboxylase in leaf mesophyll cells. The Michaelis constant for HCO_3^- (K_m (HCO_3^-)) of PEP carboxylase is approximate 8 μM, which could be easily saturated by a HCO_3^- concentration of 50 μM in the cytoplasm of mesophyll cells at physiological pH. Therefore, HCO_3^- is efficiently catalyzed to C4 acid in mesophyll cells, which is subsequently transported to the bundle-sheath cells and decarboxylated to generate concentrated CO_2 around Rubisco (Langdale et al., 2011; Fig. 2).

In contrast, the shortage of carbon supply in aquatic environments is caused not only by the low catalytic capacity of Rubisco but also by the 10,000-folds slower diffusion rate of CO_2 in aquatic conditions than that in atmospheric conditions (Jones, 1992). To acclimate to this stress, many aquatic organisms possess a biophysical CCM, which involves the active transportation of Ci into the chloroplast

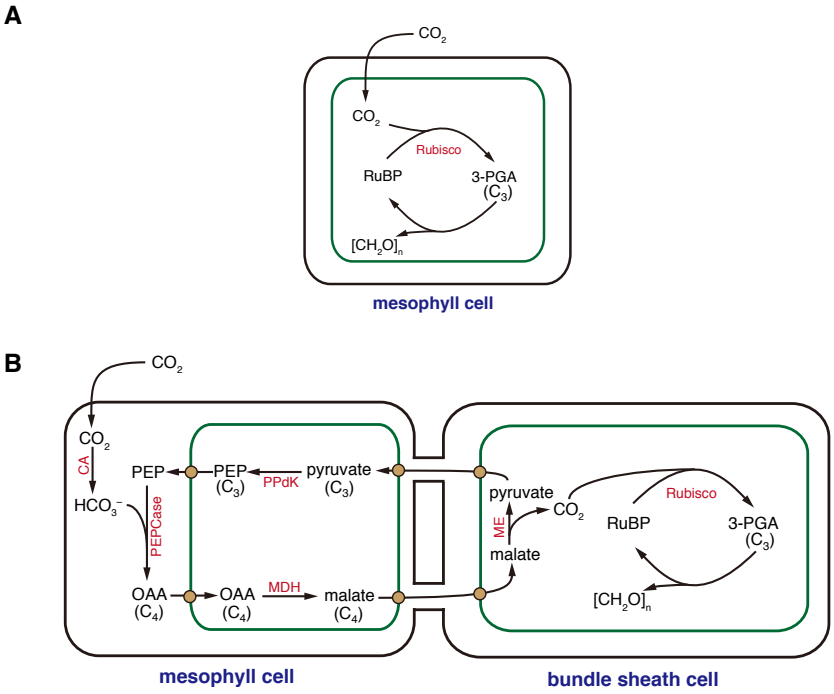

Figure 2. Schematic diagrams of C_3 Calvin–Benson–Bassham (A) and C_4 cycles for CO_2 fixation (modified from Langdale et al., 2011). (A) In C_3 plants, CO_2 is fixed in mesophyll cells by Rubisco. (B) In C_4 plants, CO_2 is first converted to C_4 acid in mesophyll cell and then transferred into bundle sheath cell for fixation by Rubisco. The green squares indicate the chloroplast envelope. The proteins involved in these pathways are shown in red. The yellow dots indicate proteins involved in transportation of intermediates. RuBP, ribulose-1,5-bisphosphate; PGA, phosphoglyceric acid; PEPCase, phosphoenolpyruvate carboxylase; OAA, oxaloacetic acid; MDH, malate dehydrogenase; PPdK, pyruvate, phosphate dikinase; ME, malic enzyme; CA, carbonic anhydrase.

stroma and conversion from CO_2 to HCO_3^- to maintain the Ci pool or from HCO_3^- to CO_2 for concentrating CO_2 at the site of Rubisco in specific microcompartments. This biophysical CCM was recognized for the fist time in the green algae *Chlamydomonas reinhardtii* (Badger et al., 1980), and the cyanobacterium *Anabaena variabilis* (Kaplan et al., 1980). The physiological evidences for Ci uptake were provided that the aquatic photosynthetic organisms has the ability to efficiently fix CO_2 even when the external CO_2 concentration is below the K_m (CO_2) for Rubisco, and that the Ci concentration inside the cell is higher than that by diffusion alone. In addition, the conversion between CO_2 and HCO_3^- was focused on because of the increased levels of CAs in cyanobacteria and microalgae in response to CO_2-limiting conditions (Aizawa and Miyachi, 1986; Fukuzawa et al., 1990). Another evidence for the CCM existence is the studies of mutants showing defects in growth rate, photosynthetic Ci affinity, internal Ci accumulation in CO_2-limitinig conditions (Moroney and Ynalvez, 2007). Remarkably, engineering the components from these mechanisms has been considered to achieve improvements in the efficiency of photosynthetic CO_2 fixation in the chloroplasts of C_3 crops (Driever et al., 2013; Lin et al., 2014; McGrath et al., 2014; Atkinson et al., 2016).

1. Inorganic carbon transport system

An active Ci transport system is essential for the operation of the CCM in aquatic organisms. In cyanobacteria, the CCM accumulates CO_2 around Rubisco in a highly efficient manner, reaching a ratio of up to 1,000-fold (Badger and Price, 2003). To achieve this, five distinct transport systems for Ci uptake have been identified (Fig. 3). Firstly, there are two single-gene systems for HCO_3^- uptake, designated as SbtA and BicA. SbtA is a Na^+/HCO_3^- symporter with high affinity but low flux rate (Shibata et al., 2002).

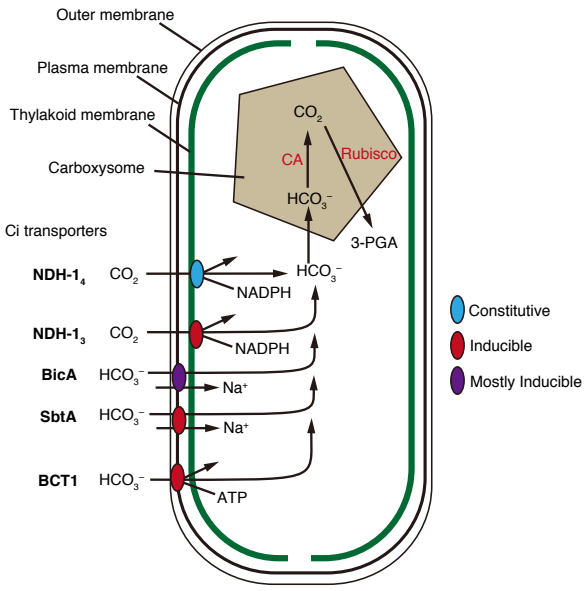

Figure 3. A model of the CO_2-concentrating mechanism (CCM) in cyanobacteria (modified from Price et al., 2011). The paths of inorganic carbon (Ci) in the cyanobacteria CCM. The ellipses indicate three types of identified Ci transporters, including constitutive (blue), inducible (red), and mostly inducible (purple). CA, carbonic anhydrase; PGA, phosphoglyceric acid. Mostly Inducible protein is accumulated in sufficient CO_2, but much higher in CO_2-limiting conditions.

In contrast, BicA, a possible Na^+/HCO_3^- symporter, exhibits low-affinity but a high-flux rate (Price et al., 2004). Secondly, an adenosine triphosphate (ATP)-binding cassette (ABC)-type high-affinity HCO_3^- transporter, named BCT1, is an inducible complex in CO_2-limiting conditions, comprised of components encoded by the four genes *cmpA–D* (Omata et al., 1999). Finally, nicotinamide adenine dinucleotide phosphate (NADPH) dehydrogenase was reported to be essential for Ci transport (Ogawa, 1991), and was detected in two complexes, nicotinamide adenine dinucleotide dehydrogenase (NDH)-1_3 and NDH-1_4 (Ohkawa et al., 2000). The inducible NDH-1_3 and constitutive NDH-1_4 CO_2 pumps are located in the thylakoid membrane and are capable of using reduced NADPH as an electron donor to power the conversion of CO_2 to HCO_3^- during operation of the CCM (Shibata et al., 2001; Zhang et al., 2004). As components of these two NHD-1-type CO_2 pumps, NADPH dehydrogenase catalyze the conversion of both CO_2 diffusing from outside of cell and leaking from the carboxysome.

In microalgae, the $K_m(CO_2)$ of Rubisco is at least two-fold higher than the 10 μM for CO_2 in the water equilibrated with air. However, cells with a CCM exhibit the affinity for CO_2 of about 1 μM, which can readily be saturated by CO_2 in water (Badger et al., 1998; Moroney et al., 1999). In the eukaryotic unicellular green alga *C. reinhardtii*, Ci transport systems facilitate Ci uptake across physiological barriers such as the plasma membrane and chloroplast envelope (Fig. 4). Two plasma-membrane-localized proteins encoded by nuclear genes, high-light activated 3 (*HLA3*) and low-CO_2 (LC)-inducible 1 (*LCI1*), have been identified as putative Ci transporters. HLA3 belongs to a multidrug-resistance-related protein subfamily of the ABC transporter superfamily (Im and Grossman, 2001; Duanmu et al., 2009b; Yamano et al., 2015).

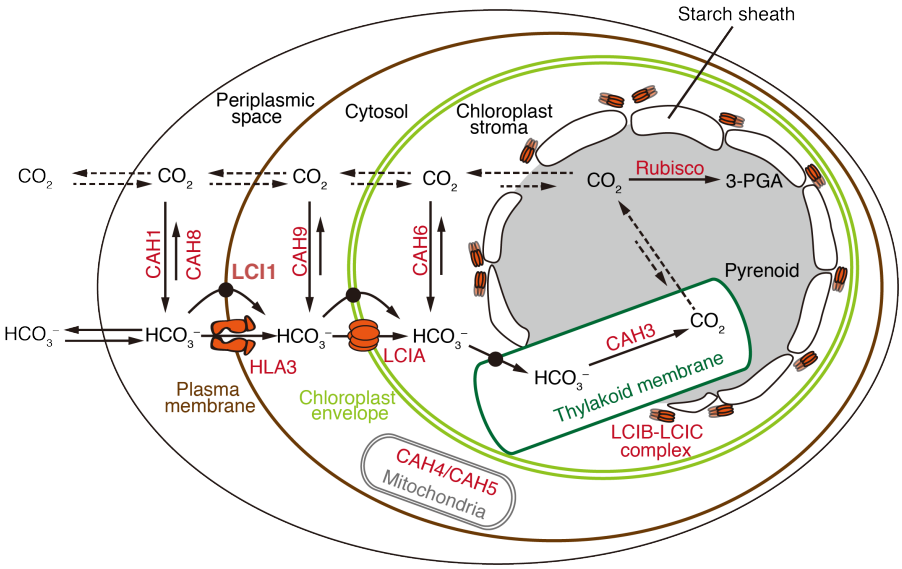

Figure 4. Schematic model of CO_2-concentrating mechanism (CCM) in *Chlamydomonas reinhardtii* in CO_2-limiting conditions. (modified from Moroney and Ynalvez, 2007; Wang et al., 2015; Yamano et al., 2015). The proposed uptake of inorganic carbon (Ci) from the extracellular space to the thylakoid lumen is illustrated. In CO_2-limiting conditions, the pyrenoid develops as a spherical structure surrounded by starch sheathes. The unknown Ci transporters are shown as closed circles. The broken lines indicate the diffusion paths of CO_2. CAH, carbonic anhydrase in *Chlamydomonas reinhardtii*.

The members of this subfamily allow alternating access to the inside or outside of cell for unidirectional transport through the central cavity formed by two transmembrane domains, whose conformation change is driven by ATP hydrolysis on its two nucleotide-binding domains (Higgins and Linton, 2004; Dawson and Locher, 2006; Hollenstein et al., 2007; Jin et al., 2012; Wilkerns, 2015). Physiologically, HLA3 appears to function in HCO_3^- uptake, because photosynthetic Ci affinity and accumulation are decreased by knockdown (Duanmu et al., 2009b) or knockout (Yamano et al., 2015) of *HLA3* but increased by the overexpression of HLA3 (Yamano et al., 2015; Gao et al., 2015), especially in alkaline conditions where HCO_3^- is the predominant type rather than CO_2. Another putative Ci transporter, LCI1 has several predicted transmembrane domains but no homologs in other species. Its expression is induced in CO_2-limiting conditions, and the overexpression of LCI1 under high-CO_2 (HC) conditions in an *lcr1* mutant in which limiting-CO_2-induced expression of *LCI1* and several other genes were impaired, increased photosynthetic Ci affinity and internal Ci accumulation (Ohnishi et al., 2010). However, simultaneous artificial overexpression of *LCI1* and LC-inducible protein A (*LCIA*) encoding a chloroplast envelope-localized HCO_3^- channel did not increase those of wild-type (WT) cells in HC conditions, even in alkaline conditions where HCO_3^- is the predominant type. In contrast, simultaneous overexpression of HLA3 and LCIA clearly raised photosynthetic Ci affinity and internal Ci accumulation (Yamano et al., 2015). Additionally, two Rhesus-like proteins RHP1 and RHP2 have been suggested to be channels for CO_2 in HC conditions, because they are paralogues of the ammonium and methylammonium transport proteins in animal and their expressions were up-regulated in HC conditions (Soupene et al., 2002). Especially, RHP1 protein has been proposed as a plasma membrane-localized CO_2 channel (Yoshihara et al., 2008), whose downregulation by RNA interference impaired growth of the *Chlamydomonas* cells in HC conditions (Soupene et al., 2004).

The chloroplast envelope is supposed to be another membrane barrier for Ci uptake in *Chlamydomonas* CCM. Although three chloroplast envelope-localized proteins, including LCIA, chloroplast carrier protein 1 (CCP1), CCP2, and Ycf10 were proposed to be involved in Ci uptake across this membrane, only LCIA has been confirmed to function in HCO_3^- uptake. LCIA belongs to a formate-nitrite transporter (FNT) family (Mariscal et al., 2006), in which proteins form a pentameric aquaporin-like channel rather than an active transporter (Wang et al., 2009; Lu et al., 2012). Although the injection of *LCIA* into *Xenopus oocytes* increased the uptake of nitrite more than that of HCO_3^- (Mariscal et al., 2006), LCIA was shown to be associated with HCO_3^- uptake in very LC (VLC) conditions from the characterization of its insertion mutant (Wang et al., 2014a; Yamano et al., 2015). Furthermore, LCIA is associated with HCO_3^- uptake into the chloroplast stroma in cooperation with HLA3 in VLC conditions, because simultaneous knockdown or knockout of *HLA3* and *LCIA* cause a dramatic decrease in photosynthetic Ci uptake (Duanmu et al., 2009b; Yamano et al., 2015) in alkaline conditions. In contrast, although knockdown of CCP1/2 led to growth defects in VLC conditions, the photosynthetic characteristics were not affected by these knockout mutations (Pollock et al., 2004). Further studies are required to determine the roles of CCP1/2, despite two possibilities that the defects in CCP1/2 in insertion

mutants were compensated for by other Ci uptake systems (Spalding, 2009) or CCP1/2 might affect the acclimation to VLC conditions indirectly by transporting unknown metabolites rather than directly in Ci uptake (Pollock et al., 2004). In addition, the chloroplast inner envelope-localized protein Ycf10 was proposed to promote efficient Ci uptake into chloroplast, because the photosynthetic Ci affinity was decreased in the mutant cells of the chloroplast *Ycf10* gene and isolated chloroplasts from *ycf10* mutant (Rolland et al., 1997).

Diatoms are a unicellular marine algae derived from secondary endosymbiosis of plastids from red algal cells (Falkowski et al., 2004), leading to the formation of a plastid endoplasmic reticulum surrounding its chloroplast. The $K_m(CO_2)$ of Rubisco in diatoms is approximately 50 µM, which is considerably higher than the CO_2 concentration in water equilibrated with air (Badger et al., 1998). To overcome the inefficiency of CO_2 fixation caused by the low-Ci affinity of Rubisco, a CCM system has been suggested in diatoms (Roberts et al., 2007; Fig. 5), based on the physiological evidence of direct uptake of CO_2 and HCO_3^- in marine diatom species (Johnston and Raven, 1996; Matsuda et al., 2001; Burkhardt et al. 2001; Trimborn et al., 2008; Nakajima et al., 2013), although a C_4-type biochemical CCM was also proposed to be a part of the diatom CCM in some species (Reinfelder et al., 2000; Kustka et al., 2014).

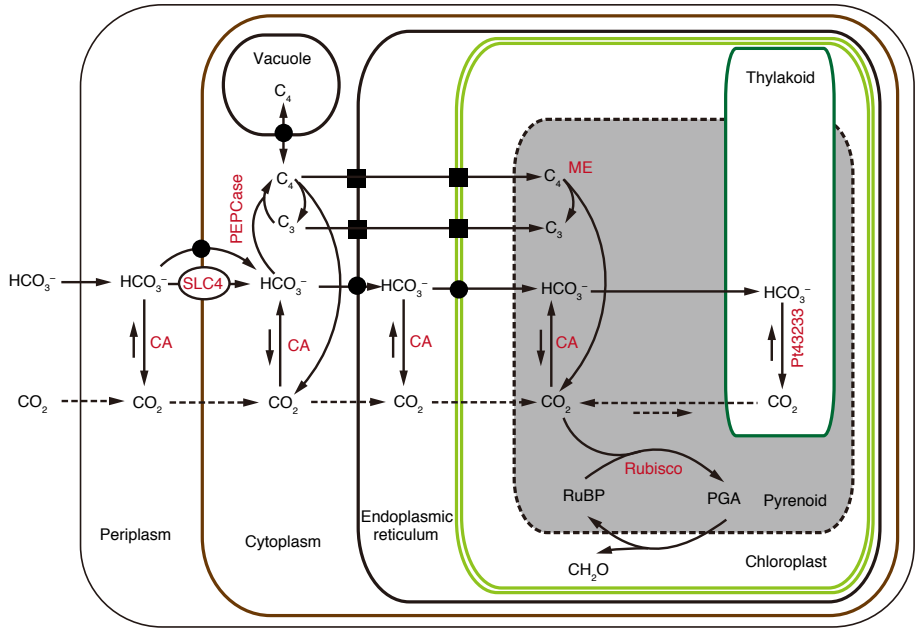

Figure 5. Schematic presentation of the possible CO_2-concentrating mechanism (CCM) in diatoms in CO_2-limiting conditions (modified from Roberts et al., 2007; Nakajima et al., 2013; Kikutani et al., 2016). The scheme shows the proposed uptake of inorganic carbon (Ci) from the extracellular space to the thylakoid lumen. The possible involvement of C_4 acid in the diatom CCM is also illustrated. The unknown Ci transporters are shown as closed circles. The transporters for C_3 or C_4 acid are indicated as closed squares. The broken lines indicate the diffusion paths of CO_2. CA, carbonic anhydrase. PEPCase, phosphoenolpyruvate carboxylase; ME, malic enzyme; RuBP, ribulose-1,5-bisphosphate; PGA, phosphoglyceric acid; SLC4, Ci transporters (Nakajima et al., 2013); Pt43233, thylakoid lumen-localized θ-CA (Kikutani et al., 2016).

As basic components for the uptake of Ci, several putative bicarbonate transporters homologous to solute carrier (SLC) 4 and SLC26-type bicarbonate transporters have been identified in model diatoms, *Phaeodactylum tricornutum* and *Thalassiosira pseudonana* (Kroth et al., 2008). Of note, an SLC4 homolog in *P. tricornutum*, known as PtSLC4-2, was characterized in the direct uptake of HCO_3^- across the plasma membrane (Nakajima et al., 2013). It was induced in CO_2-limiting conditions, and its expression increased significantly with the dissolved Ci uptake and photosynthetic activity. Furthermore, its function was inhibited by the addition of an anion-exchanger inhibitor and was dependent on the concentration of Na^+ ions, suggesting that PtSLC4-1 is a sodium-dependent HCO_3^- transporter. By examining the fluorescence of tagged proteins, some other SLC4 homologs could be embedded in chloroplast membranes as a 'chloroplast-pump' mechanism for the CCM (Hopkinson et al., 2016).

2. Carbonic anhydrases

In aqueous solution, CO_2 is in equilibrium with HCO_3^- and proton (H^+). CA causes H_2CO_3 to dissociate with a pK_1 of 6.35 and pK_2 of 10.25 (Rudenko et al., 2015). For example, the ratio of HCO_3^-: CO_2 at pH 6.2, 7.0, 7.8, and pH 9.0 is 0.7:1, 4.3:1, 28:1, and 446:1, respectively. In physiological conditions, the equilibration rate between HCO_3^- and CO_2 is slow, but CAs can accelerate both hydration and dehydration reactions in most organisms including animals, plants, and bacteria (Hewett-Emmett and Tashian, 1996). The known CAs can be grouped into at least six evolutionarily independent families, named α, β, γ, δ, ζ, and θ, based on their conserved nucleic acids sequences (Rudenko, et al., 2015; Kikutani et al., 2016). All groups are metalloenzymes that use metal ions in the active site, such as zinc or cadmium ions (Xu et al., 2008). CA was found for the first time in animal red blood cells (Meldrun et al., 1933), and animals only have the α-CAs with multiple isoforms. In aquatic photosynthetic organisms, the existence of CAs was first suggested in *Chlorella vulgaris* (Tsuzuki and Miyachi, 1979), and it was required for photosynthesis (Hogetsu and Miyachi, 1979) and CO_2 fixation (Shiraiwa et al., 1979). In contrast, cyanobacteria have both α-CAs and β-CAs (Fukuzawa et al., 1992), and the CcmM protein contains an active N-terminal γ-CA domain. A CA, known as CcmM, CcaA, or CsoS3 in different types of carboxysomes, is essential for the accumulation of HCO_3^- in the carboxysome (Pena et al., 2010; Espie and Kimber, 2011) and it is able to minimize the outward diffusion of CO_2 to the external environment when coupled with the NDH-1 CO_2 uptake systems. Diatoms possess all six types of CA (Hopkinson et al., 2016; Kikutani et al., 2016). Examples of α-CA (Fukuzawa et al., 1990) and β-CA have been found in *C. reinhardtii* (Moroney et al., 2001). Functional studies of the CCM suggest that CAs have three main roles: first, conversion between HCO_3^- and CO_2 at the cell surface to facilitate HCO_3^- or CO_2 uptake by their corresponding transporters; second, conversion of imported CO_2 to HCO_3^- in the cytosol or chloroplast stroma to prevent diffusion of CO_2 out of the cell or facilitate the transport of HCO_3^-; and third, conversion of accumulated HCO_3^- to CO_2 for CO_2 fixation by Rubisco.

In contrast to cyanobacteria, diatoms possess numerous CAs (Roberts et al., 1997; Cox et al., 2000; Lane et al., 2005; Harada et al., 2005; Lee et al., 2013) including two pyrenoidal β-CAs in *P. tricornutum*

(PtCA1 and PtCA2) (Tachibana et al., 2011), but the actual functions of most CAs are still unclear. Recent identification of the CA activity of a θ-CA, named as Pt43233 in *P. tricornutum*, emphasizes the functional importance of CAs in the diatom CCM (Kikutani et al., 2016). The depletion of Pt43233 by RNAi clearly impaired photosynthetic growth in ambient air conditions and its transcription level was maintained irrespective of CO_2 conditions. Pt43233 possessed CA activity *in vitro* and was localized to the lumen of the pyrenoid-penetrating thylakoid, where a thylakoid-luminal CA in *C. reinhardtii*, CAH3 converts HCO_3^- to CO_2 in acidic conditions in order to supply CO_2 to Rubisco (Karlsson et al., 1998).

In *C. reinhardtii*, at least six CAs have been identified. At the cell surface, a periplasmic α-CA, CAH1 has been studied extensively as a CO_2-limiting-inducible protein (Coleman and Grossman, 1984; Fukuzawa et al., 1990). It may function in the supply of HCO_3^- for plasma membrane HCO_3^- transporters or CO_2 for active CO_2 uptake by conversion between HCO_3^- and CO_2. A *CAH1* insertion mutant exhibited normal growth but only slightly deceased photosynthetic Ci affinity (Van and Spalding, 1999) in CO_2-limiting conditions. Considering the marine diatom *P. tricornutum* lacks periplasmic CAs but possesses an efficient CCM (Hopkinson et al., 2016), periplasmic CAs might be not necessary for the operation of the CCM in microalgae. It is also possible that defects in the *CAH1* mutant were masked because multiple Ci uptake systems could complement each other functionally (Wang et al., 2014a; Wang et al., 2015). Another periplamic CA, *CAH2* showed 91.8% identity with *CAH1* and its mRNA level was decreased in CO_2-limiting conditions but increased in sufficient CO_2 conditions (Fujiwara et al., 1990).

The thylakoid α-CA, CAH3 is localized to the pyrenoid-tubules after switching cells to CO_2-limiting conditions (Blanco-Rivero et al., 2012; Sinetova et al., 2012; Tirumani et al., 2014). Considering that CAH3 was suggested to be located outside of the thylakoid lumen in a recent report (Meyer and Griffiths, 2015), it might plausibly catalyze dehydration of HCO_3^- in the minitubules of the pyrenoid-tubules and directly release CO_2 into the pyrenoid matrix. To test this speculation, it would be necessary to make sure that the size of functional CAH3 protein is smaller than the minitubule lumen with minor axis of 3–4 nm and major axis of 8–15 nm (Engel et al., 2015). Correlating with the relocation into pyrenoid-tubules, CAH3 was phosphorylated in CO_2-limiting conditions, suggesting that post-translational modification might play a role in its function (Blanco-Rivero et al., 2012). So far, CAH3 is mainly considered to dehydrate HCO_3^- to CO_2 in the acidic thylakoid lumen, which is then released into the pyrenoid matrix for fixation by Rubisco, because a *CAH3* insertion mutant showed a severely retarded growth and accumulated 5-fold higher amounts of intracellular Ci than that in WT cells (Moroney et al., 1986b; Karlsson et al., 1998), although it has also been reported to function in the evolution of O_2 at the electron donor side of photosystem II (PSII) (Villarejo et al., 2002; Shutova et al., 2008). Considering the recent discovery that the θ-CA Pt43233 in the thylakoid lumen of *P. tricornutum* is critical for photosynthetic growth in CO_2-limiting conditions, the generation of ample CO_2 from HCO_3^- by CAs in the acidic thylakoid lumen for fixation by Rubisco could be an essential evolutionary event in the functionality of the pyrenoid in the algal CCM (Kikutani et al., 2016). Additionally, CAH6, a putative stroma CA has also been proposed to convert CO_2 to HCO_3^- and maintain a high Ci concentration by recapturing CO_2 leaking

from the pyrenoid (Moroney and Ynalvez, 2007). Two β-CAs, CAH4 and CAH5, are localized to the mitochondria and their expression was strongly up-regulated in CO_2-limiting conditions (Villand et al., 1997), but their contribution to the CCM is still unclear.

3. Microcompartments containing Rubisco in aquatic photosynthetic organisms

In many aquatic organisms, Rubisco proteins are enclosed within microcompartments, which maintain elevated CO_2 concentrations in the vicinity of Rubisco, both increasing carbon fixation and suppressing photorespiration. In cyanobacteria and several autotrophic prokaryotes, the polyhedral microcompartment is known as the carboxysome (Cameron et al., 2013; Fig. 6). Carboxysomes evolved as a proteinaceous microcompartments of 90–400 nm diameter in cyanobacteria (Badger et al., 2002). Two types of carboxysome, α-type and β-type, have evolved in parallel but both contribute to the CCM. The shell in either types of carboxysome is composed of 6–10 types of protein (Cannon et al., 2003; Espie and Kimber, 2011) and its Ci permeability is important for maximizing the carbon fixation (Mangan and Brenner, 2013). Of these, the protein CcmM is able to bind the large subunit of Rubisco, which is important for the aggregation as well as organization of Rubisco in the precarboxysome (Cot et al., 2008). The aggregated Rubisco serves as a nucleation cores initiated the biogenesis of the carboxysome (Cameron et al., 2013). A recent mathematical model of the cyanobacterial CCM proposed that the optimal permeability of the carboxysome outer-shell could maximize carbon fixation (Mangan et al., 2013).

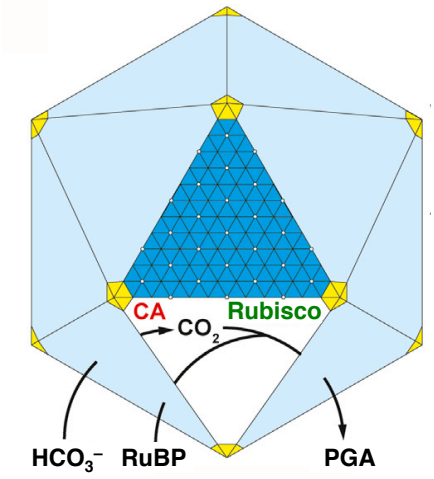

Figure 6. Schematic diagram of the carboxysome (modified from Cameron et al., 2013). The carboxysome shell is comprised of hexameric (blue) and pentameric (yellow) proteins that enclose enzymes of the Calvin–Benson–Bassham (CBB) cycle including almost all Rubisco (green). Bicarbonate (HCO_3^-) is converted to CO_2 by carbonic anhydrase (CA, red) in the carboxysome for CO_2 fixation.

In many algae, the pyrenoid has developed as a spherical proteinaceous structure surrounded with starch sheathes in the chloroplast (Fig. 7). It was described as dense and refractive bodies associated with the chloroplast for the first time (Schmitz, 1884), and it contains more than 90% of Rubisco in CO_2-limiting conditions (Morita et al., 1997). Its formation is controlled by several factors, such as Rubisco small-subunit α-helices (Meyer et al., 2012). Although active CCM was also found in some species of the pyrenoid-less free-living algal genus *Chloromonas* (Morita et al., 1998), physiological evidence indicated that the pyrenoid is associated with optimal function of the CCM (Badger et al., 1992; Meyer et al., 2012; Ma et al., 2011). Some of the thylakoid membrane penetrates into the pyrenoid, termed pyrenoid-tubules (Ohad et al., 1967). By *in situ* cryo-electron tomography, the three-dimension structures of the chloroplast and pyrenoid in *C. reinhardtii* have been elucidated (Engel et al., 2015).

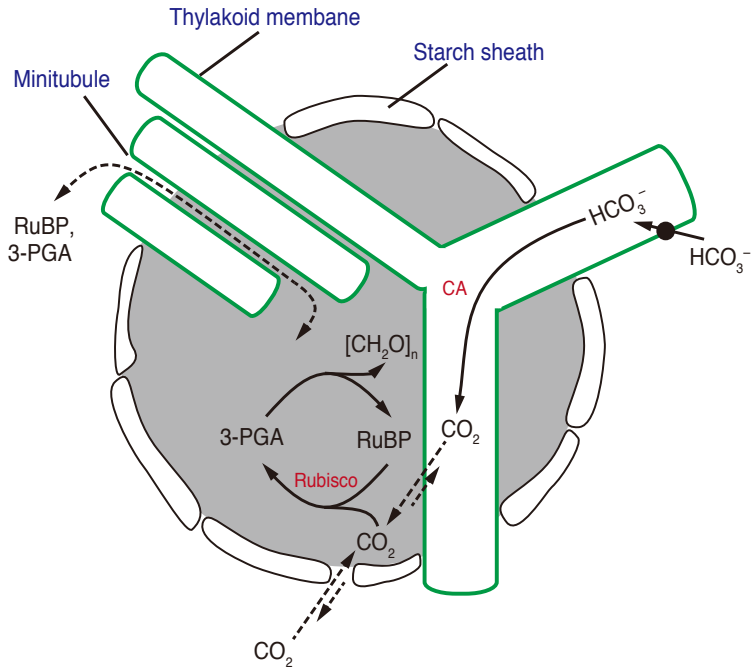

Figure 7. Schematic diagram of pyrenoid structure and the function of the pyrenoid in CO_2-concentrating mechanism (CCM) (modified from Meyer et al., 2015). The pyrenoid is surrounded by starch sheathes and encapsulates enzymes of Calvin–Benson–Bassham (CBB) cycle, including more than 90% of Rubisco. In CO_2-limiting conditions, the amount of CO_2 from passive diffusion is decreased. Most CO_2 comes from active uptake by HCO_3^- transporters (closed circle) into the thylakoid lumen, and HCO_3^- is converted into CO_2 by carbonic anhydrase (CA) in acidic lumen conditions. Subsequently, the CO_2 produced diffuses into the pyrenoid matrix for fixation by Rubisco. Small molecules, such as RuBP and 3-PGA, could diffuse between the chloroplast stroma and pyrenoid matrix through the minitubules formed by thylakoid stacks. The broken lines indicate the diffusion paths of CO_2.

Thylakoid stacks and the pyrenoid were connected by cylindrical pyrenoid tubules, and multiple parallel minitubules were bundled in each pyrenoid tubule, possibly serving as conduits for the diffusion of small molecules, such as ribulose-1,5-bisphosphate (RuBP) and 3-PGA, between the chloroplast stroma and the pyrenoid matrix. In addition, likely similar with the case of CcmM in cyanobacteria, an essential pyrenoid component 1 (EPYC1), previously named LC-inducible protein 5 (LCI5) (Somanchi et al., 1996; Im et al, 2003) possessing phosphorylated sites under LC conditions (Turkina et al., 2006), is colocalized with Rubisco throughout the pyrenoid. It may assist the formation of the pyrenoid and the packing of Rubisco in the pyrenoid in CO_2-limiting conditions by linking with Rubisco, based on the fact that an *EPYC1* insertion mutant exhibited low Rubisco content in the pyrenoid, aberrant formation of the pyrenoid, and decreased efficiency of CO_2 fixation (Mackinder et al., 2016). Other than Rubisco and EPYC1, hundreds of candidate proteins were also aggregated in pyrenoid after switching to CO_2-limiting conditions (Mackinder et al., 2016).

4. CO_2-concentrating mechanism in *Chlamydomonas reinhardtii*

C. reinhardtii has been used as a model organism in studies of the CCM for several decades (Badger et al., 1980; Fukuzawa et al., 1990; Giordano et a., 2005; Fukuzawa et al., 2012; Wang et al., 2014a), because of its short life cycle, sequenced genome (Merchant et al., 2007), and many available molecular approaches. Recently, the development of high-throughput methods for the isolation of mutants from insertion mutant libraries (Li et al., 2016) and possibility of editing its genome with the CRISPR/Cas9 system (Jiang et al., 2014; Shin et al., 2016; Baek et al., 2016) further enables the use of this organism as a leading unicellular model for photosynthetic eukaryotes. In *Chlamydomonas*, three CO_2-acclimation states, namely HC (0.5%–5% CO_2), low-CO_2 (LC; 0.03%–0.5% CO_2), and VLC (<0.03% CO_2), have been designated based on distinct growth, photosynthesis, and gene expression characteristics in response to CO_2 concentration (Vance and Spalding, 2005), suggesting a complicated but subtle regulation of the CCM. Under HC conditions, a periplasmic protein, H43, was accumulated by sensing the concentration of ambient CO_2 (Kobayashi et al., 1997; Hanawa et al., 2007). Many CO_2-inducible genes encoding putative Ci transporters and CAs, have been identified through transcriptome analyses and their functions have been further studied in corresponding mutants in terms of their physiological, genetic, cellular, and molecular aspects.

In addition to the putative proteins for Ci uptake and CAs, another soluble protein is also well characterized. In the chloroplast, LC-inducible protein B (LCIB) is dispersed throughout the chloroplast stroma in HC and LC conditions, but it is localized as a ring-like structure in the vicinity of the pyrenoid in VLC conditions (Yamano et al., 2010; Wang et al., 2014a; Wang et al., 2014b). LCIB interacted with its close homolog LC-inducible protein C (LCIC) in a hetero-hexamer complex in VLC conditions (Yamano et al., 2010; Wang and Spalding, 2014b). The proposed phosphorylation and glutathionylation of LCIB suggest that post-translational regulation could be essential for its function or related with its relocation in VLC conditions (Yamano et al., 2010; Zaffagnini et al., 2012). It appears to function in a

CO_2 uptake system for VLC acclimation, in parallel with the pathway operated by LCIA, because of the lethal phenotype by double mutations of *LCIA*/*LCIB* but only slightly retarded growth from a *LCIA* mutation in VLC conditions (Wang et al., 2014a). Additionally, LCIB is essential for survival in LC conditions due to the 'air-dier' phenotype of the *pmp1* and *ad1* mutant (Spalding et al., 1983; Wang and Spalding, 2006), which could be rescued by a *CAH3* mutation (Duanmu et al., 2009a). In addition to the involvement of LCIB in Ci uptake, another possibility in its function as a CA was strongly raised from a recent study that its homolog, Pt43233, in marine diatom *P. tricornutum* possessed CA activity *in vitro* and is localized in the lumen of the pyrenoid-penetrating thylakoid (Kikutani et al., 2016). This is consistent with previous speculation that LCIB may catalyze the hydration or dehydration between CO_2 and HCO_3^- to facilitate accumulation of Ci or to recapture CO_2 leaking from the pyrenoid (Duanmu et al., 2009b; Wang and Spalding, 2014b). The possible CA activity of LCIB might be a cause for the aggregation of LCIB in the vicinity of pyrenoid in VLC conditions.

In addition to these CCM-related genes described above, RNA-Seq transcriptome analyses have revealed several candidates for the CCM by comparing gene expression levels when shifting from sufficient CO_2 to CO_2-limiting conditions. Approximately 2,200–5,880 genes in *Chlamydomonas* are differentially expressed (Brueggeman, 2012; Fang et al., 2012; Wang et al., 2015), but only 57 genes were identified as classic LC-inducible genes (Fang et al., 2012). Future studies on these novel candidate genes could provide additional insight to promote understanding of the CCM.

5. Regulation of the CO_2-concentrating mechanism

The CCM in cyanobacteria is functional even in sufficient CO_2 (1–2%) conditions with a constitutive CO_2 pump to maintain a basal level of HCO_3^- uptake, but the induction of these high-affinity CO_2 uptake systems in CO_2-limiting conditions strongly enhances uptake capacity. The regulatory mechanisms controlling the responses to these two conditions have been studied. So far, two critical transcription factors belonging to LysR transcriptional regulators (LTTRs) family, CmpR and CcmR, have been identified to de-repress the expression of related genes. CmpR functions as a transcriptional activator targeting the operator DNA sequences of *cmpA–D* (Omata et al., 2001). In contrast, regulator CcmR (also named NdhR) mainly functions as a repressor of approximate 20 genes, including the *ndh-1*$_3$ operon and *sbtA/B* genes (Wang et al., 2004), and also has a potential activating role in the expression of some specific genes in CO_2-limiting conditions (Klahn et al., 2015). An additional regulatory factor belonging to the AbrB family, named cyAbrB2, functions in repressing the expression of *ndh-1*$_3$ and *sbtA* in HC conditions (Lieman-Hurwitz, et al., 2009). Furthermore, the transcription of CCM-related genes was also regulated by metabolic signals, such as ribulose-1,5-bisphosphate (RuBP), 2-PG, 3-PGA, NADPH, $NADP^+$, and α-ketoglutarate (Daley et al., 2012; Haimovich-Dayan et al., 2014; Burnap et al., 2015). In addition to CO_2-limiting conditions, light intensity also regulates the CCM by modulating the biosynthesis and organization of the carboxysome possibly through photosynthetic electron flow (Hihara et al., 2001; Burnap et al., 2013; Sun et al., 2016).

Regulation of the CCM in diatoms was largely unknown until the present evidences that the cytosolic cAMP level was increased during the shift from LC to HC conditions, and it repressed the expression of reporter genes driven by the promoter of *PtCA1* (Harada et al., 2006). Recently, it was reported that the CO_2/cAMP signal is involved in cross-talk with light signals in the cAMP-mediated transduction pathway and targeted three and two CO_2/cAMP-responsive elements (CCREs) in the promoter of *PtCA1 and PtCA2*, respectively (Tanaka et al., 2016).

In *C. reinhardtii*, two regulatory factors, CCM1/CIA5 and LCR1, have been identified to regulate gene expression (Yoshioka et al., 2004; Fig. 8). CCM1/CIA5 is a master regulatory factor controlling the induction of the CCM (Xiang et al., 2001; Fukuzawa et al., 2001). CCM1/CIA5 exhibits zinc-binding activity, and is constitutively expressed in both sufficient and limiting-CO_2 conditions (Kohinata et al., 2008). A *CCM1/CIA5* insertion mutant exhibited defects in acclimation responses to limiting-CO_2 conditions, especially the expression of 47 LC-inducible genes (Miura et al., 2012). As a downstream regulator of CCM1, LCR1 is an LC-inducible myeloblastosis (Myb)-type DNA-binding transcription factor regulating a subset of the genes responsive to limiting CO_2, at least including *CAH1*, *LCI1*, and *LCI6* (Yoshioka et al., 2004). The direct interaction of LCR1 with the *CAH1* promoter indicates that the LCR1 regulates the expression of genes through binding *cis*-elements. In addition to the regulation of gene expression, post-translational modification may be associated with the operation of the CCM. Some CCM-related proteins, including CAH3 (Blanco-Rivero et al., 2012), LCIB (Yamano et al., 2010), LCI5 (Turkina et al., 2006), and HLA3 (Wang et al., 2014c), possess phosphorylation sites, which could be essential for their function. Additionally, the lack of CIA6 protein with a SET methyltransferase domain impaired the development of the pyrenoid and CCM induction (Ma et al., 2011). Although LC stress in light is thought to be essential for the induction of CCM, it was also reported that CCM was induced during dark to light transition (Tirumani et al., 2014), correlating with the aggregation of the portion of Rubisco and CAH3 in pyrenoid as well as the accumulation of CAH1, LCIB, and LCIC, (Mitchell et al., 2014).

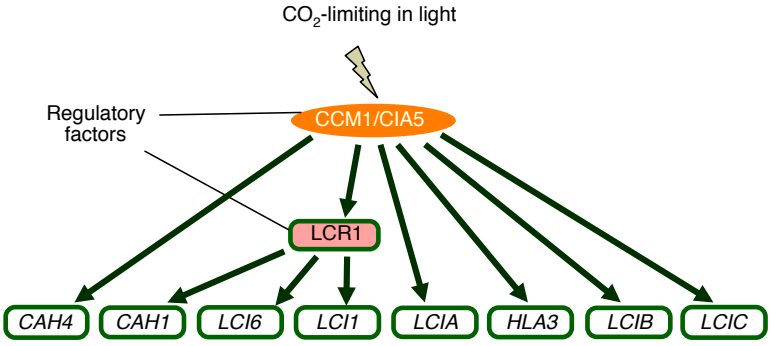

Figure 8. A model for CO_2-dependent regulatory network in *Chlamydomonas reinhardtii* (modified from Yoshioka et al., 2004)**.** Two regulatory factors including CCM1/CIA5 and low-CO_2 (LC)-inducible DNA-binding transcriptional factor (LCR1) are presented. *CAH1* and *CAH4* are genes encoding carbonic anhydrases. LC-inducible 1 (*LCI1*) and high-light activated 3 (*HLA3*) are genes encoding two plasma membrane-localized inorganic carbon (Ci) transporters. LC-inducible A (*LCIA*) is a gene encoding chloroplast envelop-localized Ci channel. LC-inducible B (*LCIB*) and LC-inducible C (*LCIC*) are genes encoding proteins for recycling of leaked CO_2 from pyrenoid. LC-inducible gene 6 (*LCI6*).

6. Calcium signaling and CO_2 response in plants

In addition to these identified signals as described above, calcium (Ca^{2+}), which plays important roles in many regulatory processes (Clapham, 2007; Kudla, et al., 2010), has been suggested to mediate CO_2 signal transduction in animals and plants (Cummins et al., 2014; Kim et al., 2010). Especially in terrestrial plants, changes in cytosolic Ca^{2+} concentrations ($[Ca^{2+}]_{cyt}$) in guard cells could be induced by both increases and decreases in external CO_2 concentrations (Schwartz et al., 1988; Webb et al., 1996; Young et al., 2006; Kim et al., 2010). Furthermore, Ca^{2+} also plays a critical role in the regulation of photosynthesis, in which the activation of several proteins was dependent on chloroplastic Ca^{2+} concentration (Hochmal et al., 2015), and the regulation of redox in chloroplast (Hochmal et al., 2016). As a molecular component related to the Ca^{2+} signal, the chloroplast Ca^{2+}-binding protein CAS was primarily identified in *Arabidopsis thaliana* and could mediate extracellular Ca^{2+} sensing in guard cells (Han et al., 2003). A hydrophobic sequence separates the peptide into an N-terminus and a C-terminus, which has a rhodanese-like domain (Fig. 9A). CAS is specifically conserved in green eukaryotic photosynthetic organisms (Fig. 9B and C) and is localized to the thylakoid membrane (Nomura et al., 2008; Vainonen et al., 2008). It was also reported that CAS mediated the transient elevation of stroma Ca^{2+} concentration ($[Ca^{2+}]_{stro}$) and cytosolic Ca^{2+} concentration ($[Ca^{2+}]_{cyt}$), which presumably regulated plant immune responses or stomata closure (Nomura et al., 2008; Weinl et al., 2008; Nomura et al., 2012). Recently, this cytosolic Ca^{2+} signal was proposed to be sensed by 14-3-3ω-mediated Ca^{2+}-dependent scaffolding, which subsequently activates a nuclear-localized transcriptional factor abscisic acid-insensitive 4 (ABI4) through phosphorylation by mitogen-activated protein kinases (MAPKs) (Guo et al., 2016).

In *C. reinhardtii*, an ortholog of CAS was also detected in the thylakoid membrane fraction (Allmer et al., 2006; Terashima et al., 2010) by proteomic analyses. It was proposed that CAS is required for photoacclimation by regulating the induction of the light-harvesting protein LHCSR3 (Peers et al., 2009; Petroutsos et al., 2011) and for forming a super complex of photosynthetic cyclic electron flow (CEF) in anaerobic conditions (Terashima et al., 2012), based on the characterization of *CAS* knockdown strains. Because *LHCSR3* is also induced by CO_2-limiting conditions during the induction of the CCM (Fang et al., 2012; Miura et al., 2004; Maruyama et al., 2014) and light signals cross-talk with CO_2 in the regulation of the *Chlamydomonas* CCM (Yamano et al., 2008), CAS could be involved in the CO_2-transduction pathway of the CCM.

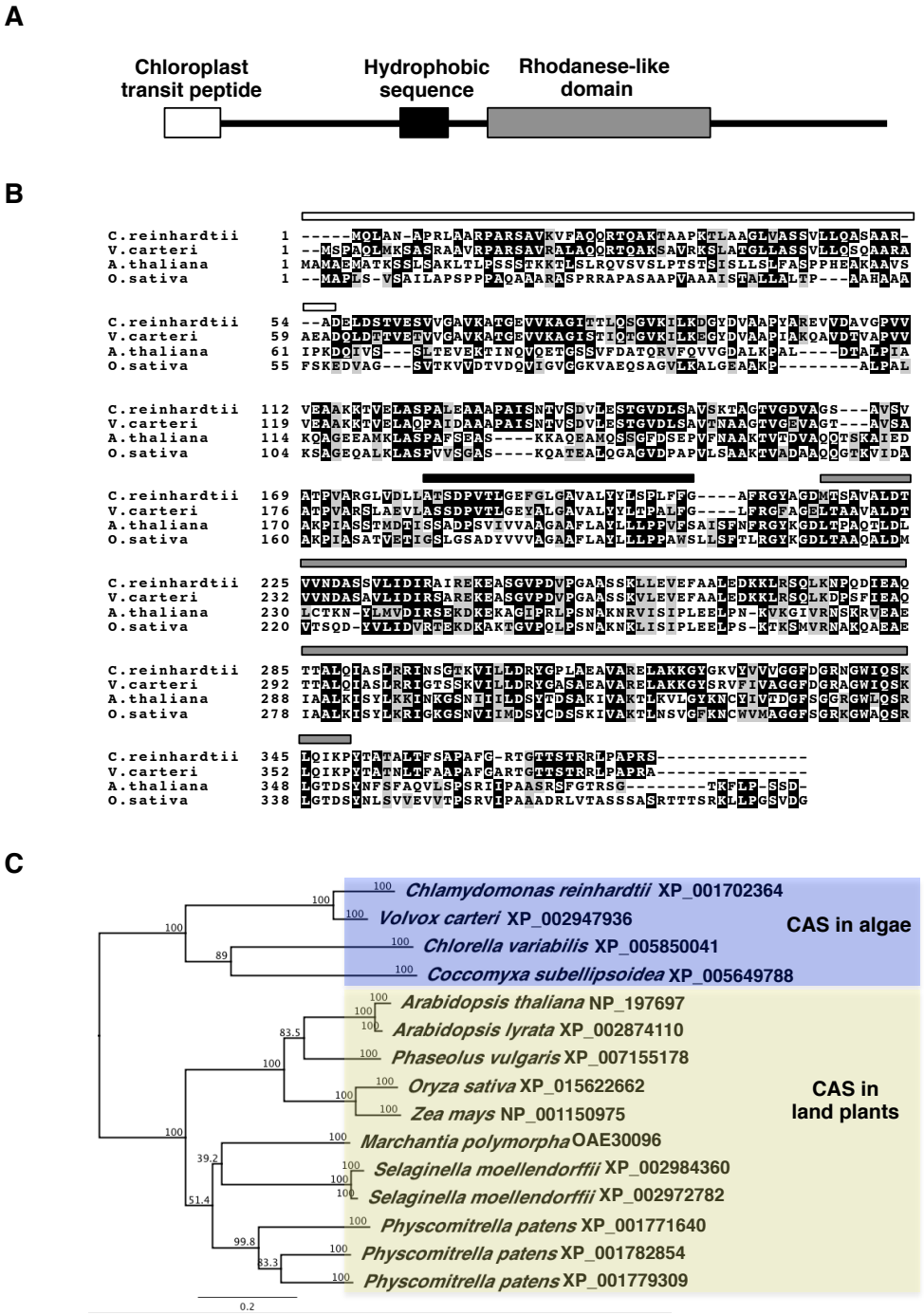

Figure 9. Domain structure and phylogenetic tree of homologous calcium (Ca^{2+})-sensing receptor (CAS). (A) Schematic presentation of the domain structure of CAS. (B) Alignment of *Chlamydomonas* CAS with the amino acid sequences of putative homologous proteins from *Chlamydomonas reinhardtii*, *Volvox carteri*, *Arabidopsis thaliana*, and *Oryza sativa*. The rectangles with white, black, and gray colors represent chloroplast transit peptide, hydrophobic sequence, and rhodanese-like domain, respectively. (C) The phylogenetic tree was constructed using the neighbor-joining method. Bootstrap values are calculated over 1,000 replicates.

Purpose

In *C. reinhardtii*, the molecular mechanism of the CCM has been studied in detail, mainly based on CCM-related genes identified by analyzing HC-requiring mutants. So far, several HC-requiring mutants have been obtained, such as *ccm1*, *cah3*, and *cia6* (Fukuzwa et al., 1998; Morony et al., 1986; Ma et al., 2010), by comparing the growth rate of DNA-tagged transformants with that of WT cells in CO_2-limiting conditions. To elucidate the molecular components in *Chlamydomonas* CCM, I generated 25,380 transgenic lines by transforming hygromycin (hyg) or paromomycin (par) resistance gene cassettes into WT cells, and screened for HC-requiring mutants.

By characterization one HC-requiring mutant, designated as H82, and its complemented strains, it was found that the disruption of the Ca^{2+}-binding protein CAS was responsible for its HC-requiring phenotype. To evaluate the causes of the HC-requiring phenotype in H82, genes whose expression was affected by the *CAS* mutation in LC conditions were identified by RNA-seq analysis. To understand the localization of CAS *in vivo*, the indirect immunofluorescence signal using an anti-CAS antibody was examined. Additionally, by examining photosynthetic Ci affinity and the accumulation of HLA3 as well as LCIA in WT cells when intracellular Ca^{2+} homeostasis was perturbed by the addition of a Ca^{2+}-chelator or calmodulin antagonist, the link between Ca^{2+} signaling and regulation of the CCM was elucidated. From these results, the chloroplast-mediated regulation of the CCM by Ca^{2+}-binding protein CAS is proposed, in addition to the regulation by CCM1/CIA5.

Material and Methods

Strains and culture conditions

For maintenance, *Chlamydomonas* strains (Table 1) were cultured at 22°C with light intensity below 10 μmol photons·m^{-2}·s^{-1} on Tris-acetate-phosphate (TAP) agar plates. *C. reinhardtii* strain C-9 (mt^-) was used as a wild-type (WT) line (Fukuzawa et al., 2001). *CCM1* insertion mutant C16 as well as its parental 5D strain (Fukuzawa et al., 2001) and a *PGRL1* insertion mutant (Tolleter et al., 2011) were characterized previously. For physiological and biochemical experiments, 5 mL or 100 mL volume of cells were pre-cultured mixotrophically in TAP medium with shaking at 25°C with 60 μmol photons·m^{-2}·s^{-1} for 24 h. Then, cells were centrifuged at 600 g for 5 min and pellets were re-suspended in 50 mL modified high-salt medium supplemented with 20 mM 3-(N-morpholino)propanesulfonic acid (MOPS) (HSM) with ammonium (NH_4^+) as nitrogen source in high-CO_2 (5% CO_2, HC) conditions at 120 μmol photons·m^{-2}·s^{-1}. For LC induction, HC-acclimated cells were centrifuged, re-suspended in 50 mL fresh HSM, and cultured in low-CO_2 (0.04% CO_2, LC) conditions at 120 μmol photons·m^{-2}·s^{-1} for indicated time period. For induction of HLA3 and LCIA in AH-1 strain, the HC-acclimated cells were centrifuged, washed with 10 mL volume of HSM medium with nitrate (NO_3^-) as nitrogen source (HSM-NO_3^-), re-suspended in 50 mL of HSM-NO_3^- medium, and cultured in HC conditions for 24 h. In all experiments, cell density was kept in mid-log phase (approximately OD_{730}=0.4) before harvesting the cells for following analyses.

Table 1. Genetic information of strains used in this study.

Name of strain	Genotype	Promoter and 3'-UTR used for gene expression	References
C-9	Wild-type and parental strain of H24, H82, and P103	N.A.	Fukuzawa et al., 2001
CC-125	Wild-type	N.A.	Harris et al., 1989
CC-1690	Wild-type	N.A.	Harris et al., 1989
H24	*uch:: aphVII*	N.A.	Wang et al., 2014
P103	*ccm1:: site mutation*	N.A.	Wang et al., 2014
H82	*cas:: aphVII*	N.A.	Wang et al., 2014
C-1	*cas:: aphVII, CAS*	Native promoter and 3'-UTR of *CAS*	This study
C-2	*cas:: aphVII, CAS*	Native promoter and 3'-UTR of *CAS*	This study
AH-1	*cas:: aphVII, HLA3, LCIA*	Tandemly duplicated enhancer elements of *NIA1* fused with minimal β_2-tublin promoter and *RbcS2* 3'-UTR in plasmid pTY2b	Yamano et al., 2015 and this study
FN-1	*cas:: aphVII, FLAG-CAS*	Native promoter and 3'-UTR of *CAS*	This study
5D	*nit1-305, cw-15*	N.A.	Fukuzawa et al., 2001
C16	*ccm1:: Nia1*	N.A.	Fukuzawa et al., 2001
L-1	*pgrl1:: aphVIII*	N.A.	Tolleter et al., 2011
L-1C	*pgrl1:: aphVIII, PGRL1*	Native promoter and 3'-UTR of *PGRL1*	Tolleter et al., 2011

N.A., not applicable; *aphVII*, hygromycin resistance gene cassette; *aphVIII*, paromomycin resistance gene cassette; *uch*, ubiquitin carboxyl-terminal hydrolase.

Transformation of cells

A 1,999-bp DNA fragment with the hygromycin (hyg)-resistant gene *aphVII* driven by β2-tubulin promoter was amplified by PCR from plasmid templates pHyg3 (Berthold et al., 2002) using PrimeSTAR GXL DNA Polymerase (TAKARA BIO, Shiga, Japan) with a forward primer HYG-F and reverse primer HYG-R (Table 2). It was performed as follows: 35 cycles of denaturation for 10 s at 98°C, annealing for 15 s at 60°C, and extension for 2 min at 68°C. Similarly, a 1,534-bp DNA fragment containing the paromomycin (par)-resistance gene *aphVIII* driven by HSP70A (heat shock protein 70 A) -RBCS2 tandem promoter (Lodha et al., 2008) was amplified by PCR from plasmid pGenD-aphVIII (Nakazawa et al., 2007) with a forward primer PAR-F and reverse primer PAR-R (Table 2). It was performed as follows: 30 cycles of denaturation for 10 s at 98°C, annealing for 15 s at 60°C, and extension for 2 min at 68°C. The PCR product was purified using a PCR purification kit (QIAGEN, Valencia, CA, USA) and the concentration was adjusted to 100 μg mL^{-1}. Transformation of *C. reinhardtii* cells without cell-wall degradation was performed as reported previously (Yamano et al., 2013). In brief, WT cells in early-log phase (approximately OD_{730}=0.25) were harvested and transformed by electroporation using a NEPA21 electroporator (NEPAGENE, Chiba, Japan). The transformants were incubated at 25°C for 24 h with gentle agitation under illumination at 1.5 μmol photons·m^{-2}·s^{-1} and then spread over the surface of TAP plates containing 30 μg mL^{-1} hyg or 10 μg mL^{-1} par. After culturing in 80 μmol photons·m^{-2}·s^{-1} for 4 days, the appeared colonies were subjected to the screening process of HC-requiring mutants.

For complementation of H82 mutant, genomic sequences of *CAS* with its own predicted promoter (~3.5 kb upstream of the 5'-UTR) were amplified using the primer set CF1 and CF0 (Table 2) and introduced into H82 cells with paromomycin resistance gene (*aphVIII*) cassette. For screening of complemented candidates, cells were cultured in HC conditions at 120 μmol photons·m^{-2}·s^{-1} to logarithmic phase in a 96-well microtiter plate containing liquid HSM medium, diluted to the optical density (approximately OD_{700}=0.04), and then transferred to LC conditions for 24 h. OD_{700} was measured using a microtiter plate reader XFluor4 (TECAN, Tokyo, Japan) and transformants showing similar OD_{700} with that of WT were selected as complemented candidates.

Table 2. Sequences of primers used in this study.

Primer name	Sequence
HYG-F	5'-GCACCCCAGGCTTTACACTTTATGCTTCC-3'
HYG-R	5'-CCATTCAGGCTGCGCAACTGTTGG-3'
PAR-F	5'-GCTTATCGATACCGTCGACCT-3'
PAR-R	5'-AACACCATCAGGTCCCTCAG-3'
UP3	5'-GACTCACCTCCCAGAATTCCTGG-3'
UP2	5'-TCGTTCCGCAGGCTCGCGTAGG-3'
UP1	5'-TCGAGAAGTAACAGGGATTCTTGTGTCATG-3'
DP4	5'-CTTCGAGGTGTTCGAGGAGACCC-3'
DP3	5'-CGCTGGATCTCTCCGGCTTCACC-3'
DP2	5'-GCCCCCGGCGCCTGATAAGG-3'
RMD227	5'-NTCGWGWTSCNAGC-3'
A1	5'-NGTCGASWGANAWGAA-3'
A2	5'-GTNCGASWCANAWGTT-3'
A3	5'-WGTGNAGWANCANAGA-3'
A4	5'-TGWGNAGSANCASAGA-3'
A5	5'-AGWGNAGWANCAWAGG-3'
A6	5'-STTGNTASTNCTNTGC-3'
A7	5'-NTCGASTWTSGWGTT-3'
F1	5'-GCGGATCAGATAATACCCCGTA-3'
R1	5'-AAGAACAGGGGGCTGAGGTAAT-3'
UPS	5'-TCATGTTTGCGGGTTGTGACTG-3'
DPS	5'-CCCCGCTCCGTGTAAATGGAGG-3'
F2	5'-CGTCCACACAGACCCTGGAC-3'
R2	5'-GCGATACACCGTTGGCTGTAG-3'
HLA3-F	5'-CGCTCTGCGCAAGTCCTTC-3'
HLA3-R	5'-CGTAGTTGACGTGGGACAGCA-3'
CBLP-F	5'-AGGTCTGGAACCTGACCAACT-3'
CBLP-R	5'-AAGCACAG GCAGTGGATGA-3'
CF1	5'- CTGACACACGTTACCACACAGCACCAC-3'
CR0	5'- ATCCGTAACCACTTCGCGCTCGTTC-3'
GST-CAS-F1	5'-CCCGGGTCGACTCGAGGATGAGCTGGACTCCACTGTGG-3'
GST-CAS-R1	5'- GATGCGGCCGCTCGAGCGAGCGGGGGGCGGGCAG-3'
GST-CAS-F2	5'- CCCGGGTCGACTCGAGCGCGGCTACGCCGGCGAC-3'
GST-CAS-R2	5'- GATGCGGCCGCTCGAGCTCGCCCAGAGTGACGGGGT-3'
GST-AtCAS-F	5'-ATTCCCGGGTCGACTCGAGGTTTCACTTCCAACATCAACTTCAATCATCTCT-3'
GST-AtCAS-R	5'-ACGATGCGGCCGCTCGAGCGTATCCATGGTCGATGAAGCAATC-3'
FLAG-CAS-F1	5'-ATCGATAAGCTTGATATCGACTACAAGGACGACGACGACAAG GATGAGCTGGACTCCACTGTGG-3'
FLAG-CAS-F2	5'-ATCGATAAGCTTGATGGGGCTACTCGAACGCATGAG-3'
FLAG-CAS-R1	5'-CTGCAGGAATTCGATGTGATGGAACATGGCAAGGGGCA-3'
FLAG-CAS-R2	5'-GTCCTTGTAGTCGATGTCGTGGTCCTTGTAGTCGCCGTCGTGGTCCTTGTAGTCAG CGCGGGCAGCAGACGCCT-3'

Screening of HC-requiring mutants

Cells grown under HC conditions for 12 h were replicated into two 96-well microtiter plates containing 200 μL liquid HSM in each well (Fig. 10). One of the plates was incubated in a chamber aerated with 0.04% CO_2 and the other in the chamber supplied with 5% CO_2 for 3 days. For every 24 h, the optical density at 700 nm (OD_{700}) was measured using a microtiter plate reader XFluor4 (TECAN, Tokyo, Japan). For the 1st screening, transformant whose OD_{700} value in HC chamber failed to reach 1.0 at 72 h were discarded and transformant whose OD_{700} value in LC chamber was less than five-times of the initial OD_{700} and that of WT were selected as candidate HC-requiring mutants. For the 2nd screening, the candidate mutants, WT and C16 cells grown in liquid HSM under HC conditions were diluted to OD_{430} of 0.15, 0.07, or 0.03, and then 3 μL of each cell suspension was spotted onto two respective HSM agar plates grown in HC or LC chambers for 9 days. WT and C16 cells were used as control.

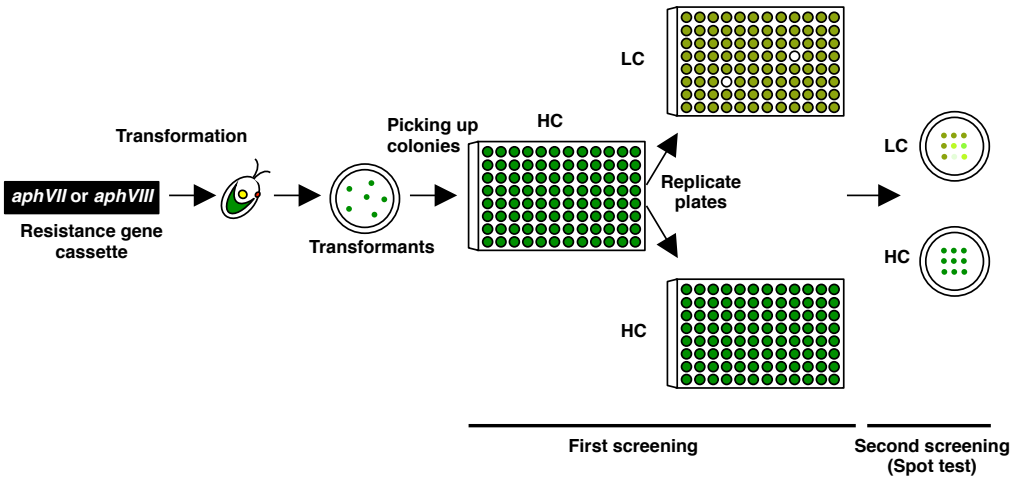

Figure 10. Schematic illustration of screening process. PCR-amplified hygromycin (hyg) or paromomycin (par) resistance gene cassettes were introduced into wild-type (WT) cells by electroporation. Colonies with resistance were picked up, cultured in 96-well microtiter plates under high-CO_2 (HC) conditions, and replicated into two plates. One plate was incubated under HC conditions, and the other one was incubated under low-CO_2 (LC) conditions. By measuring optical density at 700 nm every 12 h, HC-requiring candidates were isolated. The reproducibility of the HC-requiring phenotype was checked by a spot test in second screening.

Measurement of light-dependent CO_2-exchange activity

For measuring light-dependent CO_2-exchange (LCE) activity, HC- or LC- grown cells were centrifuged at 600 g for 5 min, and resuspended in fresh HSM at 5 μg Chl mL^{-1}. The CO_2-exchange activity was measured at 28°C using an open infrared gas-analysis system that records real-time rate of CO_2 exchange. Standard nitrogen (N2) gas balanced with 50 ppm (parts per million) CO_2 and 21% O_2 (Sumitomo Seika Chemicals) was supplied at a flow rate of 0.5 L min^{-1} to the cell chamber where the cell suspension was placed. Actinic light (2,000 μmol photons·m^{-2}·s^{-1}) was applied to the surface of the cell chamber for 5 min, and CO_2-exchange rate was measured during light illumination with a halogen projector lamp to achieve

maximal CO_2-exchange activity. The gas leaving the measurement chamber was chilled to 4°C by passing through a Dimroth condenser (NCB-1200; EYELA) and dehydrated by passing through a glass tube filled with granular $CaCl_2$. The CO_2-concentration of the gas was measured by an infrared CO_2-analyzer (model LI-7000; LI-COR).

Measurement of inorganic carbon-dependent photosynthetic oxygen evolution

The photosynthetic Ci affinity was evaluated by measuring the rate of dissolved Ci-dependent photosynthetic O_2 evolution. Cells grown in HC and LC conditions were collected and suspended in Ci-depleted 20 mM MES-NaOH buffer (pH 6.2), MOPS-NaOH buffer (pH 7.0), or HEPES-NaOH buffer (pH 7.8) with a concentration corresponding to 10 μg mL^{-1} chlorophyll. Cell suspension (1.5 mL) was transferred into the chamber of the O_2 electrode and illuminated at 350 μmol photons·m^{-2}·s^{-1} for 15 min with bubbling of N_2 gas to remove dissolved Ci. Then, the light intensity was increased to 700 μmol photons·m^{-2}·s^{-1}, and 1–10 μL of $NaHCO_3$ stock solutions (15, 150, and 750 mM) were injected into the cell suspension to yield the desired Ci concentration every 30 s. The maximal velocity of O_2-evolving activity, defined as V_{max}, was measured in the presence of 10 mM $NaHCO_3$.

Measurement of photosynthetic Ci uptake

The Ci uptake was measured by the silicone oil centrifugation method described previously (Fukuzawa et al., 1998). Cells cultured in LC conditions for 12 h were collected by centrifugation at 600 g for 5 min at room temperature and suspended in Ci-depleted 20 mM HEPES-NaOH buffer (pH 7.8) with a concentration corresponding to 25 μg Chl mL^{-1}. Cell suspension (1.5 mL) was transferred into chamber of the O_2-electrode and illuminated at 350 μmol photons·m^{-2}·s^{-1} for 15 min with bubbling of N_2 gas to remove dissolved Ci. For preparation, 60 μL silicon oil (SH550/SH556=4/7 [v/v]) was overlaid on the layer of the termination solution (1 M Glycin, 0.75% (wt/vol) SDS, adjust to pH 10.0 by NaOH). The pretreated cell suspension of 300 μL was gently overlaid on but without disturbing the silicon oil layer. After slowly adding 10 μL of 100 μM $Na^{14}HCO_3$ in the layer of cell suspension using a long tip, the tube was placed in centrifuge in balance, then immediately illuminated with 300 μmol photons·m^{-2}·s^{-1} light for 20, 40, or 80 s, collected by centrifugation at 13,000 g for 35 s, and frozen by putting into the liquid nitrogen. Subsequently, the radioactive labeled cells were suspended in alkaline buffer containing 0.1 N NaOH of 400 μL. One aliquot of 160 μL was directly subjected to the liquid scintillation counting for the evaluation of total Ci uptake. The other aliquot of 160 μL cell suspension was mixed with 0.5 N HCl of 200 μL and then placed in 75°C water bath, followed by liquid scintillation counting for determine the CO_2 fixation. The Ci accumulation was calculated by subtracting CO_2 fixation from Ci uptake. The Ci uptake was corrected by evaluating the cell volume as sorbitol impermeable space (SIS) using [^{14}C]-labeled sorbitol and ^3H_2O.

Thermal asymmetric interlaced (TAIL) PCR

For the thermal asymmetric interlaced PCR analysis of upstream flanking regions, specific primers UP3, UP2, and UP1 were used for primary, secondary, and tertiary amplifications, respectively. Similarly, for downstream flanking regions, DP4, DP3, and DP2 were used for primary, secondary, and tertiary amplifications, respectively. The degenerate primers RMD227 (Dent et al. 2005), A1, A2, A3, A4, A5, A6, and A7 (Liu et al. 1995; Liu and Whittier 1995) (Table 2), were used in each reaction. The genomic DNA (50 ng) was used as template in the primary amplification. Primary reactions with GC buffer (TAKARA BIO), 0.2 mM dNTPs, 5 pmol of specific primer, 60 pmol of degenerate primer, and 1 U of LA Taq (TAKARA BIO) were performed under the following conditions: 2 min, 95°C; 5 cycles (1 min, 94°C; 1 min, 62°C; 2.5 min, 68°C); 1 min, 94°C; 3 min, 25°C; ramping over 3 min to 68°C; 2.5 min, 68°C; 15 cycles (30 s, 94°C; 3.5 min, 68°C; 30 s, 94°C; 3.5 min, 68°C; 30 s, 94°C; 1 min, 44°C; 2.5 min, 68°C); 5 min, 68°C. The primary reaction products were diluted 50-fold, and an aliquot of 1 μL was used in secondary reactions with identical components to the primary reaction under the following conditions: 12 cycles (30 s, 94°C; 3.5 min, 68°C; 30 s, 94°C; 3.5 min, 68°C; 30 s, 94°C; 1 min, 44°C; 2.5 min, 68°C); 5 min, 68°C. The secondary reaction products were diluted 50-fold, and an aliquot of 1 μL was subjected to tertiary reactions with identical components to the primary reaction under identical conditions to the secondary reaction. The tertiary reaction products were separated by agarose gel in electrophoresis, and the visualized fragments under UV light were extracted from the gel, and analyzed by DNA sequencing.

For amplifying and sequencing the upstream and downstream flanking regions of *aphVII* cassette in genomic DNA, primers of F1, R1, UPS, and DPS were used (Table 2).

Tetrad analysis

The tetrad analysis was performed using an inverted microscope (BX41; Olympus, Japan) equipped with a micromanipulator (Narishige, Japan) and a glass needle (Singer Instruments, UK). H82 (mt^-), CC-1690 (mt^+), and CC-125 (mt^+) cells were grown in TAP medium for 12 h and then spread over the special TAP agar plates with 1/5 nitrogen source. The plates were incubated in 60 μmol photons·m^{-2}·s^{-1} light for 3 days until the colony became yellow. Subsequently, the yellow cells were sprayed out and washed two times using induction medium. For induction of gametes, each suspension was incubated under 60 μmol photons·m^{-2}·s^{-1} light for 3 h with gentle shaking (60 rpm). The suspension of H82 was gently mixed with these of CC-1690 or CC-125 strains in sterilized plates. After incubation for 1 h, each mixture was spread onto TAP agar plates with 3% (wt/vol) agar, and incubated in dark condition for 1 week. To obtain matured zygotes, unmated cells were scratched from the agar plates using sterilized blades, followed by transferring zygotes to a new TAP agar plate and separate them using needle under inverted microscope.

Immunoblotting Analysis

Chlamydomonas Cells were harvested by centrifugation at 600 g for 5 min, washed by phosphate-buffered saline (PBS) once, and suspended in PBS with protease inhibitor (EDTA-free, Cocktail, Germany). Then, cells were disrupted by sonication using Handy Sonic (Tomy) for 3 s with 25 cycles. The sonicated cells were regard as total protein sample. After centrifugation of the total protein sample at 15,000 g for 5 min, supernatant was transferred to new tube and regarded as crude soluble protein sample. Extracted soluble and total proteins suspended in sodium dodecyl sulfate (SDS) loading buffer were incubated at 37˚C for 30 min, and subsequently centrifuged at 13,000 g for 10 min. The supernatant was loaded on SDS-PAGE for electrophoresis. Next, proteins were transferred to Fluoro Trans® PVDF membrane (Life Science) using semi-dry blotting system. Membranes were blocked with 5% (wt/vol) skim milk powder (Wako, Japan) in PBS. Blocked membranes were washed using PBS containing 0.1% (vol/vol) Tween-20 (PBS-T) and treated with the following anti-serums generated from rabbit: anti-CCM1 anti-serum (1:5,000 dilution); anti-CAH1 anti-serum (1:2,500); anti-CAH3 anti-serum (1:2,000); anti-CAH6 anti-serum (1:2,000); anti-LCI1 anti-serum (1:5,000); anti-LCIA anti-serum (1:5,000); anti-HLA3 anti-serum (1:1,000); anti-LCIB anti-serum (1:5,000); anti-LCIC anti-serum (1:10,000); anti-CAS antiserum (1:5,000); anti-LHCSR3 anti-serum (1:5,000), and following commercial antibodies: anti-Histone H3 antibody (1:20,000); anti-D1 antibody (1:20,000); anti-H^+-ATPase antibody (1:2,500); and anti-FLAG antibody (1:10,000). The anti-serum against LHCSR3 generated following peptide sequence, Cys-VAAEDVFAYTKNLPGVTA. The purified antibody against C-terminus of CAS generated against following peptide sequence, Cys-RTGTTSTRRLPAPRS was used for most of the analyses. The purified antibody against N-terminus of CAS generated against following peptide sequence, Cys-DELDSTVESVVGAVKATG was only used for determining the topology of N-terminus of CAS. The antibody against D1 (Cat No. AS05084A), and H^+-ATPase (plasma membrane-localized P2-type proton transporting ATPase (PMH1)) (Cat No. AS07260) were commercial products purchased from Agrisera. For probing the primary antibody, a horseradish peroxidase (HRP)-conjugated goat anti-rabbit IgG antibody to detect described proteins other than FLAG, or goat anti-mouse IgG antibody to detect FLAG was used as a secondary antibody in dilution of 1:10,000.

RNA-sequencing assay

Total RNA was first extracted from cells cultured under HC, LC-0.3 h or LC-2 h conditions, using RNeasy Plant Mini Kit (QIAGEN) according to manufacturer's protocol. Each mRNA was obtained from 10 μg of the total RNA using Dynabeads Oligo(dT)25 (Life technologies). The complementary DNA (cDNA) libraries were prepared using NEBNext mRNA library prep kit for Illumina (NEB), as described in previous report (Fujiwara et al., 2015). Sequencing was performed on HiSeq 2500 system (Table 3). The resulting reads were aligned to v5.5 of the C. reinhardtii genome annotation, downloaded from Joint Genome Institute (https://phytozome.jgi.doe.gov/pz/portal.html). Alignments were performed using Tophat program following previous report (Trapnell et al., 2012). The FPKM (Fragments Per Kilobase of

Table 3. Summary of RNA-seq samples and sequence alignment.

Sample	Sequencer	Read length (bp)	Total number of clean bases (Gb)	Total number of clean reads	Reads with paired-end alignments to 1 output stream(s)	Percentage of total reads (%)
WT-HC-1	Illumina HiSeq™ 2500	100	8.35	47,265,130	27,609,316	58.41
WT-HC-2	Illumina HiSeq™ 2500	100	8.21	45,637,471	29,885,519	65.48
WT-LC-20min-1	Illumina HiSeq™ 2500	100	9.68	58,266,403	23,808,590	40.86
WT-LC-20min-2	Illumina HiSeq™ 2500	100	8.32	46,300,307	29,881,377	64.54
WT-LC-2h-1	Illumina HiSeq™ 2500	100	8.57	47,940,877	31,067,123	64.80
WT-LC-2h-2	Illumina HiSeq™ 2500	100	10.01	57,546,663	29,885,519	51.93
H82-HC-1	Illumina HiSeq™ 2500	100	8.34	46,983,516	30,403,878	64.71
H82-HC-2	Illumina HiSeq™ 2500	100	7.59	42,574,570	27,063,569	63.57
H82-LC-20min-1	Illumina HiSeq™ 2500	100	9.50	53,019,310	34,222,317	64.55
H82-LC-20min-2	Illumina HiSeq™ 2500	100	10.35	57,397,611	38,222,209	66.59
H82-LC-2h-1	Illumina HiSeq™ 2500	100	7.91	43,967,647	28,932,872	65.80
H82-LC-2h-2	Illumina HiSeq™ 2500	100	6.79	37,781,602	24,637,228	65.21
C1-HC-1	Illumina HiSeq™ 2500	100	6.42	38,382,258	16,394,246	42.71
C1-HC-2	Illumina HiSeq™ 2500	100	7.16	40,414,944	25,098,869	62.10
C1-LC-20min-1	Illumina HiSeq™ 2500	100	6.71	37,685,632	23,073,042	61.23
C1-LC-20min-2	Illumina HiSeq™ 2500	100	7.40	40,831,129	27,740,665	67.94
C1-LC-2h-1	Illumina HiSeq™ 2500	100	8.32	47,822,947	29,906,711	62.54
C1-LC-2h-2	Illumina HiSeq™ 2500	100	8.45	46,527,856	29,890,701	64.24

Sequencing details and alignment summary are provided for each individual sample lane.

In each condition, sequencing data were obtained from two biological replicates.

exon per Million mapped fragments) values were calculated using the Cufflinks program, and the differentially expressed transcripts were identified using the Cuffdiff program.

Quantitative real-time PCR

Total RNA was extracted from cells grown under HC or LC conditions using an RNeasy Plant Mini Kit (QIAGEN) and any remaining genomic DNA was digested with DNase (QIAGEN) in accordance with the manufacturer's instructions. First strand cDNA was synthesized using Superscript III Reverse Transcriptase (Life Technology, Carlsbad, CA, USA). Quantitative real-time PCR was performed using SYBR Premix Ex Taq GC (TAKARA BIO) and a LightCycler 480 Instrument (Roche, Mannheim, Germany) following the manufacturer's instructions. *CBLP* encoding a Chlamydomonas Beta Subunit – Like Polypeptide was used as an internal control. The primers used were HLA3-F/R and CBLP-F/R (Table 2). The amplification conditions were as follows: 5 min denaturation at 95°C; 40 cycles at 95°C for 10 s, at 55°C for 30 s and at 68°C for 1 min. Melting curves for each PCR product were determined by measuring the decrease in fluorescence with increasing temperature from 60 to 95°C.

Plasmid construction

To generate the expression plasmid for *CAS* fused with FLAG sequence with its own promoter, two genomic fragments were amplified by primer set FLAG-CAS-F2/R2 for promoter and transit peptide sequence and by FLAG-CAS-F1/R1 for the remaining sequence of *CAS* (Table 2). The FLAG sequence was included in primers FLAG-CAS-F1 and FLAG-CAS-R2. These two fragments were then simultaneously cloned into pBlueScript II SK(+) using an In-Fusion reaction (Clontech, Mountain View, USA). The N-terminal chloroplast transit peptide was determined as amino acids 1-54 of *Cr*CAS, as described previously (Allmer et al., 2006). All PCR reactions were performed using Prime STAR GXL DNA Polymerase (Takara, Japan) and the nucleotide sequence were verified by sequencing. The fragments containing the promoter, tagged *CAS* sequence, and *3'-UTR* were amplified and co-transformed into H82 cells with a paromomycin resistance gene cassette, *aphVIII*. In the case of *Flag-tagged CAS*, the native promoter of the *CAS* gene was used. The nucleotide sequences of primers were listed in Table 2.

Generation of complemented strains expressing tagged CAS protein

Transformed cells were selected by spreading cell suspensions over TAP agar plates containing 10 μg mL^{-1} paromomycin. For screening of complemented strains, the growth rates of each candidate in liquid medium were compared under HC and LC conditions.

Indirect immunofluorescence assay

Cells grown in mid-logarithmic phase were harvested by centrifugation and, the pellet was rinsed with PBS two times. Cell suspensions were spotted onto poly-L-lysine-treated glass slides (Poly-Prep Slides, Sigma) and air-dried for 5 min in 120 μmol photons·m^{-2}·s^{-1} at room temperature. Cells were fixed with 4% (wt/vol) formaldehyde in PBS for 20 min at room temperature, and then incubated in 100% methanol at -30˚C for 20 min to remove the chlorophyll. The methanol was pre-chilled in -30˚C overnight. The immunofluorescence staining was performed as described previously (Yamano et al., 2015). Purified

antibodies against CAS (C-terminus) and LCIB generated in rabbit, and commercial antibody FLAG were used at a dilution of 1: 500, 1:200, 1:500, respectively as primary antibodies. After washing membrane 6 times by PBS-T, Alexa Fluor 488 goat anti-rabbit IgG (Life Technologies) was used in 1:500 dilution to detect CAS and LCIB protein, or Alexa Fluor 488 goat anti-mouse IgG (Abcam) was used in 1:2,000 dilution to detect FLAG as secondary antibodies. Finally, the digital fluorescence and transmission images were acquired using a confocal fluorescence microscopy TCS SP8 (Leica) with a 488-nm laser line and then deconvoluted using Huygens Essential software (Scientific Volume Imaging B.V., Netherlands).

Expression of recombinant protein in *Escherichia coli*

Full-length cDNA of CAS from *Chlamydomonas reinhardtii* or from *Arabidopsis thaliana* was synthesized using Superscript III Reverse Transcriptase (Life Technology). The transmit peptide of *Cr*CAS was determined as described previously (Allmer et al., 2006). The transmit peptide of *At*CAS was predicted using the ChloroP predictor. N-terminus and C-terminus were amplified using specific primers (Table 2), and cloned into *XhoI* sites of pGEX-6p-1 vector using the In-Fusion reaction (Clontech, Mountain view, USA). Recombinant GST-tagged CAS and GST proteins were expressed in E.coli BL21 (DE3) (Life Technologies, Carlsbad, CA) by incubation in the presence of 0.5 mM isopropyl-*β*-D-thiogalactopyranoside (IPTG) with gentle shaking at 20˚C for 6 h. Next, the recombinant proteins were extracted, loaded on the GSTrap FF columns (GE Healthcare), cleaved on-column with PreScission Protease (GE Healthcare) for 24 h, and harvested following manufacture's instructions. Protein concentrations were measured using a protein assay kit (Bio-Rad) by plotting on standard curve of bovine serum albumin (BSA).

Blue Native-PAGE

Cells corresponding to the amount of 200 µg chlorophyll were suspended in 200 µL PBS in presence of EDTA-free protease inhibitor (Roche), and disrupted using Handy Sonic (Tomy) on ice. The disrupted sample was incubated with 0.5% (vol/vol) n-Dodecyl-β-D-maltoside (DDM, Dojindo) in loading buffer [0.5% (wt/vol) CBB G-250, 50 mM 6-aminocaproic acid, 10 mM Bis-Tris/HCl (pH 7.0), 10 mM PMSF, and 10% (vol/vol) glycerol]. After incubation on ice for 30 min, the sample was centrifuged at 20,000 g for 10 min and the supernatant was loaded on the NativePAGE Novex 4-16% Bis-Tris gel (Invitrogen) following the manufacture's instructions. NativeMarker Unstained Protein Standard (Invitrogen) was used as a size marker. After electrophoresis, transferred membrane was incubated in denature buffer containing 50 mM Tris-HCl (pH 7.4), 2% (wt/vol) SDS, 0.8% (vol/vol) mercaptoethnaol at 50˚C for 30 min. Rinsed membrane with deionized water two times was subjected to immunoblotting assay using antibody against the C-terminus of CAS.

Calcium-binding assay

Each recombinant protein of 0.42 nmol was separated by 15% SDS-PAGE and transferred onto Fluoro Trans® PVDF (Life Science) membrane by semi-dry blotting system. GST protein was used as negative control. The membranes were washed with buffer containing 5 mM $MgCl_2$, 60 mM KCl, 10 mM MES-KOH (pH 6.5), and then incubated in the same buffer with the addition of $^{45}CaCl_2$ (PerkinElmer, 370 $MBq \cdot mL^{-1}$) to 74 $kBq \cdot mL^{-1}$ for 10 min, and rinsed in 50% (vol/vol) ethanol for 5 min, as descried preciously (Maruyama et al., 1984). The protein-bound ^{45}Ca was exposed to the Imaging plate (Fuji) for 24 h and visualized by autoradiography.

Subcellular fractionation

HC- or LC- grown C-9 cells for 12 h were harvested by centrifugation at 600 g for 5 min. Suspended in PBS with protease inhibitor (EDTA-free, Cocktail, Roche, Germany), cells were disrupted by sonication and centrifuged at 2,000 g for 5 min at 4˚C. The supernatants were transferred to a new tube without disturbing the debris and centrifuged at 60,000 g for 1 h at 4˚C to obtain soluble (supernatant) and insoluble fractions (pellet).

For isolation of thylakoid membranes in small-scale, 100 mL C-9 cells were cultured in HC or LC conditions for 12 h, harvested by centrifugation at 600 g for 5 min at room temperature. After washed by fresh liquid HSM and solution 1 (0.3 M sucrose, 1 mM $MgCl_2$, 25 mM HEPES-NaOH, pH 7.5), the pellet was suspended in 100 μL solution 1 in 2.0 mL tube. Next, cells were disrupted by vortexing with 800 mg of Zirconia/Silica beads (0.5 mm diameter; BioSpec Products) for 5 min and transferred to 1.5 mL tube. To remove unbroken cells and chloroplasts, the cell samples were centrifuged at 760 g for 2 min at 4 ˚C. Then, supernatant was pelleted at 5,000 g for 20 min at 4 ˚C. After washed using 1.5 mL solution 2 (0.3 M sucrose, 10 mM EDTA, 5 mM HEPES-NaOH, pH 7.5), the pellet was suspended in 1.25 mL solution 3 (1.8 M sucrose, 10 mM EDTA, 25 mM HEPES-NaOH, pH 7.5). Then, the suspension was transferred to Ultra-Clear centrifuge tube (13×51 mm, BECKMAN COULTER) and overlaid with 0.5 mL solution 4 (1.3 mM sucrose, 10 mM EDTA, 5 mM HEPES-NaOH, pH 7.5) and 1.25 mL solution 5 (0.5 mM sucrose, 10 mM EDTA, 5 mM HEPES-NaOH, pH 7.5) for discontinuous sucrose gradient centrifugation at 208,000 g for 15 min at 4˚C using Optima TLX ultracentrifuge (BECKMAN COULTER). The green band in the 1.3-M sucrose layer was collected in a new 1.5 mL tube, diluted with solution 6 (10 mM EDTA, 5 mM HEPES-NaOH, pH 7.5), and pelleted by centrifugation at 5,000 g for 30 min at 4˚C. The pellet was then resuspended in solution 6 at 0.8 mg $Chl^{-1} \cdot mL^{-1}$ for immunoblotting assay.

To isolate the chloroplast envelopes, the intact chloroplast fraction was isolated from 10 L of strain CC-400 cells acclimated to LC conditions according to previous report (Mason et al., 2006). Cells was harvested by centrifugation at 3,000 g for 10 min at 4˚C, and washed with 100 mL 50 mM HEPES-KOH pH 7.5. After pelleting by centrifugation at 3,000 g for 5 min at 4˚C, the pellet was resuspended in appropriate volume of 50 mM HEPES-KOH pH 7.5 to adjust the chlorophyll amount to 1 mg. Immediately before disrupting cells by passing through 27-gauge needle of syringe, dilute aliquots

containing 0.3 mg of chlorophyll per mL by adding 6 mL isolation buffer (300 mM sorbitol, 50 mM HEPES-KOH (pH7.5), 2 mM Na-EDTA (pH8.0), 1 mM $MgCl_2$, 1% (wt/vol) BSA). Then, the whole cells, crude chloroplast and thylakoid was collected by centrifugation at 750 g for 2 min at 4˚C, and gently suspended by 2 mL isolation buffer. By Percoll gradient centrifugation at 4,200 g for 15 min in 15 mL BD Falcon tube, thylakoid fraction and intact chloroplast fraction were obtained from 20-45% (vol/vol) and 45-65% (vol/vol) interfaces, respectively. The chloroplast fraction was diluted by 50 mL isolation buffer and collected by centrifugation at 750 g for 2 min at 4˚C. The pellet was then suspended in 0.6 M sucrose buffer (0.6 M sucrose, 10 mM Tris-HCl (pH 7.4), 1 mM EDTA). Aliquots of 1 mL suspension sample were frozen in -20˚C for 1 h, and then melted in 37˚C for 5 min (4 times). Then, the homogenate by PELLET PESTLE was mixed with 1.8 M sucrose buffer (1.8 M sucrose, 10 mM Tris-HCl (pH 7.4), 1 mM EDTA) to adjust the sucrose concentration to 1.3 M, and transferred to Ultra-Clear centrifuge tube (13 ×51 mm, BECKMAN COULTER). The 1.3 mL of 1.2 M sucrose buffer (1.2 M sucrose, 10 mM Tris-HCl (pH 7.4), 1 mM EDTA) and 0.3 M sucrose buffer (0.3 M sucrose, 10 mM Tris-HCl (pH 7.4), 1 mM EDTA) was overlaid successively for discontinuous gradient centrifugation at 113,000 g, 2 h, 4˚C. The yellow band was collected, diluted by buffer (10 mM sucrose, 1 mM EDTA), and pelleted by centrifugation at 113,000 g, 1 h, at 4˚C. The pellet was suspended by addition of PBS with protease inhibitor (EDTA-free, Cocktail, Roche, Germany), and subjected to immunoblotting assay.

Isolation of thylakoids and protease treatment

The fraction from 20-45% (vol/vol) of Percoll gradient centrifugation was used for the isolation of thylakoids for determining the topology of CAS. The isolation of thylakoid membranes by discontinuous sucrose gradient centrifugation was performed as describe in subcellular fractionation.

Thylakoid fraction (0.05 mg chlorophyll mL^{-1}) was suspended in the reaction buffer containing trypsin (Sigma) with indicated concentrations, and incubated on ice for 30 min. Proteolysis was stopped by adding SDS loading buffer and heat it at 100˚C for 5 min. The samples were analyzed after denaturing gel electrophoresis and immunoblotting, and then probed by the antibodies against the N-terminus of CAS, C-terminus of CAS, or CAH3.

Fluorescence distribution of calcium indicator

HC- or LC-acclimated cells were collected at 600 g for 5 min, and washed one time using fresh Ca^{2+}-free HSM (without MOPS and Hutner's trace elements). Then cells were adjust to 1×10^7 cells mL^{-1}, and incubated in Ca^{2+}-free HSM medium with 1 mM EGTA, 15 μM Calcium Green-1, AM, and 0.02% (wt/vol) pluronic F-127 at room temperature in 10–20 μmol photons$\cdot m^{-2}\cdot s^{-1}$ light for 30 min. The addition of EGTA is to minimize the interference coming from the binding of free Ca^{2+} to the extracellular hydrolyzed Ca^{2+} indicator, as described previously (Lam et al., 2005). The Calcium Green-1, AM signal was generated by excitation at 488 nm and emission between 500-550 nm. The digital fluorescence and transmission images were acquired using a confocal fluorescence microscopy TCS SP8 (Leica).

Measurement of Ci concentration in the culture medium

Cells were removed from the supernatant by centrifuged at 1000 g for 5 min. Then, 20 μL of the supernatant was injected into the gas-stripping column of the gas chromatograph (GC) through a glass hypodermic needle. Ci concentration was measured using gas chromatograph (GC-8A; Shimadzu) equipped with a methanizer (MTN-1; Shimadzu) following the manufacture' s instruction.

Spectroscopic analysis

Light-induced absorption changes at 705 nm were measured using a JTS-10 spectrophotometer (BioLogic, France) as previously described (Alric et al., 2010). HC- or LC- grown cells in 120 photons·m^{-2}·s^{-1} were pelleted at 15,000 g for 2 min at room temperature, resuspended in HSM (10 μg chlorophyll mL^{-1}), and were mixed with the same volume of HSM containing 20% (wt/vol) Ficoll. Actinic light intensity was 82 photons·m^{-2}·s^{-1}. Measuring pulse duration was 10 μs.

Results

1. Isolation and characterization of high-CO_2-requiring mutants

1.1 Isolation of high-CO_2-requiring mutants of *C. reinhardtii* by DNA-tagging

In order to obtain HC-requiring mutants, approximately 25,380 transformants (9,964 for hyg and 15,416 for par resistance) was generated by transforming WT cells with *aphVII* or *aphVIII* cassettes (Fig. 10). For the first screening, the growth rates of cells grown in HC and LC chambers were compared by measuring the OD_{700} value of each transformant. Of these, 655 transformants showing retarded growth rates in LC conditions were selected as candidates of HC-requiring mutants. For the second screening, these candidates were spotted onto high-salt medium supplemented with 20 mM MOPS (HSM) agar plates for testing their growth rate in HC or LC conditions. Eventually, three mutants designated as H24, H82, and P103, displayed significantly retarded growth in LC conditions (Fig. 11), although the WT cells could grow well in LC conditions as well as HC conditions.

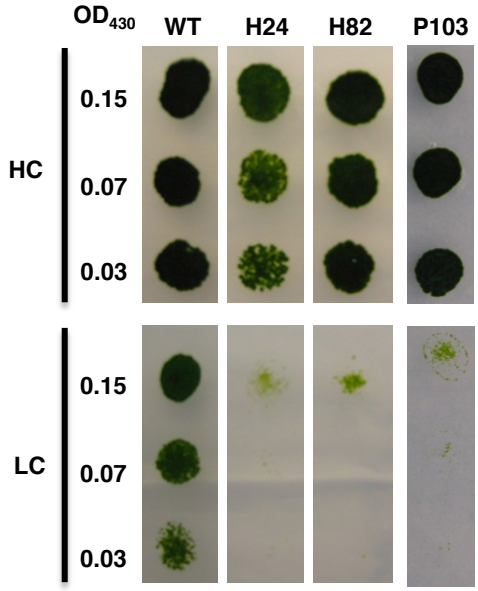

Figure 11. Spot test of wild-type (WT) and high-CO_2 (HC)-requiring mutants H24, H82, and P103. Cells grown to logarithmic phase were diluted to the indicated optical density at 430 nm (OD_{430}=0.15, 0.07, or 0.03). Then 3 µL of each cell suspension was spotted on HSM plates and incubated for 9 days in growth chambers supplied with HC or low-CO_2 (LC) in continuous light at 120 µmol photons·m^{-2}·s^{-1}.

1.2 Photosynthetic characteristics of the high-CO_2-requiring mutants

To carry out a preliminary evaluation of the photosynthetic characteristics of these three mutants, the photosynthetic affinities for Ci were evaluated by measuring the rates of photosynthetic O_2-evolution against dissolved Ci concentrations in cells grown in 80 μmol photons·m^{-2}·s^{-1} light. As a control, HC-requiring mutant, strain C16 with an insertion mutation in *CCM1* was used. In LC conditions, the Ci concentration required for half maximal velocity ($K_{0.5}$ (Ci)) of C16, H82, and P103 cells were increased to 482.0, 525.6, and 312.4 μM, respectively, compared with 48.8 μM in WT cells (Fig. 12 and Table 4), indicating that photosynthetic Ci affinity was drastically decreased in these mutants. In contrast, LC-acclimated H24 showed the typical photosynthetic responses of cells with normal CCM induction in the range of 10–100 μM Ci but exhibited approximately 70% of maximal photosynthetic rate at 100 μM Ci (Fig. 12). Although the photosynthetic rate of WT cells reached a maximum at 100 μM Ci and retained its activity, the photosynthetic rate of H24 was attenuated in the range of 100–500 μM Ci. Subsequently, the photosynthetic rate increased again at higher concentrations of Ci, reaching a maximum at 1.5 mM Ci. Although this biphasic response of the photosynthetic curve caused a slight decrease in the $K_{0.5}$ (Ci) value of 50.4 μM, it attenuated photosynthetic activity between 100 and 500 μM Ci, corresponding to LC conditions, could cause the retarded growth of H24 cells.

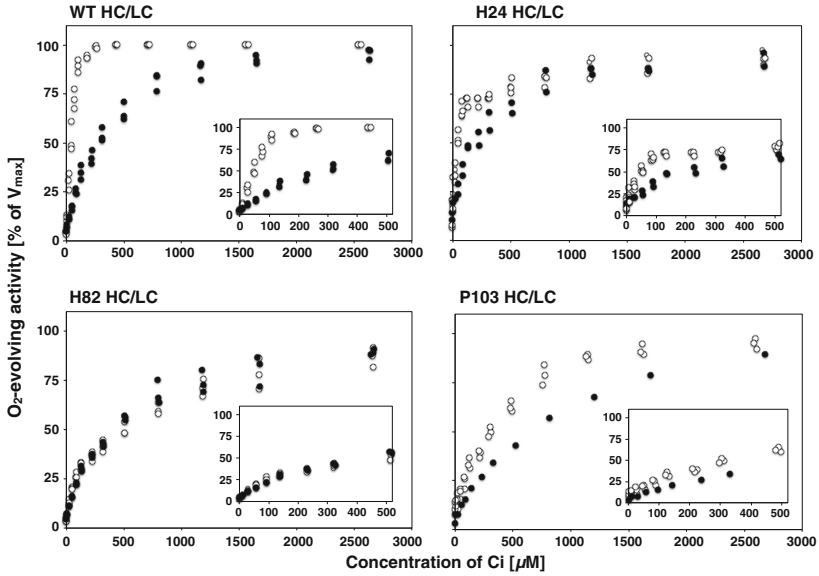

Figure 12. Oxygen-evolving activity of wild-type (WT) and high-CO_2 (HC)-requiring mutants H24, H82, and P103 in response to external dissolved inorganic carbon (Ci) concentration. WT and mutants were grown in HC (closed circles) or low-CO_2 (LC, open circles) conditions for 12 h with continuous light at 80 μmol photons·m^{-2}·s^{-1}. Photosynthetic oxygen-evolution was measured in the presence of various concentrations of $NaHCO_3$. Insets show plots at external dissolved Ci concentration below 500 μmol.

Table 4. Oxygen-evolving activity of wild-type (WT) and mutants cells.

Strain name	Growth conditions	V_{max} of O_2-evolving activity [μmol O_2 mg $Chl^{-1}h^{-1}$]	$K_{0.5}$ (Ci) [μM]
WT	HC	184.7 ± 13.2	298.7 ± 43.3
	LC	197.7 ± 18.7	47.8 ± 5.8
C16	HC	195.3 ± 19.0	675.9 ± 75.9
	LC	245.5 ± 24.0	482.0 ± 27.8
H24	HC	102.6 ± 2.0	149.6 ± 69.2
	LC	92.0 ± 8.5	50.4 ± 9.1
H82	HC	184.6 ± 27.4	425.2 ± 17.5
	LC	179.5 ± 12.3	525.6 ± 75.1
P103	HC	N.D.	N.D.
	LC	168.8 ± 11.1	312.4 ± 9.9

Data are shown ± standard deviation, which were obtained from three independent experiments. V_{max} was obtained in the presence of 10 mmol $NaHCO_3$. Ci, inorganic carbon; HC, high-CO_2; LC, low-CO_2; N.D., not determined; V_{max}, maximum O_2-evolving activity.

Next, to evaluate the Ci uptake activity of these mutants, the light-dependent CO_2 exchange (LCE) activities were measured (Fig. 13). In LC conditions, C16, H24, H82, and P103 showed significantly decreased LCE activities of 19.7 (16.3%), 10.9 (9.1%), 13.5 (11.2%), and 19.7 (16.4%) μmol CO_2 mg Chl^{-1} h^{-1}, respectively, compared with 120.2 μmol CO_2 mg Chl^{-1} h^{-1} of WT cells, suggesting defects in Ci uptake activity in LC conditions.

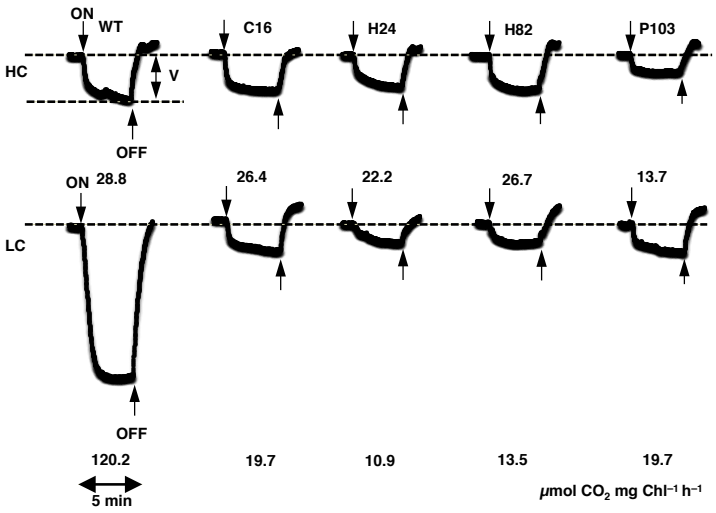

Figure 13. Light-dependent CO_2-exchange (LCE) activity of wild-type (WT) and high-CO_2 (HC)-requiring mutants. Cells were grown in low-CO_2 (LC) conditions for 12 h. The maximum difference in the CO_2 concentrating from the basal level within 5 min, shown as 'V' was defined as the LCE activity. The LCE activities of cells corresponding to 5 μg mL^{-1} of chlorophyll are indicated below the profiles. Arrows indicate when actinic light was turned on and off, respectively.

1.3 Accumulation of CO_2-concentrating mechanism-related proteins in high-CO_2-requiring mutants

It was speculated that the absence of some CCM-related proteins led to the HC-requiring phenotype of the mutants. In order to examine the accumulation profiles of CCM-related proteins in these mutant, soluble or membrane proteins were extracted from WT, C16, H24, H82, and P103 cells grown in HC or LC conditions for 12 h. These protein samples were probed with antibodies against CCM-related proteins, including CCM1, CAH1, CAH3, CAH6, LCI1, HLA3, LCIA, LCIB, and LCIC (Fig. 14).

In the P103 mutant, CCM1 was not detected, and the accumulation profiles of the CCM-related proteins examined were similar to that of C16, suggesting that P103 could be a *CCM1* mutant. By sequencing the genomic region of *CCM1* in P103, a deletion of adenine in the second exon was found (AAAAA in WT and AAAA in P103). This could cause a frame shift, producing a truncated CCM1 with 161 amino acid residues (Fig. 15). In WT cells, CCM1, CAH3, and CAH6 were accumulated constitutively irrespective of the environmental CO_2 conditions. Although CCM1 and CAH6 accumulated normally in H24 and H82 cells, a slight decrease in CAH3 was observed in C16, H24, H82, and P103 cells. Accumulation levels of LCIB and LCIC in H24 and H82 cells were similar to that of WT cells with slight accumulation in HC conditions and induced in LC conditions. In LC-acclimated H24 and H82 cells, accumulation of HLA3 or both HLA3 and LCIA, respectively, was not detected (Fig. 14), which are LC-inducible membrane proteins associated with HCO_3^- transport (Duamnu et al., 2009; Yamano et al., 2015).

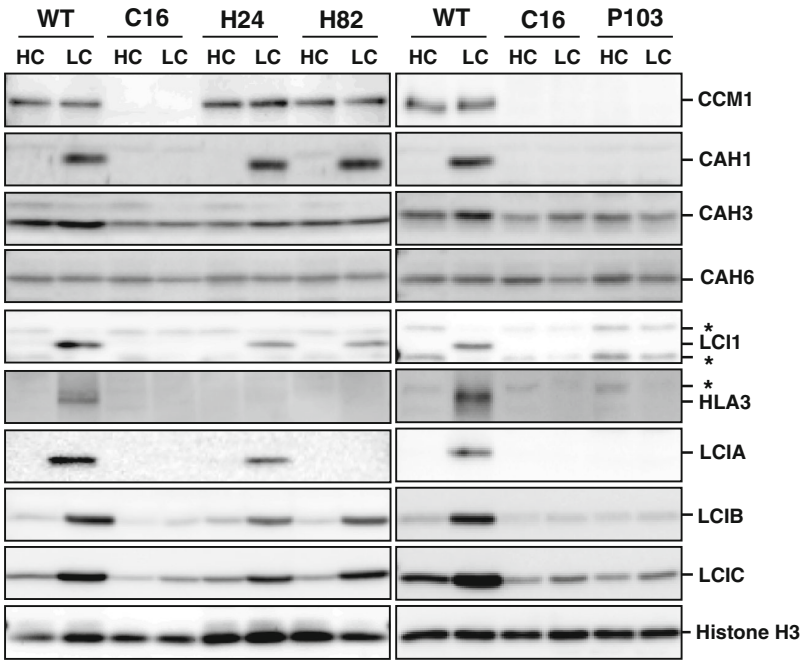

Figure 14. Accumulation of CCM-related proteins. Accumulation of CCM-related proteins in wild-type (WT), C16, H24, H82, and P103 cells was analyzed by immunoblotting analysis. Cells were grown in high-CO_2 (HC) conditions for 12 h and then shifted to HC or low-CO_2 (LC) conditions for 12 h. Histone H3 was used as a loading control. Asterisks indicate the nonspecific protein bands.

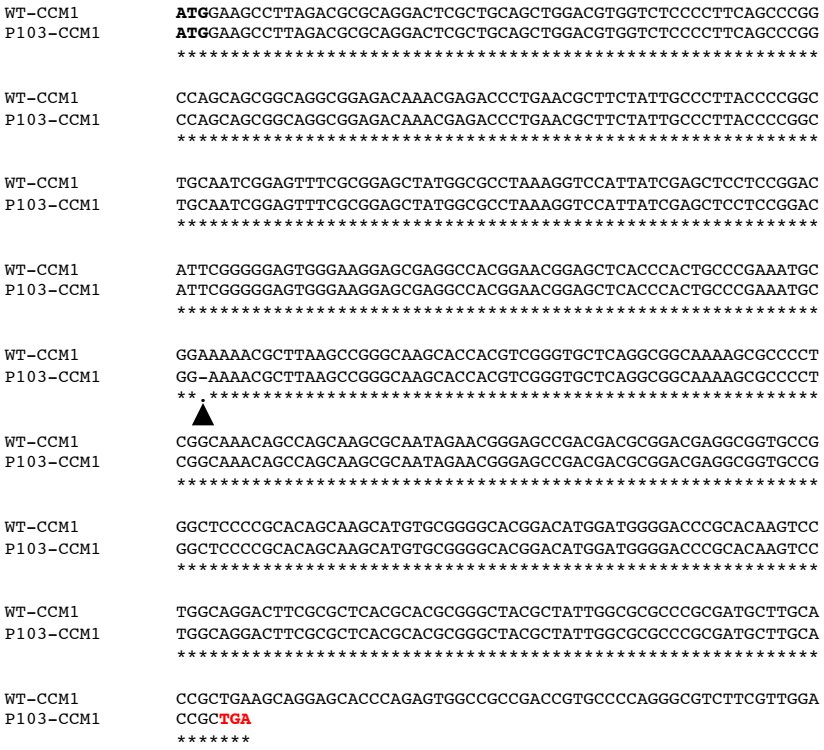

Figure 15. Alignment of *CCM1* exons between wild-type (WT) and P103 cells. The PCR-amplified *CCM1* gene in P103 mutant was sequenced. Its coding DNA sequence was compared with that of WT. The black triangle indicates the mutation site. The start codon is marked with bold letter. The stop codon is marked in red.

1.4 Insertion site of the hygromycin resistance gene cassettes in high-CO_2-requiring mutants

To determine the flanking regions of the *aphVII* cassette in the genome of these mutants, TAIL-PCR was performed. Both upstream and downstream sequences adjacent to the insertion sites were amplified and sequenced using UP primers targeted to the promoter region or DP primers targeted to the 3'-UTR of the *aphVII* cassette and degenerate primers, respectively. The alignment of the obtained nucleotide sequences from the genomic DNA of H82 to the *C. reinhardtii* genomic sequence database Phytozome v.9.1 yielded a match to locus *Cre12.g497300* encoding a Ca^{2+}-sensing receptor, named CAS (Fig. 16A). Specifically, the obtained sequence from the UP side matched a sequence in the fourth intron and that from the DP side matched a sequence in the fifth exon, correlating with a deletion of 92-bp in the *CAS* gene. Furthermore, this *aphVII* insertion was also determined by PCR using primer sets of F1/UP-S, DP-S/R1, and DP-S/R2. A fragment of 365-bp was amplified from the genomic DNA of WT cells, but a fragment with size of 7-kb was amplified from the genomic DNA of H82 using F1/R1 primers targeting the fourth intron and fifth exon, thereby confirming the *aphVII* insertion in *CAS* gene (Fig. 16B). Because the length of the *aphVII* cassette was 1,999 bp, 3.3 copies of *aphVII* cassette could be tandemly inserted into the *CAS* gene.

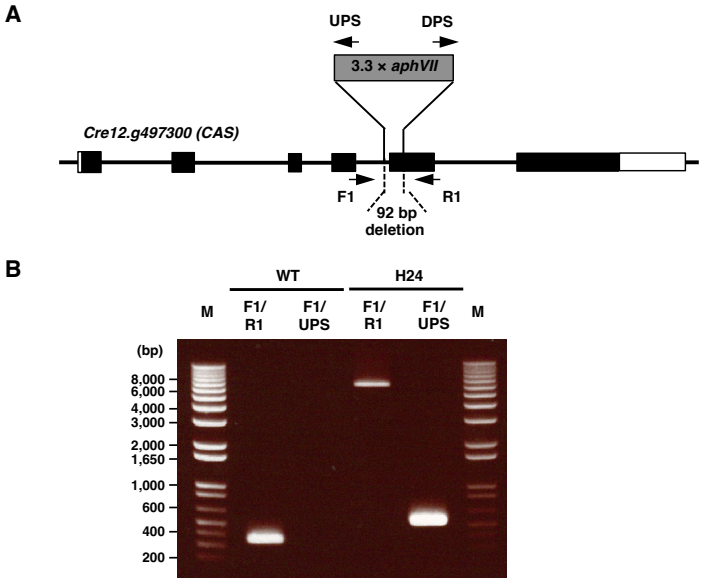

Figure 16. Molecular characterization of the H82 mutant. (A) Schematic representation of the *aphVII* insertion into the genome of the H82 mutant. The *UTR*, exon, and *aphVII* are shown as white, black, and gray boxes, respectively. (B) Confirmation of *aphVII* insertion by genomic PCR. Genomic PCR was performed using the primer sets depicted in (A). WT, wild-type; bp, base pair; M, marker.

In contrast, the hyg resistance gene cassette in H24 was inserted in the tenth exon of an ubiquitin carboxyl-terminal hydrolase (*UCH*) gene (Fig. 17A). A fragment of 0.7-kb was amplified from the genomic DNA of WT cells but a fragment of 4.2-kb was amplified from the genomic DNA of H24 using F2/R2 primers targeting to the tenth exon (Fig. 17B), suggesting that 1.8 copies of the *aphVII* cassette could be tandemly inserted into *UCH* gene.

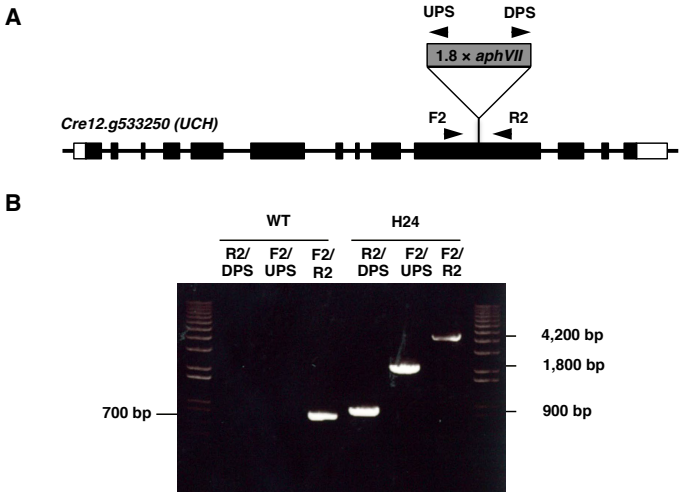

Figure 17. Molecular characterization of the H24 mutant. (A) Schematic representation of the *aphVII* insertion into the genome of the H24 mutant. The *UTR*, exon, and *aphVII* are shown as white, black, and gray boxes, respectively. (B) Confirmation of *aphVII* insertion by genomic PCR. Genomic PCR was performed using the primer sets depicted in (A). WT, wild-type; bp, base pair; M, marker.

1.5 Tetrad analysis in high-CO_2-requiring mutants

In order to evaluate a genetic link between the HC-requiring phenotype and insertion of the hyg resistance cassette, H82 or H24 cells were cross-mated with WT strain CC-125 or CC-1690. In total, 48 progenies generated from 12 complete tetrads (A–L from H82 × CC-125 in Fig. 18) were obtained, and the linkage between the HC-requiring phenotype and hyg resistance was analyzed. All progenies exhibiting the HC-requiring phenotype possessed hyg resistance and an *aphVII* insertion detected by PCR, suggesting that the HC-requiring phenotype in H82 cells was closely linked with the insertion of the hyg resistance gene cassette in the *CAS* gene. In contrast, in 8 progenies of 2 complete tetrads from H24 × CC-1690, 50% of progenies showing retarded growth in LC conditions failed to survive in the presence of hyg (Fig. 19).

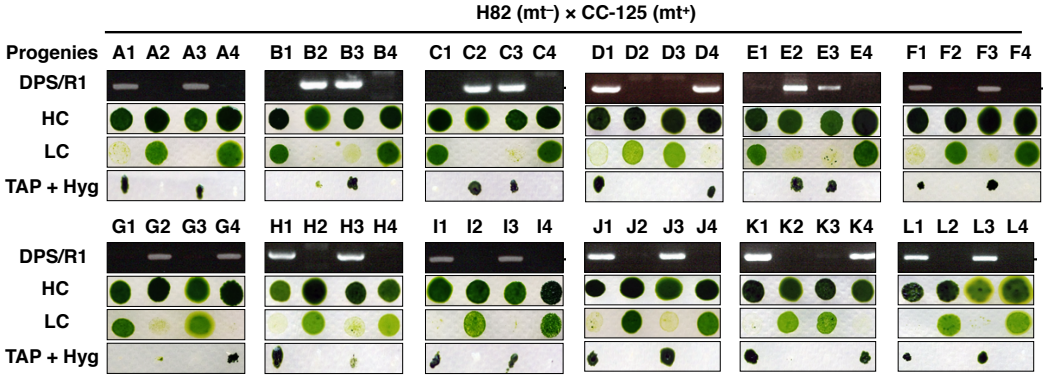

Figure 18. Tetrad analysis of the H82 mutant. Genetic linkage of the hygromycin (hyg) insertion, hyg resistance, and high-CO_2 (HC)-requiring phenotype. Genomic DNA was extracted from tetrad progenies (A–L), obtained from crosses of H82 (mt^-) and CC-125 (mt^+) strains. Genomic PCR was performed with primer sets depicted in Figure 16A. LC, low-CO_2.

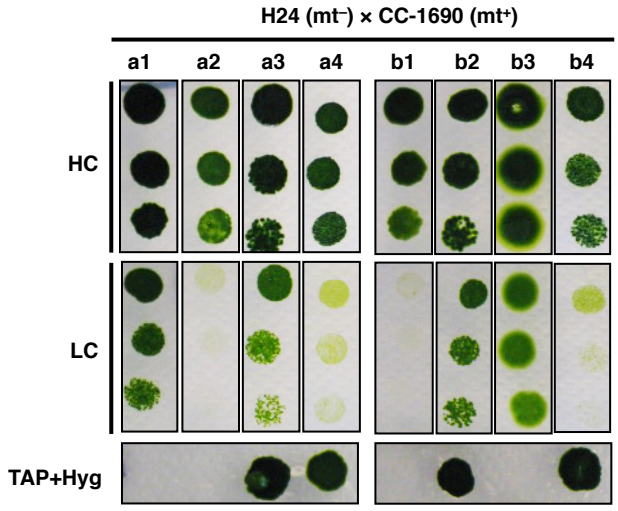

Figure 19. Tetrad analysis of the H24 mutant. Genetic separation of the high-CO_2 (HC)-requiring phenotype and hyg resistance. Tetrad progenies (a and b sets) were obtained from crosses of H24 (mt^-) and CC-1690 (mt^+) strains. LC, low-CO_2.

2. Photosynthetic characteristics of complemented strains of the *CAS* insertion mutant

2.1 Complementation in growth rate of H82 by introduction of the *CAS* gene

In order to examine whether the disruption of *CAS* by insertion of the hyg-resistance gene cassette is responsible for the phenotype of H82, an 8.2-kb PCR-amplified genomic DNA fragment containing the WT *CAS* gene with its own predicted promoter was co-transformed into H82 cells with a par-resistance gene cassette, *aphVIII* (Fig. 20A). From 774 par-resistant transformants, two strains showing similar growth rates to that of WT cells in liquid medium in LC conditions were isolated and designated as C-1 and C-2 (Fig. 20B). In liquid culture, the respective doubling times of 7.6 h and 7.8 h of C-1 and C-2 were shorter than the 13.0 h of H82 in LC conditions, indicating that the slower growth rate in H82 was caused by the *CAS* mutation. Furthermore, the addition of excess Ca^{2+} (3.06 mM) did not restore the growth rate caused by the loss of CAS in H82 cells.

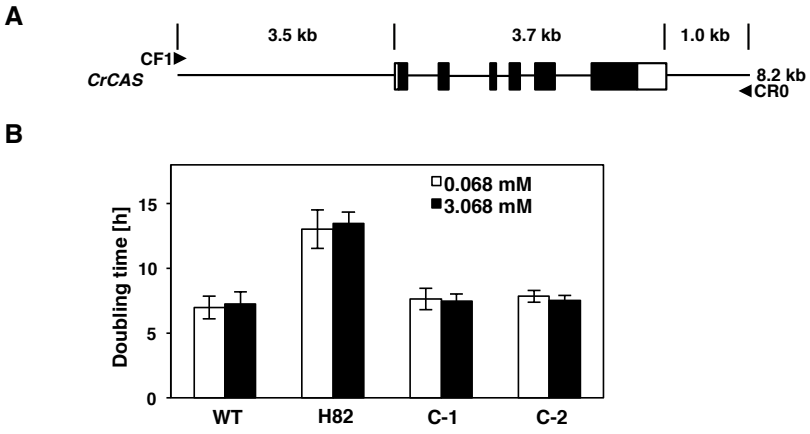

Figure 20. The growth rate of H82 and its complemented strains. (A) Schematic representation of the fragment introduced into H82 cells for complementation. The solid rectangles indicate the exons of the *CAS* gene. The open rectangles represent the 5'-UTR (left) and 3'-UTR (right). This fragment was amplified using primers CF1 and CR0. (B) The doubling time of wild-type (WT), H82, and its complemented strains (C-1 and C-2) in low-CO_2 (LC) conditions at pH 7.0.The optical density at 730 nm was measured at four time-points (0, 12, 24, and 36 h) for calculating the doubling time.

2.2 The defects in growth rate of H82 cells is partially rescued in dim light

It was reported that induction of the CCM is dependent on limiting-CO_2 conditions as well as on light intensity (Yamano et al., 2008). To examine whether the HC-requiring phenotype of the *CAS* insertion mutant H82 was dependent on light intensity, the growth rate was measured on agar plates at different light intensities (Fig. 21A). At pH 7.0, when exposed to LC conditions and dim light (10 μmol photons·m^{-2}·s^{-1}), H82 cells showed a slower growth rate than complemented strains (C-1 and C-2), but the growth rate of H82 cells in dim light was increased, compared with that of it in either mild light (120 μmol photons·m^{-2}·s^{-1}) or strong light (300 μmol photons·m^{-2}·s^{-1}) conditions. As a control, the growth rate of a *PGRL1* mutant (L-1) was equivalent to that of its complemented strain (L-1C) in dim light but reduced in mild light and strong light conditions, supporting a previous report that a *PGRL1* insertion mutant

exhibited a light-dependent HC-requiring phenotype in spots tests (Dang et al., 2014). These results indicated that light intensity had an effect on the HC-requiring phenotype of H82 cells, and they were more sensitive to CO_2-limiting stress than the L-1 strain in dim light. In HC conditions, L-1 cells showed obviously retarded growth compared with L-1C cells in strong light, in which H82 cells showed a similar growth rate to that of C-1 and C-2 cells. These results indicated that L-1 cells were more sensitive to high-light stress than H82 cells.

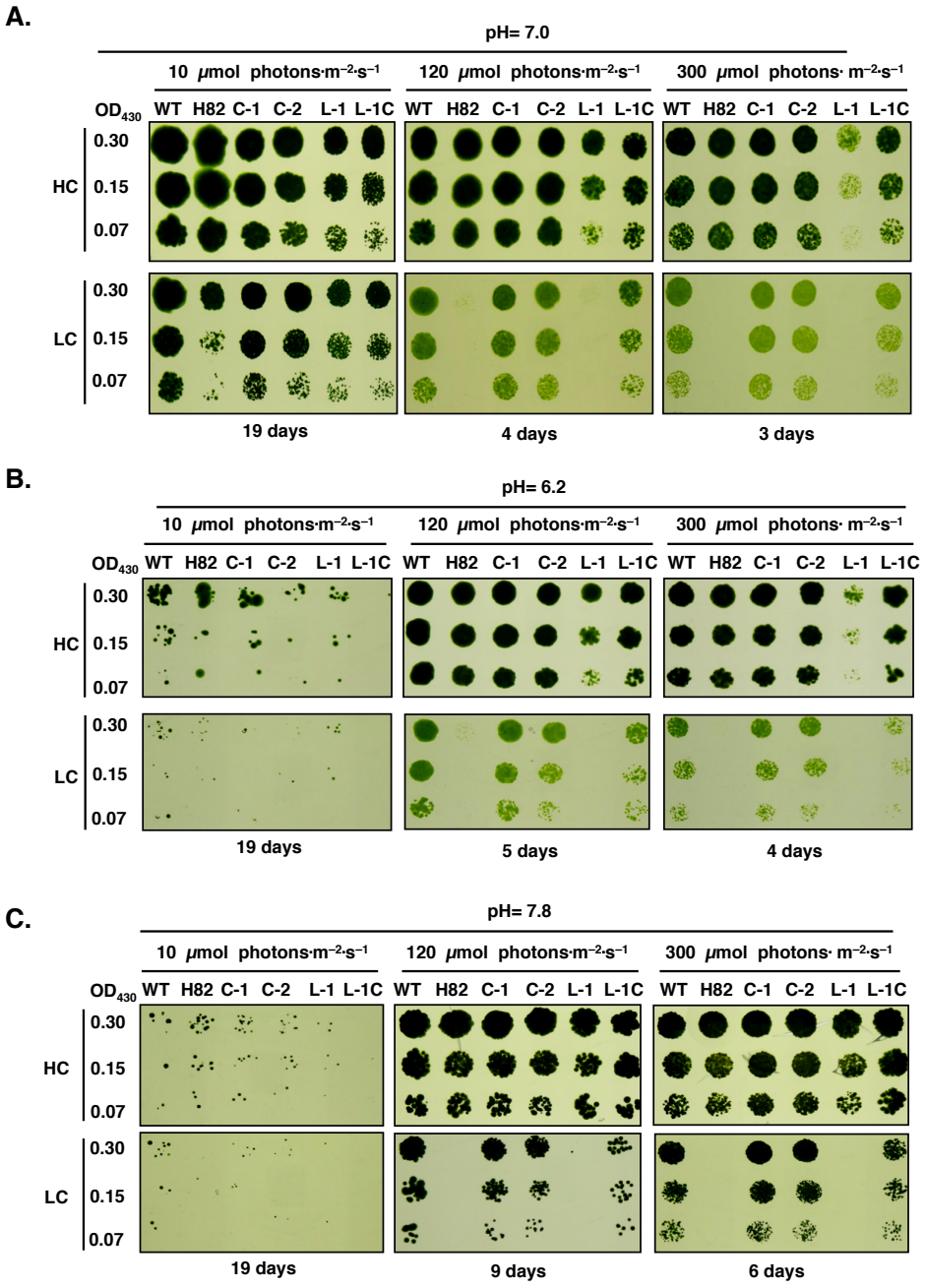

Figure 21. Spot test of wild-type (WT), H82, *pgrl1* mutant (L-1), and their respective complemented strains grown in high-CO_2 (HC) and low-CO_2 (LC) conditions. Cells grown to logarithmic phase were diluted to the indicated optical density (OD_{430}=0.3, 0.15, or 0.07). Then, 3 μl of each cell suspension was spotted onto HSM agar plates with different pHs (7.0 (A), 6.2 (B), and 7.8 (C)) and incubated in HC or LC chambers with indicated light intensity for the indicated periods.

Even at pH 6.2 and pH 7.8, H82 cells showed an HC-requiring phenotype in both mild light and strong light conditions (Fig. 21B and C). In dim light, the growth of all strains was significantly attenuated, possibly because that cells suffered enhanced damage from acidic or alkali stress in dim light, compared with that in mild light or strong light. In contrast, although the L-1 strain also exhibited severely retarded growth in LC conditions at both pH 6.2 and pH 7.8, the defects in growth of L-1 cells caused by strong light in HC conditions was clearly rescued at pH 7.8 (Fig. 21C).

2.3 Restored photosynthetic characteristics in complemented strains of H82

To evaluate induction of the CCM in LC conditions, photosynthetic affinities for Ci were evaluated by measuring the rates of photosynthetic O_2-evolution of WT, H82, and its complemented strains (C-1, and C-2). At pH 7.8 (ratio of HCO_3^-:CO_2 =28:1), the Ci concentration required for half maximal velocity ($K_{0.5}$ (Ci)) in C-1 and C-2 cells was 58 ± 8 μM and 59 ± 6 μM, respectively, which was similar to that of 50 ± 8 μM in WT cells and approximately 19 times lower than that of 1,087 ± 113 μM in H82 cells (Table 5 and Fig. 22A).

Table 5. Photosynthetic parameters of wild-type (WT) and transformant cells.

pH	Strain name	Growth conditions	V_{max} of O_2-evolving activity [μmol O_2 mg Chl^{-1} h^{-1}]	$K_{0.5}$ (Ci) [μM]
6.2	WT	LC-NH_4^+ for 12 h	296 ± 16	28 ± 3
	H82	LC-NH_4^+ for 12 h	253 ± 32	167 ± 13
	C-1	LC-NH_4^+ for 12 h	300 ± 23	25 ± 4
	C-2	LC-NH_4^+ for 12 h	303 ± 26	25 ± 2
7.0	WT	LC-NH_4^+ for 12 h	230 ± 22	31 ± 3
	H82	LC-NH_4^+ for 12 h	214 ± 11	618 ± 84
	C-1	LC-NH_4^+ for 12 h	228 ± 22	34 ± 2
	C-2	LC-NH_4^+ for 12 h	227 ± 9	32 ± 1
7.8		HC-NH_4^+	248 ± 6	235 ± 12
		LC-NH_4^+ for 2 h	235 ± 2	72 ± 9
		LC-NH_4^+ for 2 h, 0.5 mM BAPTA	222 ± 9	144 ± 14
		LC-NH_4^+ for 2 h, 0.5 mM BAPTA and 0.75 mM $CaCl_2$	240 ± 5	63 ± 12
	WT	LC-NH_4^+ for 2 h, 0.1% DMSO (Mock)	253 ± 15	59 ± 18
		LC-NH_4^+ for 2 h, 50 μM W-7	168 ± 18	157 ± 22
		LC-NH_4^+ for 2 h, 75 μM W-7	152 ± 21	235 ± 48
		LC-NH_4^+ for 2 h, 50 μM W-5	235 ± 2	52 ± 6
		LC-NH_4^+ for 2 h, 75 μM W-5	236 ± 17	57 ± 13
		LC-NH_4^+ for 12 h	233 ± 24	50 ± 8
		LC-NO_3^- for 12 h	197 ± 5	44 ± 16
	H82	LC-NH_4^+ for 12 h	217 ± 24	1,087 ± 113
		LC-NO_3^- for 12 h	249 ± 17	793 ± 91
	C-1	LC-NH_4^+ for 12 h	239 ± 29	58 ± 8
		LC-NO_3^- for 12 h	205 ± 11	35 ± 7
	AH-1	LC-NH_4^+ for 12 h	207 ± 19	1,008 ± 70
		LC-NO_3^- for 12 h	207 ± 11	430 ± 66
	C-2	LC-NH_4^+ for 12 h	231 ± 21	59 ± 5
	FN-1	LC-NH_4^+ for 12 h	233 ± 4	53 ± 4

The data are shown ± standard deviation, which were obtained from three independent experiments.
HC, high-CO_2 (aerated with 5.0%); $K_{0.5}$ (Ci), Ci concentration required for half maximal velocity; LC, low-CO_2 (aerated with 0.04%); V_{max}, maximum rate of photosynthesis; WT, wild-type; BAPTA, 1,2-bis (*o*-aminophenoxy) ethane-N, N, N, N'-tetraacetic acid.

Even at pH 6.2 (HCO_3^-: CO_2=0.7:1) and pH 7.0 (HCO_3^-: CO_2=4.3:1), the respective $K_{0.5}$ (Ci) values of the complemented strains were approximately 6.0-fold and 19.0-fold lower than that of H82 cells (Table 5 and Fig. 22B). Because the maximum rates of photosynthesis (V_{max}) of the these strains were similar to each other in each pH condition (Table 5), the decreased Ci affinity in H82 cells could be partly explained by a defect in Ci uptake activity. The accumulation and fixation of [^{14}C]-labeled Ci in H82 cells was 0.13 mM and 0.34 nmol per μL sorbitol impermeable space (SIS) after 80 s of illumination, respectively, which was lower than 0.22 mM and 1.34 nmol μL SIS^{-1} of C-1 cells (Fig. 22C and D). Correspondingly, the photosynthetic LCE activities in C-1 and C-2 cells were recovered to similar levels of that in WT cells (Fig. 22E).

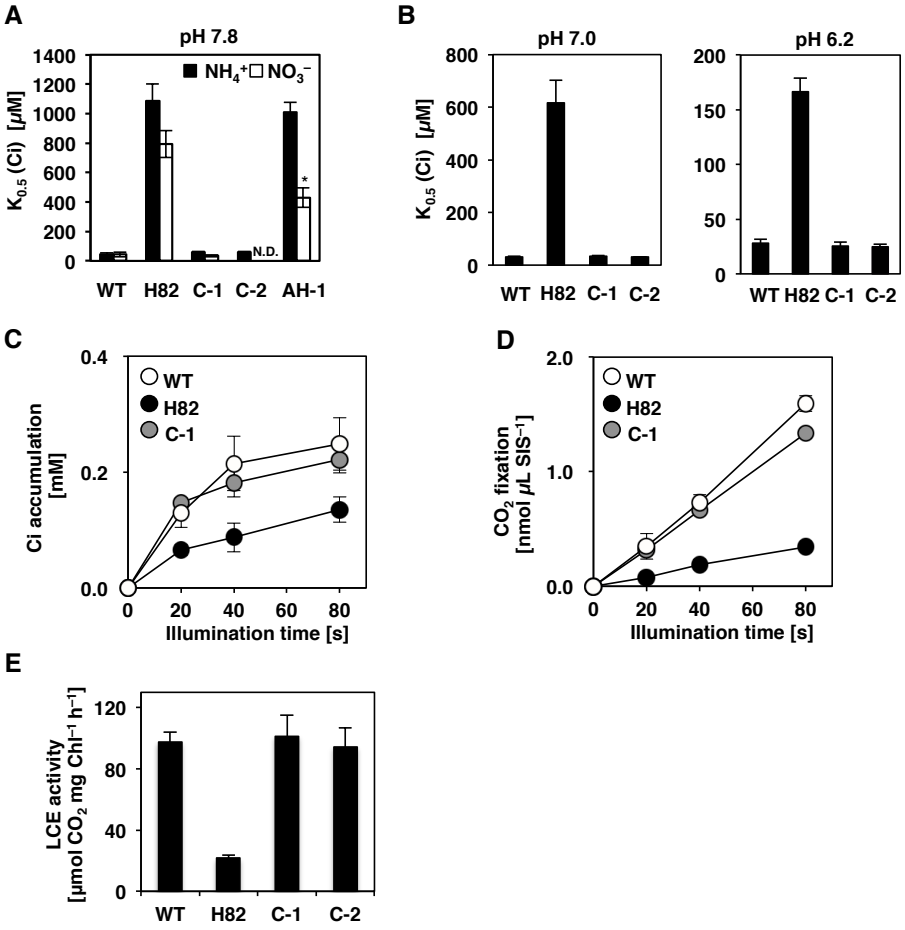

Figure 22. Photosynthetic characterization of H82 and its complemented strains. (A) Photosynthetic inorganic carbon (Ci) affinity of wild-type (WT), H82, its complemented strains (C-1 and C-2), and transgenic H82 cells containing inducible genes of HLA3 and LCIA (AH-1) cells grown in medium with NH_4^+ or NO_3^- as nitrogen sources in low-CO_2 (LC) conditions for 12 h. Photosynthetic O_2-evolving activity was measured in external dissolved Ci concentrations at pH 7.8, and the Ci concentration required for half maximal velocity ($K_{0.5}$ (Ci)) was calculated. Data in all experiments are mean values ± standard deviation (SD) from three biological replicates. *P <0.01 by Student's test. N.D., not determined. (B) Photosynthetic Ci affinity of WT, H82, C-1, and C-2 in medium with NH_4^+ as nitrogen source in LC conditions for 12 h. Photosynthetic O_2-evolving activity was measured at pH 7.0 or 6.2. (C and D) Accumulation (C) and fixation (D) of Ci in WT, H82, and C-1 cells. Cells were grown in LC conditions for 12 h, and the intracellular Ci concentration and carbon fixation were measured using a silicone-oil layer method. SIS, sorbitol impermeable space. (E) Light-dependent CO_2-exchange (LCE) activity of WT, H82, C-1, and C-2. Cells were grown in LC conditions for 12 h.

2.4 Cyclic electron flow activity is not inhibited in H82 in low-CO_2 conditions

It was reported that photosynthetic CEF is increased in CO_2-limiting conditions (Lucker and Kramer, 2013) as well as in anaerobic conditions where down-regulation of CAS resulted in a strong inhibition of CEF activity (Terashima et al., 2012), it was possible that CAS-dependent CEF might contribute to the CCM. In order to determine whether disruption of *CAS* also impaired CEF activity in LC conditions, we measured light-induced absorption changes at 705 nm, which reflect the redox state of P_{700} in H82 and C-1 cells. The P_{700} in the cells was oxidized by actinic light illumination whereas P_{700}^{+} was reduced by CEF after cessation of actinic light illumination (dark-recovery) in the presence of 3-(3,4-dichlorophenyl)-1,1-dimethylurea (DCMU), which blocks electrons from PSII. The dark-recovery kinetics were significantly slowed down in the presence of 2,5-dibromo-3-methyl-6-isopropylbenzoquinone (DBMIB), which blocks electrons in CEF (Alric et al., 2010) (Fig. 23A and B), suggesting that both H82 and C-1 strains have CEF activity. When switching from HC to LC conditions for 12 h, H82 cells showed a similar decease in half-times ($t_{1/2}$) of P_{700}^{+} re-reduction to C-1 strain after the cessation of the actinic light in the presence of DCMU (Fig. 23B), suggesting that the CEF is not affected by the lack of CAS protein in LC conditions at 120 μmol photons·m^{-2}·s^{-1}.

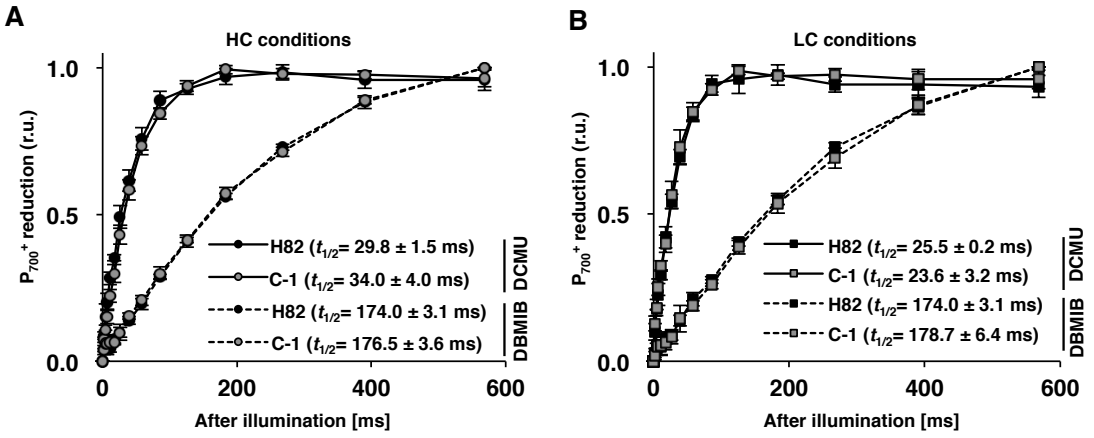

Figure 23. P_{700}^{+} reduction kinetics of H82 and C-1 cells grown in high-CO_2 (HC) (A) or low-CO_2 (LC) (B) conditions. The kinetics were measured after actinic light illumination for 10 s and then switching to dark periods. These curves show the kinetics of P_{700}^{+} reduction after cessation of actinic light exposure. The kinetics were recorded in the presence of 10 μM 3-(3,4-dichlorophenyl)-1,1-dimethylurea (DCMU) (solid line) or 10 μM DCMU and 2 μM 2,5-dibromo-3-methyl-6-isopropylbenzoquinone (DBMIB) (broken line). The time periods required for half reduction of P_{700}^{+} ($t_{1/2}$) were calculated. Data in all measurements are mean values ± SD from three biological replicates.

2.5 Recovery of the accumulation of HLA3 and LCIA in complemented strains of H82

In addition to recovery of the accumulation of CAS and photosynthetic affinities against Ci in C-1 and C-2, LC-induced accumulation in HLA3 and LCIA were also restored (Fig. 24*A*). Furthermore, another complemented strain, FN-1, expressing FLAG-tag fused CAS also showed restored photosynthetic affinities and accumulation of HLA3 and LCIA, correlated with the accumulation of recombinant FLAG-CAS protein (Fig. 24B and C and Table 5). To further evaluate the contribution of the defect in the accumulation of HLA3 and LCIA to the decreased Ci affinity in H82 cells, strain AH-1 was generated, in which two chimeric plasmids, pTY2b-LCIA and pTY2b-HLA3 (Yamano et al., 2015), were introduced into H82 cells and HLA3 and LCIA could be induced by switching the nitrogen source from NH_4^+ to NO_3^- (Fig. 24D). Although the $K_{0.5}$ (Ci) value of 1,008 ± 70 μM in AH-1 cells was similar to that of 1,087 ± 113 μM in H82 cells in NH_4^+ conditions, that of AH-1 cells decreased to 430 ± 6 μM from 793 ± 91 μM in H82 cells by expression of both HLA3 and LCIA in inductive NO_3^- conditions (Fig. 22A and Table 5). However, the $K_{0.5}$ (Ci) value in AH-1 cells was still approximately 10-fold higher than those in WT and C-1 cells. These results suggested that decreased Ci affinity in H82 cells was partially caused by the defects in the accumulation of HLA3 and LCIA, but other additional factors could be responsible for the HC-requiring phenotype of H82 cells.

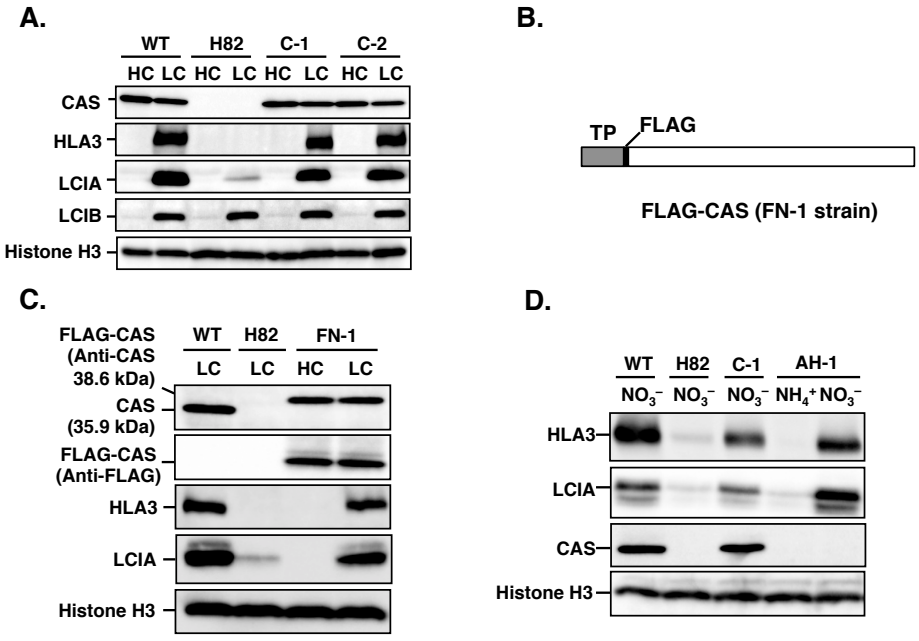

Figure 24. Accumulation of CAS, HLA3, LCIA, and LCIB in wild-type (WT), H82, C-1, C-2, FN-1, and AH-1 cells. (A) Cells were grown in medium with NH_4^+ as the nitrogen source in high-CO_2 (HC) or low-CO_2 (LC) conditions for 12 h. Histone H3 was used as a loading control. (B) Schematic representation of recombinant CAS proteins in complemented strain (FN-1) expressing FLAG-tagged CAS. The gray, solid, and open rectangles indicated the transit peptide (TP), FLAG-tag, and CAS, respectively. (C) Accumulation levels of LCIA, HLA3, and recombinant CAS in FN-1 cells were recorded. Cells were grown in HC or LC conditions for 12 h. (D) Cells were grown in medium with NH_4^+ or NO_3^- as nitrogen sources in LC conditions for 12 h.

3. CAS-dependent regulation of CO_2-concentrating mechanism-related components

3.1 CAS-dependent expression of nuclear-encoded low-CO_2-inducible genes

In order to evaluate the alternative causes of decreased Ci affinity of H82 cells other than HLA3 and LCIA, genes whose expression was affected by the *CAS* mutation were screened by RNA-seq analysis. WT, H82, and C-1 cells were grown in HC or LC conditions for 0.3 and 2 h, and the respective transcriptome profiles were compared. After exposure to HC and LC conditions for 0.3 h, no gene other than *CAS* was affected by the mutation. On the other hand, in LC conditions for 2 h, the expression levels of 44 genes in addition to *CAS* were significantly different (*false discovery rate* [FDR] < 0.05) in H82 cells from those in WT and C-1 cells (Table 6). Among them, 22 genes were included in the 47 LC – inducible genes regulated by CCM1 (Miura et al., 2004). Particularly, the expression levels of 13 genes were decreased more than fourfold by the *CAS* mutation, including *HLA3*, *LCIA, DNJ31* encoding putative DnaJ-like chaperonin, *CAH4* and *CAH5* encoding mitochondrial carbonic anhydrases, *PPP30* encoding Type 2C protein phosphatase, *CCP1* and *CCP2* encoding putative chloroplast envelope membrane proteins, low-CO_2-inducible gene D (*LCID*), *LHCSR3.1* and *LHCSR3.2* encoding LHCSR3, and two unknown genes (*Cre12.g541550* and *Cre26.g756747*).

Table 6. Genes differentially expressed in H82 cells with a FDR<0.05, compared with those in wild-type (WT) and C-1 cells in LC conditions for 2 h.

[a]Gene ID	Gene name	Average FPKM in WT			Average FPKM in H82			Average FPKM in C-1			Description of gene product	q value (WT LC2h vs. H82 LC 2h)	q value (C-1 LC2h vs. H82 LC 2h)	q value (WT LC2h vs. C-1 LC 2h)	WT LC2h FPKM / H82 LC 2h FPKM	C-1 LC2h FPKM / H82 LC 2h FPKM
		HC	LC 0.3h	LC 2h	HC	LC 0.3h	LC 2h	HC	LC 0.3h	LC 2h						
Cre02.g097800	***HLA3***	2.1	55.0	152.3	2.5	22.4	7.0	1.9	35.4	154.3	Plasma membrane-localized ATP-binding cassette transporter associated with HCO_3^- uptake	2.14.E-03	2.14.E-03	9.98.E-01	21.8	22.1
Cre12.g497300	***CAS***	367.7	152.1	264.9	6.0	6.1	7.1	99.4	95.2	89.2	Thylakoid membrane-localized calcium-binding protein containing Rhodanese-like domain	2.14.E-03	2.14.E-03	3.92.E-02	37.4	12.6
Cre03.g204577	***DNJ31***	3.0	4.0	13.2	2.6	2.9	2.9	3.0	3.3	26.6	DnaJ-like chaperonin	2.14.E-03	2.14.E-03	2.13.E-01	4.6	9.3
Cre05.g248400	***CAH4***	7.4	756.1	2335.8	3.0	499.4	296.1	6.4	712.7	2329.5	Mitochondrial carbonic anhydrase, CA4	2.14.E-03	2.14.E-03	9.98.E-01	7.9	7.9
Cre05.g248450	***CAH5***	8.5	749.9	2134.9	3.4	485.7	289.7	6.4	694.1	2243.7	Mitochondrial carbonic anhydrase, CA5	2.14.E-03	2.14.E-03	9.98.E-01	7.4	7.7
Cre07.g334750	***PPP30***	2.4	16.4	15.2	2.2	16.0	3.2	1.6	33.0	20.2	Type 2C protein phosphatase containing Stage II sporulation protein E (SpoIIE) (PF07228) domain	5.41.E-03	2.14.E-03	8.71.E-01	4.8	6.4
Cre06.g309000	***LCIA***	2.5	626.8	798.5	2.1	533.6	151.1	0.6	911.0	866.5	Chloroplast envelope-localized possible anion channel associated with inorganic carbon uptake; Nitrite transporter (NAR1) homolog	2.14.E-03	2.14.E-03	9.98.E-01	5.3	5.7
Cre04.g223300	***CCP1***	3.1	466.2	632.6	2.4	308.7	137.7	0.7	428.7	700.0	Low-CO_2-inducible chloroplast envelope protein (LIP36-1)	2.14.E-03	2.14.E-03	9.97.E-01	4.6	5.1
Cre12.g541550	**-**	7.7	6.7	24.3	33.6	15.5	6.8	48.3	27.0	34.4	[b]-	2.14.E-03	2.14.E-03	4.55.E-01	3.6	5.1
Cre26.g756747	**-**	1.3	157.5	41.0	1.0	137.8	13.6	0.4	279.4	67.1	[b]-	2.14.E-03	2.14.E-03	2.34.E-01	3.0	4.9
Cre04.g222800	***LCID***	10.5	39.3	61.9	5.8	30.0	17.6	4.2	59.2	82.2	Homolog of low-CO_2-inducible protein B (LCIB)	2.14.E-03	2.14.E-03	6.97.E-01	3.5	4.7
Cre08.g367400	***LHCSR3.2***	1.6	245.1	164.3	2.0	236.3	46.0	1.7	340.6	208.8	Stress-related chlorophyll a/b binding protein 3	2.14.E-03	2.14.E-03	8.02.E-01	3.6	4.5
Cre08.g367500	***LHCSR3.1***	1.6	290.1	191.8	1.9	263.9	49.7	2.9	341.6	223.2	Stress-related chlorophyll a/b binding protein 3	2.14.E-03	2.14.E-03	9.39.E-01	3.9	4.5
Cre04.g222750	***CCP2***	5.5	150.4	199.3	3.4	151.7	69.9	3.4	234.5	280.6	Low-CO_2-inducible chloroplast envelope protein (LIP36-2)	2.14.E-03	2.14.E-03	6.49.E-01	2.9	4.0
Cre06.g281600	***LCI23***	4.2	36.0	86.3	5.4	53.2	28.6	6.6	69.8	104.8	Low-CO_2-inducible septin-like protein	2.14.E-03	2.14.E-03	8.91.E-01	3.0	3.7
Cre02.g088551	**-**	5.2	14.0	22.2	4.1	12.5	8.9	5.9	22.3	32.1	[b]-	2.14.E-03	2.14.E-03	4.27.E-01	2.5	3.6
Cre11.g467617	***LCI19***	4.2	15.2	28.0	3.8	16.2	8.8	3.5	19.3	29.5	Low-CO_2-inducible gamma hydroxybutyrate dehydrogenase	2.14.E-03	2.14.E-03	9.98.E-01	3.2	3.4
Cre09.g399400	***TGL15***	11.6	8.7	15.2	1.4	2.9	3.6	1.9	4.9	12.0	Triacylglycerol lipase	2.14.E-03	2.14.E-03	7.20.E-01	4.2	3.3
Cre05.g234652	**-**	17.7	29.3	50.5	13.5	32.5	17.4	17.3	47.6	55.9	Predicted protein with CobW domain	2.14.E-03	2.14.E-03	9.76.E-01	2.9	3.2
Cre10.g439700	***CGL28***	6.5	56.5	58.4	6.4	64.5	25.7	4.8	122.9	82.2	RNA binding protein	3.88.E-03	2.14.E-03	5.99.E-01	2.3	3.2
Cre09.g391726	**-**	5.5	17.0	16.2	14.8	48.1	30.6	62.0	116.0	96.9	[b]-	2.86.E-02	2.14.E-03	2.14.E-03	0.5	3.2
Cre17.g720950	***SRD3***	14.4	89.7	28.2	11.4	91.5	14.1	17.2	223.0	43.5	Putative 3-oxo-5-alpha-steroid 4-dehydrogenase	1.29.E-02	2.14.E-03	2.81.E-01	2.0	3.1
Cre02.g080800	**-**	2.8	8.2	10.6	2.7	9.7	4.6	2.1	14.8	14.1	[b]-	2.14.E-03	2.14.E-03	6.04.E-01	2.3	3.1
Cre03.g162800	***LCI1***	2.6	2144.6	2496.1	2.3	1403.0	927.0	1.5	1833.1	2674.8	Plasma membrane-localized protein associated with inorganic carbon transport	2.18.E-02	1.61.E-02	9.98.E-01	2.7	2.9
Cre03.g168100	**-**	7.4	18.5	32.9	6.6	17.1	17.0	8.9	33.0	46.9	[b]-	3.02.E-02	2.14.E-03	4.75.E-01	1.9	2.8
Cre03.g151650	***SMM7***	2.5	24.2	16.1	1.8	27.3	5.1	1.8	35.4	13.4	Lysine methyltransferase	2.14.E-03	2.14.E-03	8.26.E-01	3.2	2.6
Cre10.g463370	**-**	6.8	2.5	3.8	2.7	1.8	1.3	3.3	2.4	3.2	Putative smooth-muscle-myosin-light-chain kinase	8.15.E-03	2.79.E-02	9.30.E-01	3.0	2.6
Cre02.g077750	***FAP211***	2.7	3.1	4.1	4.5	5.1	9.0	5.8	13.0	22.9	Flagellar-associated protein	2.14.E-03	2.14.E-03	2.14.E-03	0.5	2.5
Cre03.g183300	**-**	19.8	46.3	18.6	10.5	42.9	7.9	14.5	59.3	19.3	Predicted protein with starch-binding domain	2.45.E-02	2.36.E-02	9.98.E-01	2.4	2.5
Cre03.g189350	**-**	80.3	69.2	129.6	50.2	54.1	47.2	53.3	79.7	112.0	[b]-	2.14.E-03	2.14.E-03	9.12.E-01	2.8	2.4
Cre06.g295450	***HPR1***	65.8	158.6	144.4	39.6	211.7	71.8	61.7	283.8	166.2	Hydroxypyruvate reductase	3.49.E-02	1.50.E-02	9.49.E-01	2.0	2.3
Cre05.g241950	***ASC2***	217.0	191.7	374.2	174.9	184.6	152.9	239.0	287.3	351.3	Voltage-dependent anion-selective channel	6.84.E-03	2.45.E-02	9.98.E-01	2.5	2.3
Cre09.g398500	**-**	60.6	35.3	66.2	10.7	16.8	22.7	14.7	28.8	51.7	[b]-	2.14.E-03	5.41.E-03	7.53.E-01	2.9	2.3
Cre09.g404750	***SRR2***	8.7	6.3	11.5	3.3	3.9	5.6	2.7	5.5	12.1	Scavenger receptor cysteine-rich (SRCR) protein	6.84.E-03	2.14.E-03	9.98.E-01	2.1	2.2

Table 6. Genes differentially expressed in H82 cells with a FDR<0.05, compared with those in wild-type (WT) and C-1 cells in LC conditions for 2 h.

[a]Gene ID	Gene name	Average FPKM in WT			Average FPKM in H82			Average FPKM in C-1			Description of gene product	q value (WT LC2h vs. H82 LC 2h)	q value (C-1 LC2h vs. H82 LC 2h)	q value (WT LC2h vs. C-1 LC 2h)	WT LC2h FPKM / H82 LC 2h FPKM	C-1 LC2h FPKM / H82 LC 2h FPKM
		HC	LC 0.3h	LC 2h	HC	LC 0.3h	LC 2h	HC	LC 0.3h	LC 2h						
Cre06.g281450	***SRR22***	12.3	8.6	12.6	3.3	3.9	5.5	3.2	5.4	11.5	Scavenger receptor cysteine-rich (SRCR) protein	2.14.E-03	9.41.E-03	9.71.E-01	2.3	2.1
Cre14.g621650	***MCT1***	72.9	93.2	101.6	48.0	87.5	48.0	56.7	99.6	98.9	Acyl-carrier-protein, S-malonyltransferase	1.80.E-02	3.02.E-02	9.98.E-01	2.1	2.1
Cre07.g343050	-	7.7	16.6	26.0	7.9	16.0	13.7	6.5	14.8	28.0	[b]-	2.94.E-02	1.18.E-02	9.93.E-01	1.9	2.1
Cre12.g531900	-	33.4	41.0	48.6	16.6	36.7	22.8	26.7	47.8	45.3	[b]-	1.80.E-02	3.11.E-02	9.98.E-01	2.1	2.0
Cre09.g398250	-	60.3	33.2	42.2	10.6	17.3	19.9	15.8	30.3	39.1	[b]-	1.61.E-02	2.79.E-02	9.95.E-01	2.1	2.0
Cre01.g030350	***CGL41***	2.2	3.5	3.5	3.4	6.5	8.9	4.0	4.0	17.4	Predicted RbcX protein	2.14.E-03	3.71.E-02	2.14.E-03	0.4	2.0
Cre17.g710300	-	18.3	10.0	4.6	20.8	23.3	11.6	19.9	21.1	22.6	Pherophorin (DUF3707)	2.14.E-03	3.84.E-02	2.14.E-03	0.4	2.0
Cre13.g573250	-	30.8	32.1	25.8	13.0	25.4	13.3	17.6	41.6	24.5	Thiosulfate sulfurtransferase with Rhodanese-like domain	1.80.E-02	4.84.E-02	9.98.E-01	1.9	1.8
Cre02.g093750	***NRX2***	11.2	9.8	7.6	8.7	18.9	17.1	7.4	14.2	8.9	Nucleoredoxin 2	2.14.E-03	2.45.E-02	8.99.E-01	0.4	0.5
Cre12.g546550	***FEA1***	277.5	36.5	4.7	136.0	26.5	17.2	172.6	65.9	6.4	Fe-assimilating protein; High-CO_2 inducible protein H43	2.14.E-03	9.41.E-03	6.27.E-01	0.3	0.4
Cre05.g244400	-	1.6	2.4	2.1	3.1	6.7	6.2	2.1	3.4	1.9	Nucleotide-diphospho-sugar transferase	2.94.E-02	2.94.E-02	9.97.E-01	0.4	0.3

[a]Gene ID, Phytozome gene accession number
[b]Gene product which is not annotated

(Continued)

Of note, these genes, such as HLA3 and LCIA, were transiently induced at 0.3 h even in H82 cells, but their expression level could be not maintained at the same levels as in WT or C-1 cells at 2 h, unlike the case of *LCIB* (Fig. 25A). To further evaluate the effect of CAS on the expression of these CAS-dependent genes in LC conditions, the mRNA levels of *HLA3* was examined by qRT-PCR in H82 cells and its complemented strain C-1 grown in HC or LC conditions for 0.3, 2, and 12 h. Similar to its expression pattern in RNA-seq analysis, *HLA3* was similarly induced in both the H82 and C-1 cells in LC conditions for 0.3 h, but the mRNA abundance of *HLA3* in C-1 cells was 15 times higher than that in the H82 mutant in LC conditions for 2 h (Fig. 25B). Even in LC conditions for 12 h, four-times higher mRNA abundance was still observed in C-1 cells than the case in H82 cells.

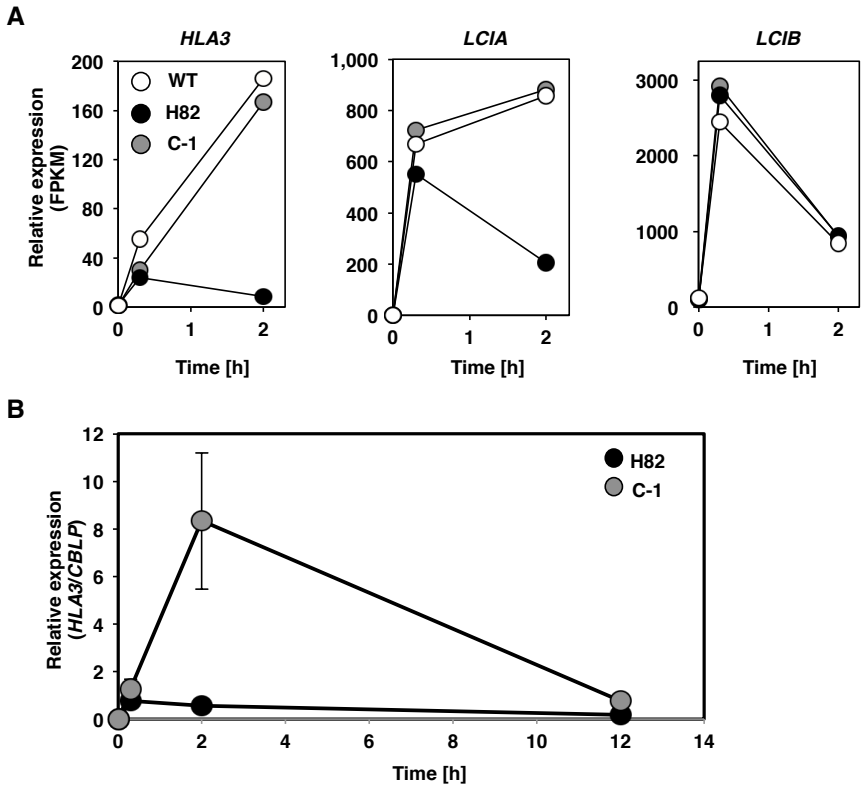

Figure 25. Time course of relative expression of HLA3, LCIA, and LCIB. (A) Time course of fragments per kilobase of exon per fragments mapped (FPKM) values of LCIA, HLA3, and LCIB in wild-type (WT), H82, and C-1 cells by RNA-seq analysis. Each strain grown in high-CO_2 (HC, 0 h) conditions was transferred to low-CO_2 (LC) conditions for 0.3 or 2 h. FPKM values calculated from two biological replicates. (B) The expression of *HLA3* was analyzed in H82 and C-1 cells at the indicated time points by qRT-PCR. *CBLP* gene encoding *Chlamydomonas* beta subunit-like polypeptide was used as an internal standard. Data in all experiments are mean values ± SD from three biological replicates. Each strain grown in HC (0 h) conditions was transferred to LC conditions for 0.3, 2, or 12 h.

3.2 Time-dependent accumulation of HLA3, LCIA, and LHCSR3 in low-CO_2-grown H82 cells

In order to evaluate whether the time-dependent defects in transcriptional abundance of gene*s* in H82 cells could affect their protein amounts, the accumulation levels of HLA3, LCIA, and LHCSR3 were examined in WT, H82, and C-1 cells in a time-dependent manner. After shifting to LC conditions for 2 h, significant accumulation of HLA3, LCIA, and LHCSR3 was detected in WT and C-1 cells (Fig. 26A). The accumulation levels of LCIA in H82 cells were approximately four-fold, eight-fold, and 16-fold lower than that in WT and C-1 cells in LC at 2 h, 4 h, and 12 h, respectively, indicating its gradually decreased accumulation in H82 cells. In the case of HLA3, its accumulation was not detected in H82 in HC or LC conditions (Fig. 26B). These results indicated that CAS regulates HLA3 and LCIA to a different extent during the induction of the CCM. Considering that the expression of HLA3 was also regulated by LCIA (Yamano et al., 2015), the defective accumulation of HLA3 in H82 mutant could be resulted from the decreased accumulation of both CAS and LCIA. In contrast, the accumulation of LHCSR3 in H82 cells was two-fold lower than the case in WT after switching to LC conditions for 2 h or 4 h, whereas similar accumulation levels of LHCSR3 were detected in each strain at 12 h. These results suggested that CAS only regulates LHCSR3 accumulation at an early stage of CCM induction.

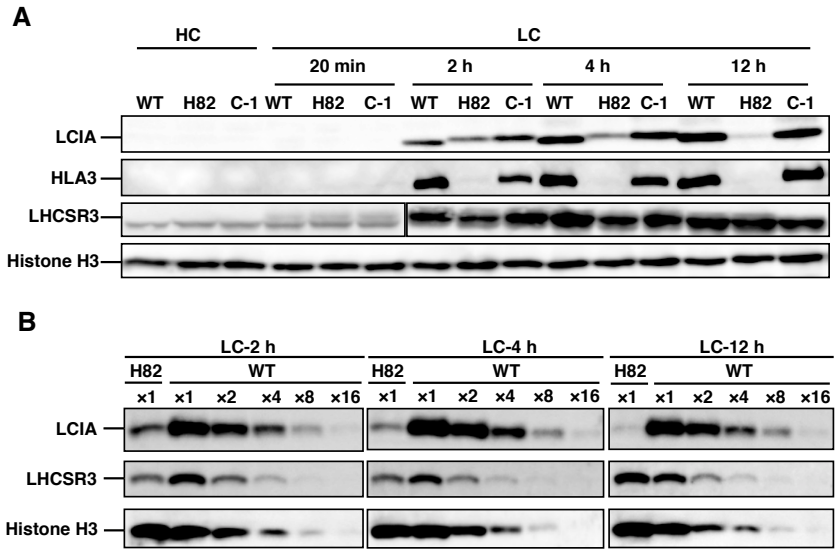

Figure 26. Accumulation of HLA3, LCIA, and LHCSR3 in wild-type (WT), H82, and C-1 cells. (A) High-CO_2 (HC)-grown cells were transferred to low-CO_2 (LC) conditions for 0.3, 2, 4, or 12 h before sampling. Cells were illuminated in 120 μmol photons·m^{-2}·s^{-1}. Histone H3 was used as a loading control. (B) To compare the accumulation levels of these proteins in H82 cells with that of WT cells, aliquots of total cell protein corresponding to 1 μg of chlorophyll were loaded in the lane designated ×1, and the same amount of protein was serially diluted 2–16 times and loaded in the lanes designated ×2, ×4, ×8, and ×16, respectively .

3.3 Poor inorganic carbon consumption in the culture medium of H82 locked the mutant cells in a low-CO_2 state and caused different LCIB location

In order to further examine alternative causes of decreased photosynthetic Ci affinity of H82 cells, the localization of LCIB in LC conditions with illumination was focused on because previous reports showed that aberrant LCIB localization occasionally resulted in decreased photosynthetic Ci affinity (Yamano et al., 2014). As shown in previous reports (Wang et al., 2006; Yamano et al., 2010; Duanmu et al., 2009a), indirect immunofluorescence signals derived from an anti-LCIB antibody were observed as a ring-like structure around pyrenoid in WT and C-1 cells bubbled with ambient air (0.04% CO_2) (Fig. 27A). On the other hand, fluorescent signals were not aggregated but dispersed mainly along the chloroplast envelope in H82 and AH-1 cells (Fig. 27A).

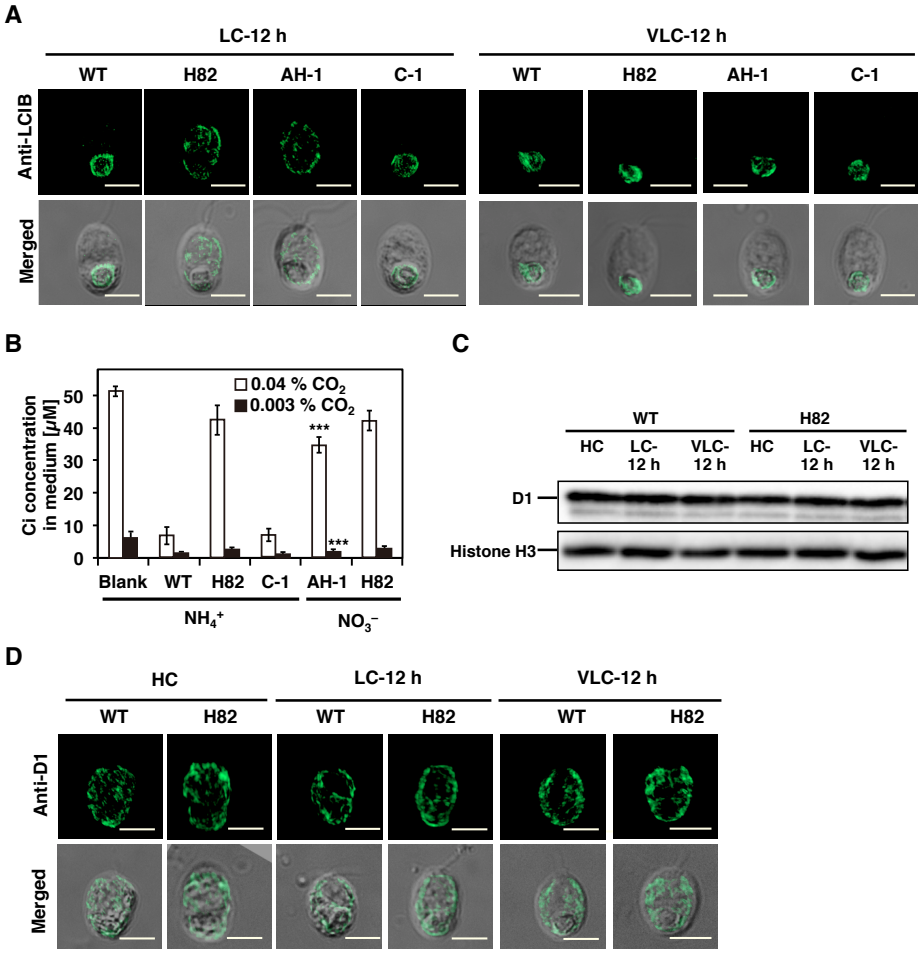

Figure 27. Subcellular localization of LCIB and D1 in H82 mutant and inorganic carbon (Ci) concentration in growth medium. (A) Localization of LCIB in wild-type (WT), H82, AH-1, and C-1 cells using an indirect immunofluorescence assay. High-CO_2 (HC)-grown cells were transferred to low-CO_2 (LC) or very LC (VLC) conditions for 12 h. AH-1 cells were cultured in HSM medium with NO_3^- (HSM-NO_3^-) as the nitrogen source. Each image is placed with the flagella facing upward on the panel. Merged indicates the merger of a fluorescence image with its differential interference contrast (DIC) image. Scale bars, 5 μm. (B) Measurement of Ci concentrations in HSM medium with NH_4^+ (HSM-NH_4^+) as the nitrogen source or HSM-NO_3^- medium after culturing cells in 0.04% or 0.003% CO_2 for 12 h. Blank means the Ci concentrations in culture medium without cells. Data in all experiments are mean values ± SD from three biological replicates. The difference of the Ci concentration in medium between AH-1 and H82 cells was evaluated. ***P<0.1 by Student's t test. (C and D) Accumulation (C) and subcellular localization (D) of D1 in HC-, LC-, and VLC-grown WT and H82 cells.

These results raised two possibilities. First, CAS directly regulates the changes in LCIB, or second, CO_2 acclimation state in H82 cells is locked in the LC state where LCIB is dispersed in the chloroplast but not in the VLC state where LCIB is in the vicinity of the pyrenoid. In order to examine these two possibilities, I measured the Ci concentrations in the culture medium without cells or that cultured with WT, H82, and C-1 cells aerated with ambient air for 12 h (Fig. 27B). Although the Ci concentrations in the culture medium without cells was 51.3 μM, the Ci concentrations in medium cultured with WT and C-1 cells were decreased to 6.8 μM and 7.2 μM, respectively, reaching the upper limit of the VLC state (Vance and Spalding, 2005; Wang and Spalding, 2014a; Wang and Spalding, 2014b; Yamano et al., 2015) because a large portion of Ci could be removed from the medium through active Ci consumption by these cells. In contrast, the Ci concentration in medium cultured with H82 and AH-1 cells was 42.3 μM and 38.1 μM, respectively, which were definitely in the range of the LC state (Vance and Spalding, 2005; Wang and Spalding, 2014b). These results suggested that the aberrant localization of LCIB in H82 cells could have resulted from the remaining Ci concentrations in the culture medium, which was insufficient to induce the relocation of LCIB around the pyrenoid. In fact, when H82 and AH-1 cells were grown with 0.003% CO_2 for 12 h, where the Ci concentrations were 1.8 μM and 2.9 μM, respectively (Fig. 27B), these cells also displayed a typical ring-like structure of LCIB in the vicinity of the pyrenoid (Fig. 27*A*). In order to compare the localization of photosynthetic proteins with the dynamic relocation of LCIB and CAS in response to CO_2 and light, the accumulation and fluorescence signals of the photosystem II reaction center protein D1 were observed (Fig. 27C and D). The fluorescence signal of D1 protein was predominantly observed in the chloroplast region outside of the pyrenoid in HC-, LC-, and VLC-grown WT and H82 cells (Fig. 27D), supporting the previous report that D1 protein was localized to the thylakoid membrane outside of pyrenoid in *C. reinhardtii* cells (Gunning and Schwartz, 1999; Blanco-Rivero et al., 2012). Neither the accumulation nor the localization of D1 was affected by CO_2 concentrations or by the defect in *CAS* (Fig. 27C and D), although I cannot exclude the possibility that other photosynthesis related proteins other than D1 could change their localization in response to CO_2 and light. This point should be clarified in the future analyses.

4. Subcellular localization of CAS in *Chlamydomonas reinhardtii*

4.1 Localization and topology of CAS protein in *C. reinhardtii*

In order to examine the localization of CAS, total protein, soluble/insoluble, chloroplast envelope, and thylakoid membrane fractions were extracted and probed with antibodies against CAS, thylakoid membrane-localized D1, soluble protein LCIB, plasma membrane-localized H^+-ATPase, and chloroplast envelope-localized LCIA (Fig. 28A-C). CAS was predominately detected in the insoluble and thylakoid membrane fractions where thylakoid membrane protein D1 was enriched, as shown in the previous proteome analyses (Allmer et al., 2006; Terashima et al., 2010).

Next, in order to determine the topology of *Cr*CAS in the thylakoid membrane, intact thylakoid membranes were isolated, subjected to trypsin treatment, and analyzed by immunoblotting using two anti-CAS antibodies that could specifically target the N-terminus or C-terminus of CAS, respectively. Both the N-terminus and C-terminus of CAS were digested and removed by trypsin (Fig. 28D). This suggests that CAS could be anchored to the thylakoid membrane, and both the Ca^{2+}-binding domain in the N-terminus and the rhodanese-like domain in the C-terminus were exposed to the stromal side, as in the case of *Arabidopsis* CAS (*At*CAS) (Normura et al., 2008). As a control, a thylakoid lumen-localized carbonic anhydrase, CAH3 (Karlsson et al., 1998), was not affected significantly by incubation with trypsin.

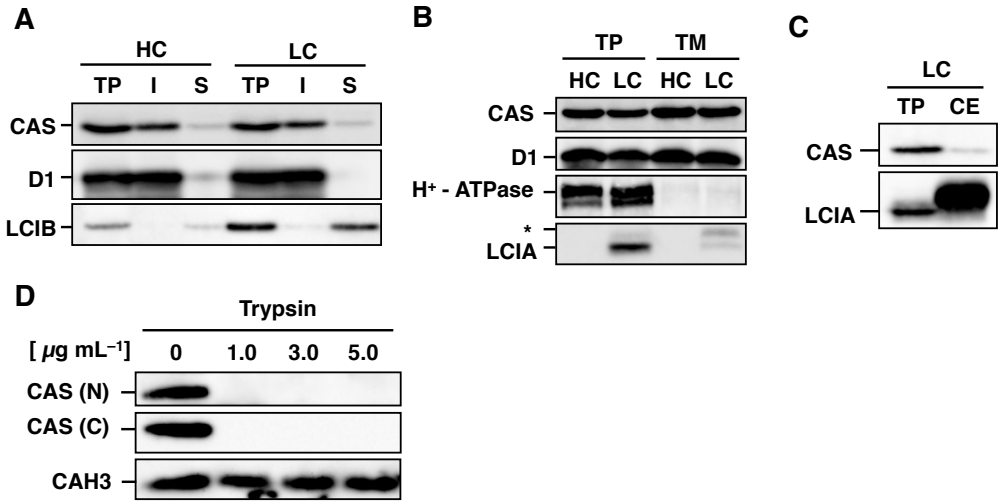

Figure 28. Localization and topology of *Cr*CAS by subcellular fractionation. (A, B, and C) Immunoblotting analysis in soluble, insoluble, thylakoid membrane, and chloroplast envelope fractions with antibodies against CAS, D1, LCIB, H^+-ATPase, and LCIA. Cells were grown in high-CO_2 (HC) or low-CO_2 (LC) conditions for 12 h. Asterisks indicate nonspecific bands. TP, total protein; S, soluble fraction; I, insoluble fraction; TM, thylakoid membrane fraction; and CE, chloroplast envelope fraction. (D) Topology of *Cr*CAS. The thylakoid fraction (0.05 mg chlorophyll mL^{-1}) isolated from CC-400 cells was suspended in buffer containing trypsin at the indicated concentrations or no protease. The proteins were separated by 15% SDS-PAGE and probed by N-terminal (N)-, C-terminal (C) -specific anti-CAS antibodies or an anti-CAH3 antibody.

4.2 Relocation of thylakoid membrane-localized CAS in low-CO_2-light conditions

In order to examine the detailed subcellular localization of CAS *in vivo*, an indirect immunofluorescence assay using an anti-CAS antibody was conducted. In HC conditions with light illumination at 120 µmol photons·m^{-2}·s^{-1} (HC-light), fluorescent signals were observed as dispersed speckles in the chloroplast region (Fig. 29A). In contrast, after switching to LC conditions in light (LC-light), the fluorescent signals were gathered in the pyrenoid after 2 h, and the gathering was observed as tubule-like structures inside the pyrenoid at 12 h. As a control, immunofluorescence signals were hardly detected in H82 cells. These localization patterns were also consistent with the results of indirect immunofluorescent signals in a complemented strain FN-1 expressing FLAG-tag-fused CAS using anti-FLAG antibody (Fig. 29B). Furthermore, the aggregated tubule-like signals were dispersed throughout the chloroplast when transferred to HC-light conditions (Fig. 29C).

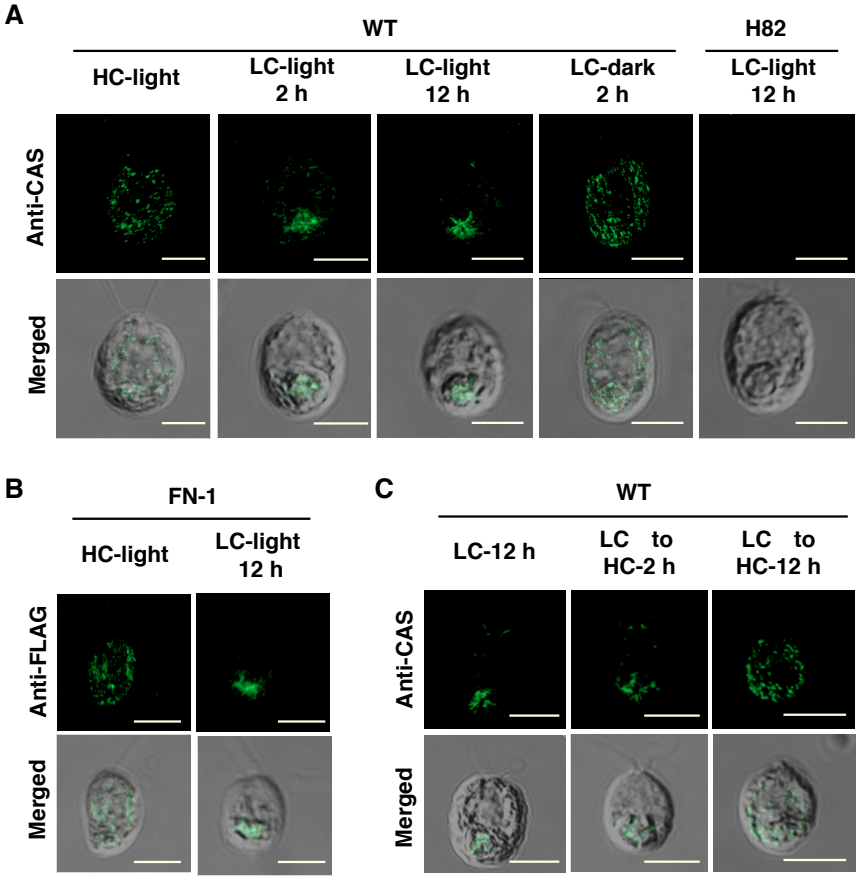

Figure 29. Subcellular localization of *Cr*CAS. (A) Localization of CAS in wild-type (WT) and H82 cells was assessed using an indirect immunofluorescence assay with an anti-CAS antibody. Cells grown in high-CO_2 (HC) conditions were shifted to low-CO_2 (LC) conditions for 2 h or 12 h in light, and then the LC-acclimated cells (12 h) were transferred from light to dark for 2 h. Each image is placed with the flagella facing upward on the panel. Merged indicates the merger of a fluorescence image with its differential interference contrast (DIC) image. Scale bars, 5 µm. (B) Localization of FLAG-CAS in complemented strain FN-1 using an indirect immunofluorescence assay with an antibody against FLAG as the primary antibody. Cells grown in HC conditions were shifted to LC conditions for 12 h in the light. (C) Time course of changes in CAS localization in cells from LC to HC in WT cells by an indirect immunofluorescence assay. LC-acclimated cells were shifted to HC conditions for 2 and 12 h in the light before sampling.

Changing localization in the chloroplast in response to CO_2 was also observed in the case of LCIB, and light as well as CO_2 could affect its localization (Yamano et al., 2010). Similarly, the gathered fluorescent signals of CAS in LC-acclimated cells became diffuse after switching from LC-light to LC conditions in the dark (LC-dark) for 2 h (Fig. 29A). Considering the fact that the changes of CAS localization in the pyrenoid as well as the accumulation of HLA3, LCIA, and LCIB were suppressed in the presence of DCMU and DBMIB (Fig. 30A-C), and that these inhibitors also suppress the CCM (Badger et al., 1980), the localization of CAS to the pyrenoid could be important for regulation of the CCM in LC-light conditions where the CCM was active.

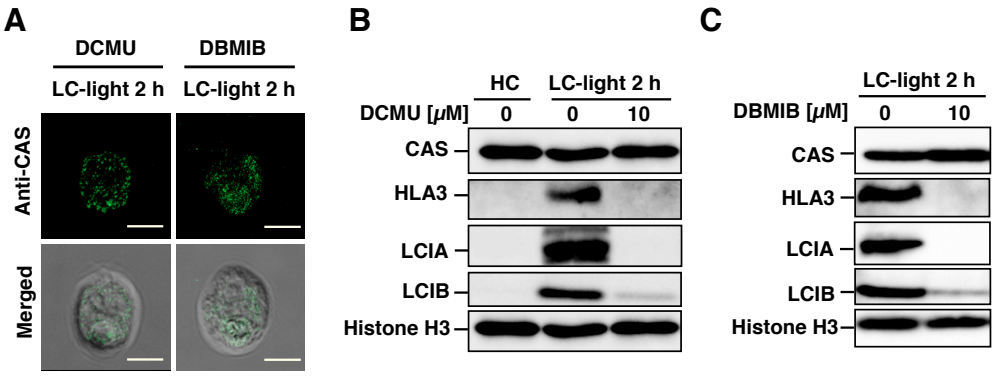

Figure 30. Subcellular localization of CAS and accumulation of CAS, HLA3, LCIA, and LCIB in the presence DCMU or DBMIB. (A) The effect of 3-(3,4-dichlorophenyl)-1,1-dimethylurea (DCMU, 10 μM) or 2,5-dibromo-3-methyl-6-isopropylbenzoquinone (DBMIB, 10 μM) on the localization of CAS in wild-type (WT) cells. High-CO_2 (HC)-grown cells were centrifuged, re-suspended in fresh HSM medium containing the indicated chemicals, and switched to low-CO_2 (LC) conditions for 2 h. (B and C) Accumulation of proteins in WT cells grown in the ethanol (mock, solvent used for inhibitors), DCMU (10 μM), or DBMIB (10 μM).

4.3 Relocation of CAS is independent of *de novo* protein synthesis and the lack of CCM1 protein

Next, in order to determine whether the aggregation of CAS in LC-light conditions was related to *de novo* protein synthesis, the effect of cycloheximide (CHX) was examined. By transferring from HC-light to LC-light conditions or from LC-light to LC-dark conditions, a change in the localization of fluorescent signals derived from CAS was observed in the presence of CHX (Fig. 31A). It was suggested that LC-induced CAS-relocation was not related to *de novo* protein synthesis, differing from the case of LCIB (Yamano et al., 2014).

Furthermore, the addition of CHX inhibited the accumulation of LCIB but not CAS in LC conditions (Fig. 31B). Because both the accumulation of CAS and its relocation in response to CO_2 were not impaired in strain C16, a *CCM1* insertion mutant (Fukuzawa et al., 2001) (Fig. 31C and D), the relocation of CAS could be regulated by external CO_2 concentration irrespective of the presence of CCM1/CIA5.

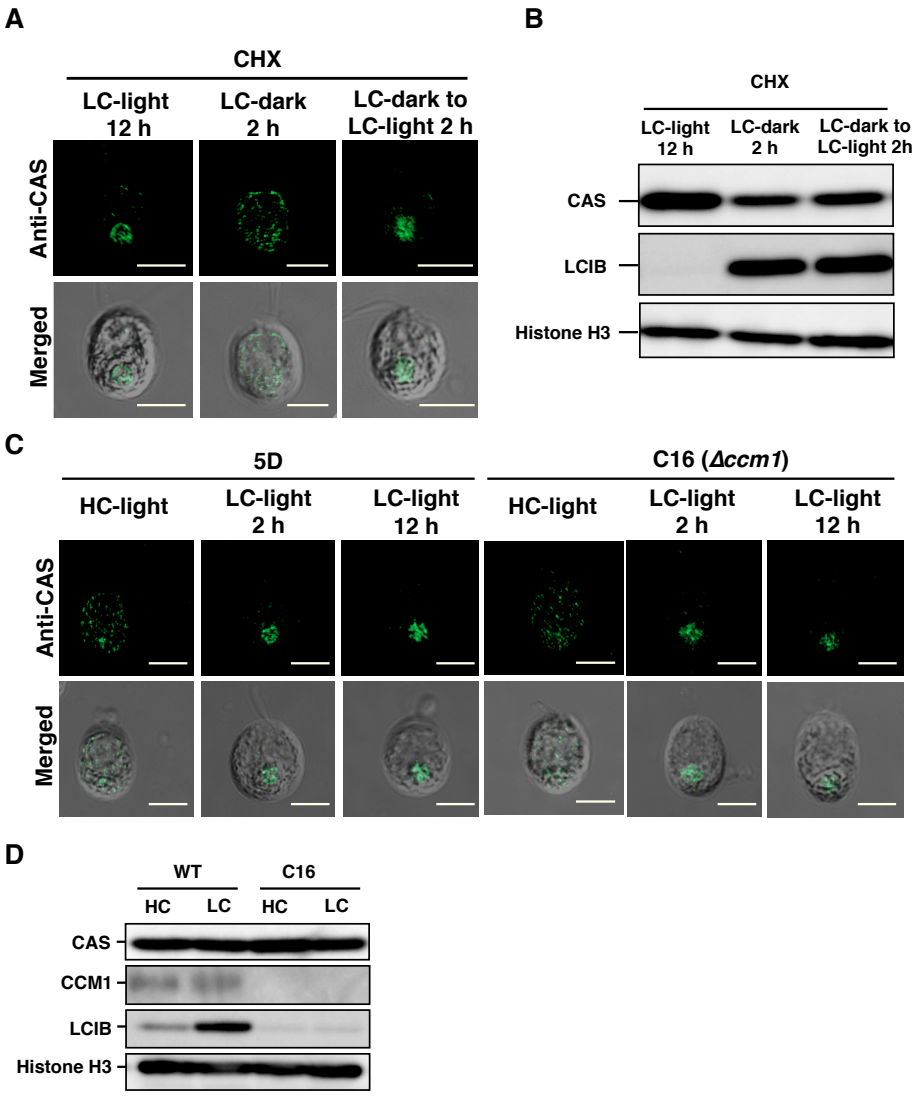

Figure 31. Subcellular localization of *Cr*CAS and accumulation of CAS and LCIB in the presence of cycloheximide (CHX) or the *CCM1* insertion mutant. (A) The effect of CHX (10 μg mL^{-1}) on the localization of CAS in wild-type (WT) cells. For CHX treatments, high-CO_2 (HC)-grown cells were transferred to low-CO_2 (LC)-light conditions in the presence of CHX for 12 h. The LC-light acclimated cells were subjected to LC-dark conditions in the presence of CHX for 2 h. The LC-dark-acclimated cells were transferred to LC-light conditions with or without CHX for 2 h. For all panels, each image is placed with the flagella facing upward on the panel. Merged images show the fluorescence image superimposed with its differential interference contrast image. Scale bars, 5 μm. (B) The effect of CHX on the accumulation of CAS and LCIB. (C) Localization of CAS in a *CCM1* insertion mutant, C16, and its parental 5D strain using an indirect immunofluorescence assay. Cells grown in HC-light conditions were shifted to LC-light conditions for 2 h or 12 h. (D) Accumulation of CAS in WT C-9 strain and C16 cells grown in HC or LC conditions for 12 h in light.

5. CAS functions in protein complexes

It was reported previously that the *Cr*CAS interact with ANR1 and PGRL1 in CEF complex of approximately 1,000 kDa in anaerobic conditions (Iwai et al., 2010; Terashima et al., 2012). To examine whether the *Cr*CAS is present as a complex *in vivo* in LC conditions, blue native gel electrophoresis was performed after dissociation of protein from membrane using 0.5% n-dodecyl β-D-maltoside (Fig. 32). In both HC and LC conditions, the CAS signal was detected in complexes with sizes of predominantly 240 kDa or 120 kDa. This suggested that CAS is part of protein complexes that do not change in apparent size or abundance when switching from HC to LC conditions. In the preliminary analysis of these two complexes using liquid chromatography tandem mass spectrometry (LC-MS/MS), only CAS protein was detected as predominant component.

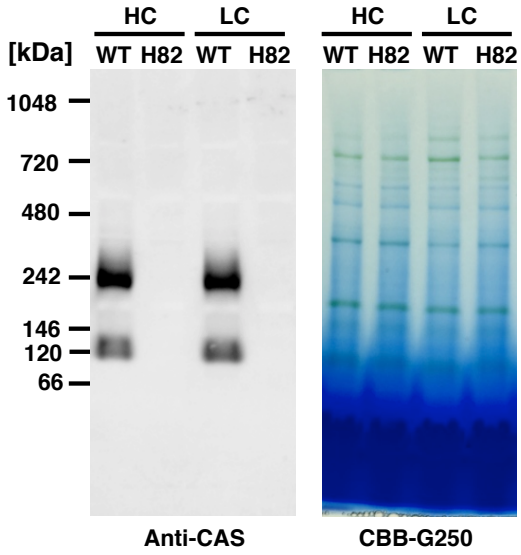

Figure 32. Molecular mass of native CAS protein. Wild-type (WT) and H82 cells were grown in high-CO_2 (HC) or low-CO_2 (LC) conditions for 12 h. Total proteins were dissociated using 0.5% n-dodecyl β-D-maltoside and separated by blue-native PAGE, in which the gel was stained by Coomassie Brilliant Blue-G250 (right). The PVDF membrane was subjected to an immunoblotting assay using an anti-CAS (C) antibody.

6. Calcium-binding activity of *Chlamydomonas* CAS

It was reported that *At*CAS has Ca^{2+}-binding sites in its N-terminus (Han et al., 2003). In order to evaluate the Ca^{2+}-binding activity of *Chlamydomonas* CAS (*Cr*CAS), recombinant proteins containing the N- and C-terminus of *Cr*CAS and N-terminus of *At*CAS were prepared (Fig. 33A). When blotting with ^{45}Ca, a radioactive signal was detected with the N-terminus of *Cr*CAS, as in the case of *At*CAS, but not the C-terminus of *Cr*CAS. (Fig. 33B). As a control, no signal was detected in GST protein. After adding an extra 10 mM $CaCl_2$ to the binding solution, the radioactive signal was weaker (Fig. 33B), presumably because of competition with ^{45}Ca for the Ca^{2+}-binding sites of CAS. These results indicate the Ca^{2+}-binding activity in the N-terminus of *Cr*CAS.

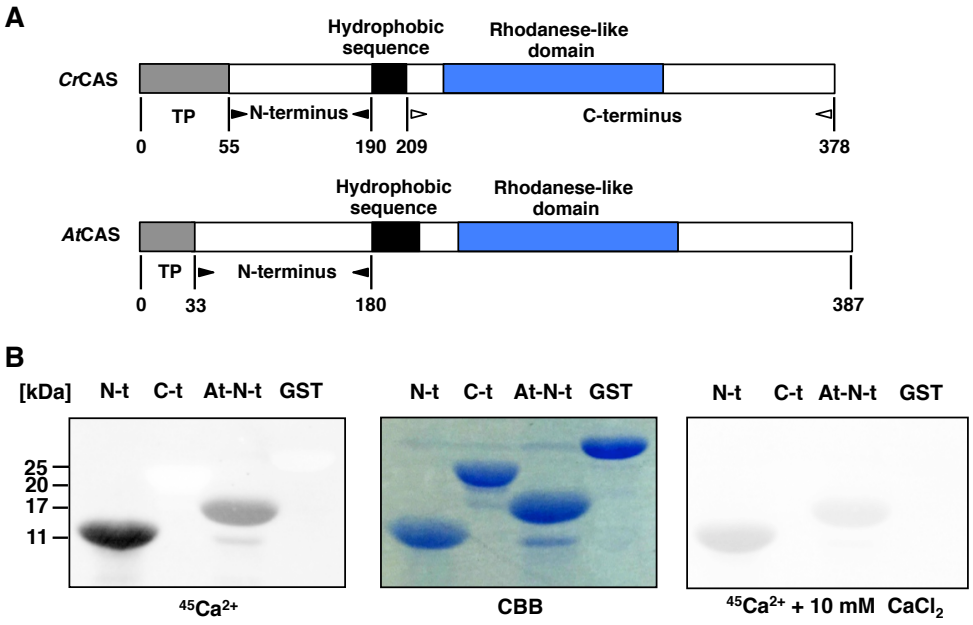

Figure 33. Ca^{2+}-binding activity of *Cr*CAS *in vitro*. (A) The N-terminus and C-terminus of CAS are separated by a hydrophobic sequence. The gray, solid, and blue rectangles indicate the transit peptide, hydrophobic sequence, and rhodanese-like domain, respectively. The numbers below the illustration represent the positions from the initial amino acid. The transit peptide of *At*CAS was predicted using the ChloroP program. (B) ^{45}Ca blotting analysis of the N- and C-terminnus (N-t and C-t, respectively) of the CAS protein. Purified recombinant N-t, C-t, N-terminus of *At*CAS (At-N-t), and GST with the same number of molecules were loaded, stained with Coomassie Brilliant blue (B, middle), and probed with ^{45}Ca in the absence (B, left) or presence (B, right) of 10 mM cold $CaCl_2$. kDa, kilodalton.

7. Calcium-dependent regulation of the CO_2-concentrating mechanism

In order to elucidate the link between Ca^{2+} signal via CAS and the regulation of HCO_3^- transporters, the accumulation of HLA3 as well as LCIA in WT cells cultured in the presence of cell-impermeable calcium specific chelator, 1,2-bis (*o*-aminophenoxy) ethane-N, N, N, N'-tetraacetic acid (BAPTA), was examined in LC conditions. The accumulation of HLA3 and LCIA was dramatically decreased by the addition of 0.5 mM BAPTA (Fig. 34A), correlating with a two-fold (72 ± 9 μM to 144 ± 14 μM) increase in $K_{0.5}$ (Ci) value (Fig. 34B). Because the addition of 0.75 mM $CaCl_2$ rescued the accumulation of HLA3 and LCIA and the $K_{0.5}$ (Ci) value, extracellular Ca^{2+} is required for the accumulation of HLA3 as well as LCIA and for the photosynthetic affinity against Ci. Similarly, the accumulation of LHCSR3 was decreased by the addition of BAPTA.

To further examine the regulation of these HCO_3^- transporters by an intracellular Ca^{2+} signal, the impact of N-(6-aminohexyl)-5-chloro-1-naphthalenesulfonamide hydrochloride (W-7), a membrane-permeable calmodulin antagonist on the accumulation of HLA3 and LCIA and photosynthetic Ci affinity was examined. In the presence of W-7, concentration-dependent effects of decreased accumulation of HLA3 and LCIA were observed as in the case of LHCSR3 (Fig. 34C) (Petroutsos et al., 2011; Maruyama et al., 2014), and concomitantly $K_{0.5}$ (Ci) was increased from 59 ± 18 μM (Mock) to 235 ± 48 μM in the presence of 75 μM W-7 (Fig. 34D). On the other hand, the addition of N-(6-aminohexyl)-1-naphthalenesulfonamide hydrochloride (W-5), a biologically inactive calmodulin antagonist, did not show any significant effects. As a control, LCIB was accumulated normally in the presence of both chemicals. These results suggested that a calmodulin-mediated Ca^{2+} signal could be involved in the LC-induced accumulation of HLA3 and LCIA. Additionally, the addition of BAPTA or W-7 had no effect on changes in CAS and LCIB localization (Fig. 34E).

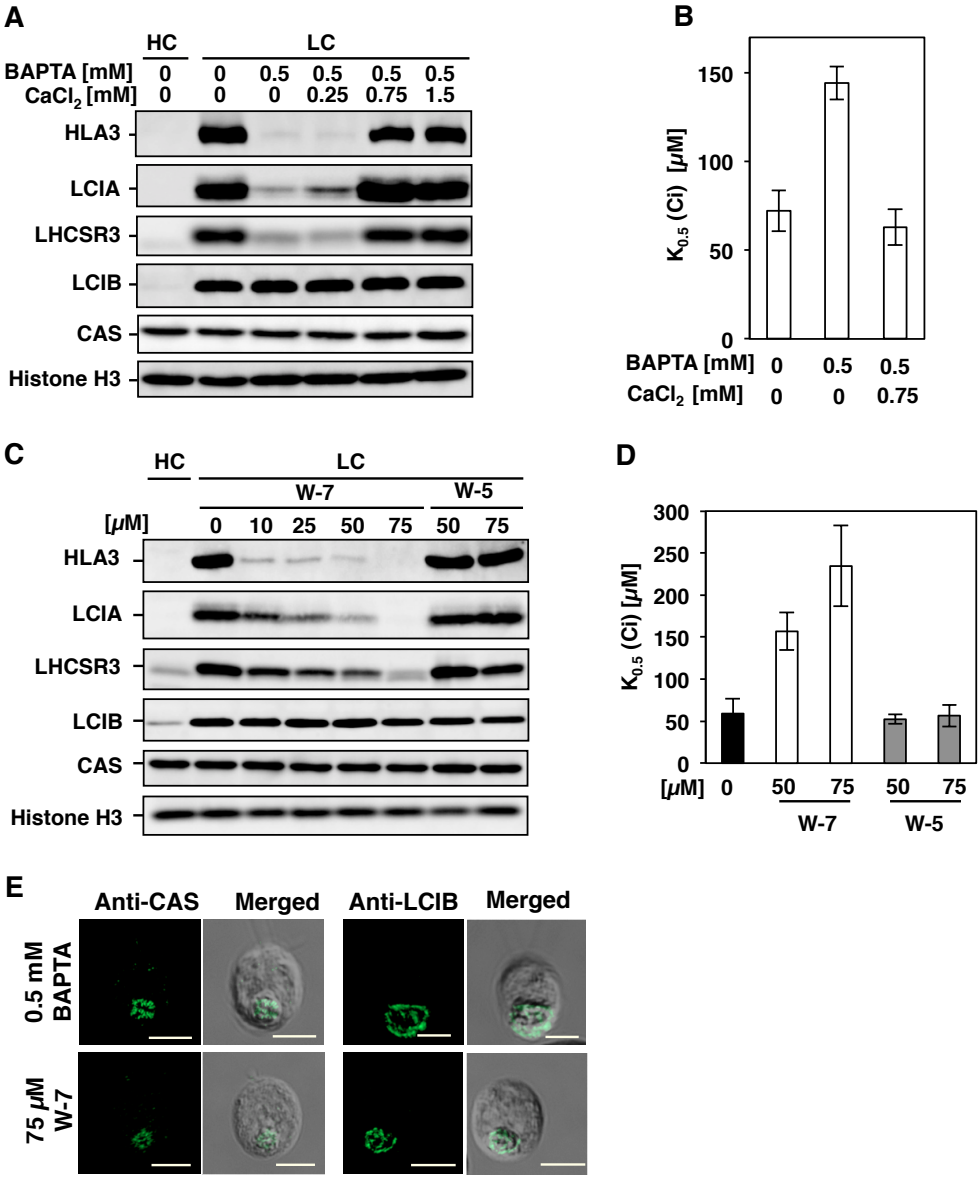

Figure 34. The effects of extracellular calcium (Ca^{2+}) chelator 1,2-bis (*o*-aminophenoxy) ethane-N, N, N, N'-tetraacetic acid (BAPTA) or N-(6-aminohexyl)-5-chloro-1-naphthalenesulfonamide hydrochloride (W-7) on the accumulation of HLA3, LCIA, LHCSR3, LCIB, and CAS (A and C), on inorganic carbon (Ci) affinity (B and D), and on the localization of CAS as well as LCIB (E) in low-CO_2 (LC) conditions. High-CO_2 (HC)-grown wild-type (WT) cells were centrifuged, re-suspended by fresh HSM medium in the presence of the indicated chemicals and cultured in LC conditions for 2 h. In the absence of any indicated additional reagents, HSM liquid medium contained 0.068 mM $CaCl_2$. N-(6-aminohexyl)-1-naphthalenesulfonamide hydrochloride (W-5), an inactive calmodulin antagonist, was used as a control for W-7. (A and C) Histone H3 was used as a loading control. (B and D) Photosynthetic O_2-evolving activity was measured at pH 7.8. Data in all experiments indicate mean value ± standard deviation (SD) from three biological replicates. (E) The localization of CAS and LCIB was examined by indirect immunofluorescence assay.

8. Increased fluorescence signal of a calcium indicator in the pyrenoid in response to CO_2 and light

Because *At*CAS had low Ca^{2+}-binding affinity (Han et al., 2003), a high Ca^{2+} concentration should be required for the Ca^{2+}-binding of CAS. It raised the possibility that the subcellular regions where free Ca^{2+} is enriched could be associated with CAS localization. To test this hypothesis, we monitored the fluorescence of Calcium Green-1 AM, a Ca^{2+}-sensitive fluorescent dye, in WT and H82 cells (Fig. 35A). In both HC and LC conditions, apparent fluorescent signals were detected in regions that overlapped with chlorophyll. Notably, high levels of fluorescent signals were observed in the region of the pyrenoid in both WT and H82 cells, especially in LC-light conditions, thereby suggesting that free Ca^{2+} might be concentrated in the pyrenoid. These increased fluorescent signals in LC-light conditions were not impaired by the *CAS* mutation (Fig. 35A) or by the addition of BAPTA or W-7 (Fig. 35B).

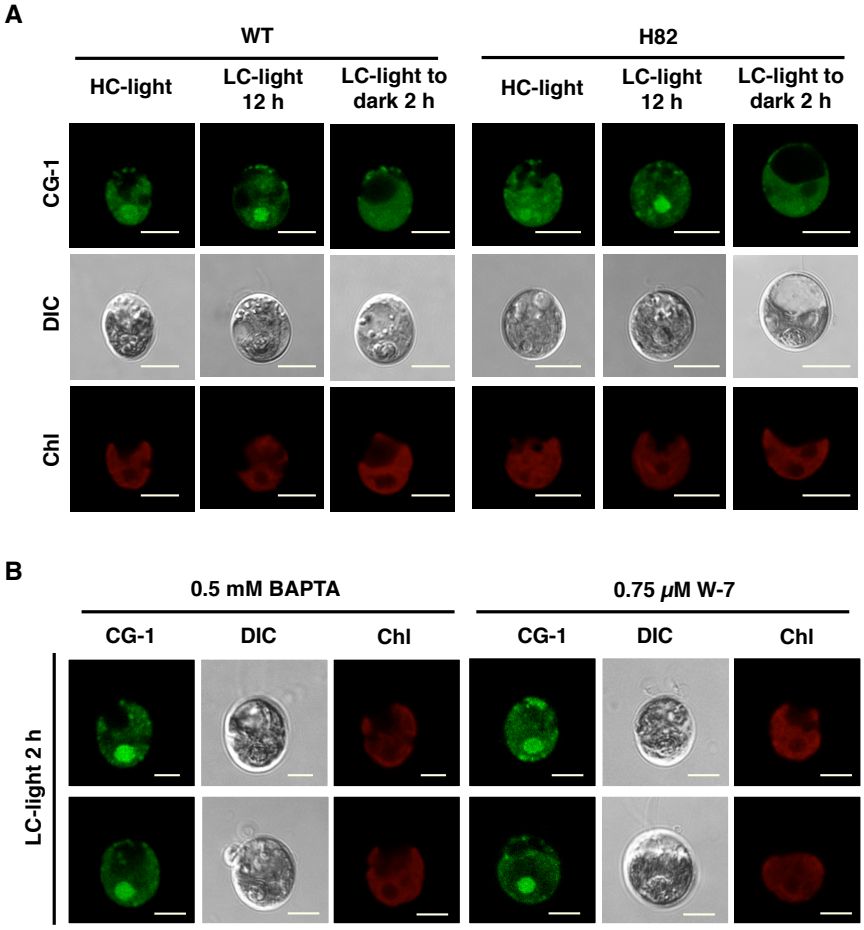

Figure 35. Calcium Green-1, AM (CG-1) fluorescence in wild-type (WT) and H82 cells, and the effect of 1,2-bis (*o*-aminophenoxy) ethane-N, N, N, N'-tetraacetic acid (BAPTA) or N-(6-aminohexyl)-5-chloro-1-naphthalenesulfonamide hydrochloride (W-7) on the fluorescence of Calcium Green-1 AM. (A) Cells were grown in high-CO_2 (HC) or low-CO_2 (LC) conditions for 12 h in light or cells in LC-light conditions were transferred to LC-dark conditions for 2 h, then incubated with CG-1 at room temperature for 30 min. Fluorescence images derived from CG-1 treatments and chlorophyll (Chl) are shown. Each image is placed with the flagella facing upward on the panel. DIC, differential interference contrast image. Scale bars, 5 μm. (B) Cells were grown in LC-light conditions for 2 h. The chemical being tested was added to fresh medium before shifting from HC to LC conditions.

In contrast, the fluorescent signals in the pyrenoid were decreased after shifting from LC-light to LC-dark conditions for 2 h. Additionally, the signal intensities of the Ca^{2+} indicator in chloroplast region were slightly stronger in H82 than in WT cells after switching to LC conditions for 12 h (Fig. 35A), suggesting a higher free Ca^{2+} concentration in the chloroplast of H82 cells. Considering that the depletion of CAS protein does not affect the total cellular Ca^{2+} content (Petroutsos et al., 2011), increased free Ca^{2+} could be caused by the redistribution of internal Ca^{2+}.

Discussion

Genes responsible for the high-CO_2-requiring phenotype in mutants

In this study, I isolated three HC-requiring mutants defective in the induction of the CCM. The decreased growth rates and decreased LCE activity of the obtained mutants in LC conditions indicated that supplying HC is essential for their survival. The P103 mutant showed a similar accumulation profile of the examined CCM-related proteins to that in C16 cells (Fig. 14), strongly implying that the lack of CCM1 protein caused by a frame shift was responsible for its HC-requiring phenotype. In the H24 mutant, only HLA3 of the CCM-related proteins examined was absent. It was reported that knockdown (Duanmu et al., 2009b) or knockout (Yamano et al., 2015) of HLA3 alone resulted in only modest decreases in photosynthetic Ci affinity and Ci uptake in neutral pH conditions. However, H24 cells exhibited severe retarded growth in LC conditions, as shown in spot tests performed at pH 7.0 (Fig. 11). This was possibly because the absence of HLA3 was not the main cause of the HC-requiring phenotype, and the accumulation of other proteins related to the CCM could be absent. Furthermore, although an *aphVII* cassette was inserted in the *UCH* gene in H24 cells, two of its hyg-sensitive progenies failed to grow in LC conditions (Fig. 19), suggesting that the *aphVII* insertion in the *UCH* gene was not linked to its HC-requiring phenotype. This means that the HC-requiring phenotype in H24 may not be caused by the disrupted *UCH* gene. In contrast, accumulation of HLA3 and LCIA in the H82 mutant was significantly decreased compared with that in WT cells in LC conditions (Fig. 14). Considering that *aphVII* insertion into CAS, as confirmed by PCR, was closely linked with the HC-requiring phenotype in all progenies examined, the genetic locus responsible for the HC-requiring phenotype as well as the defective accumulation of HLA3 and LCIA appeared to contain the *CAS* gene.

High-CO_2-requiring phenotype caused by the *CAS* mutation

By characterization of the *CAS* insertion mutant and its complemented strains, the disrupted *CAS* gene was responsible for the HC-requiring phenotype of H82 (Fig. 20-22). The defects in the photosynthetic Ci affinity and LCE activity caused by the *CAS* mutation was similar to that affected by the lack of the master regulator CCM1 (Table 4; Fig. 13), suggesting an important physiological roles of CAS in the CCM. Furthermore, the HC-requiring phenotype of H82 was partially rescued in dim light, supporting a previous conclusion that induction of the CCM is also dependent on light intensity, in addition to the CO_2-limiting conditions (Yamano et al., 2008). Additionally, the retarded growth rate caused by the loss of CAS in H82 cells was not rescued by the addition of excess Ca^{2+} (3.06 mM), although the defects in photoacclimation by downregulated CAS protein could be rescued by the addition of excess Ca^{2+} (3.06 mM) to the culture medium (Petroutsos et al., 2011). It was suggested that the existence of CAS protein could be important for restoring the growth of H82 cells by the addition of excess Ca^{2+} in the culture medium.

CAS-dependent expression of nuclear-encoded low-CO_2-induced genes

RNA-seq analyses of the *CAS* insertion mutant and its complemented strains revealed that CAS is required for maintaining the expression of at least 13 nuclear-encoded LC-induced genes after induction (Table 6 and Fig. 25). Of those genes regulated by CAS, *HLA3* and *LCIA*, whose accumulation was decreased in H82 cells (Fig. 24A), are involved in cooperative HCO_3^- uptake activity into the chloroplast stroma for operation of the CCM. However, simultaneous expression of HLA3 and LCIA in H82 cells could only rescue 46% of the decreased Ci affinity (Fig. 22A), suggesting that some of the 11 CO_2-limiting-inducible genes other than *HLA3* and *LCIA* could contribute to the operation of the CCM in *Chlamydomonas* cells. For example, the putative chaperone, DNJ31-like protein responds to CO_2-limiting stress and its expression was regulated by the master regulator CCM1 (Fang et al., 2012). PPP30 belongs to the Type 2C protein phosphatases family that was reported to regulate the MAPK pathway of stress signaling (Fuchs et al., 2013). Considering that several important components of the CCM, such as CAH3 and LCIB, possess putative phosphorylation sites (Blanco-Rivero et al., 2012; Yamano et al., 2010), PPP30 might be involved in the CCM by catalyzing the dephosphorylation of these proteins. In addition, the mRNA abundance and accumulation of LHCSR3 were decreased by the lack of CAS in LC conditions at 2 h (Table 6 and Fig. 26), supporting the previous report that down-regulation of CAS protein in *Chlamydomonas* decreased the accumulation levels of LHCSR3 (Petroutsos et al., 2011). Because the mRNA abundances of these 12 genes except for an unannotated gene (*Cre12.g541550*) were also decreased by the *CIA5* mutation (Fang et al., 2012), CAS could be required for maintaining the mRNA levels of these LC-induced genes after initial induction by CCM1/CIA5. The fact that accumulation of CCM1 was not inhibited by the loss of CAS protein (Fig. 14) and vice versa (Fig. 31D), and that CAS could change its localization to pyrenoid-tubules in response to LC-light conditions irrespective of CCM1 (Fig. 31C), suggest that CCM1 and CAS could individually function in the regulation of CCM. Considering the recent report that *At*CAS regulates nuclear gene expression though the nuclear transcription factor ABI4 (Guo et al., 2016), the CAS-mediated expression of these CAS-dependent genes could involve a possible transcription factor. Further studies of the corresponding insertion mutants with disruption of these CAS-dependent genes could clarify their roles in the CCM and the relationship between CCM1 and CAS.

Aggregation of CAS protein in the pyrenoid in response to CO_2 and light

Thylakoid membrane-localized CAS changed its localization from dispersed region in HC-light or LC-dark conditions, where the CCM was inactive, to an aggregated tubule-like structure in the pyrenoid in LC-light conditions, where the CCM is active (Fig. 29A). This means that the aggregation of CAS to the pyrenoid occurs in response to the availability of environmental light and CO_2 is important for regulation of the CCM. Considering that pyrenoid is penetrated by some of the thylakoid membrane, which are termed pyrenoid tubules (Ohad et al., 1967), it is possible that CAS could be localized in or along the pyrenoid tubules in LC-light conditions and could change its localization reversibly in response to CO_2

and light (Fig. 29C). The change in CAS localization was independent of *de novo* protein synthesis (Fig. 31A), which was different from the case of LCIB (Yamano et al., 2014), suggesting that aggregated CAS is not newly synthesized and CAS itself could move in response to light and CO_2 conditions. This distinct localization of CAS could be explained by the thylakoid membrane remodeling observed previously in varying light conditions (Chuartzman et al., 2008), although the actual mechanism for the change in localization requires further analysis.

The photosynthetic electron transport chain is comprised of a series of proteins, which could be over-reduced because of the suppressed activity of photosynthetic CO_2 fixation in CO_2-limiting conditions and the continuous production energized electron in light. As inhibitors of photosynthetic electron transfer, DCMU and DBMIB could alleviate the reduction of some photosynthetic electron transport-related proteins, such as plastocyanin, cytochrome b6f complex, and PSI. Considering that the CAS relocation was inhibited by the addition of DCMU or DBMIB (Fig. 30A), it is possible that the over-reduction of these proteins is triggers of CAS relocation. To know whether the relocation of CAS is dependent on the energy carrier, ATP, the effect of inhibitors of ATP synthesis, such as carbonyl cyanide p-trifluoromethoxyphenyl hydrazone (FCCP), should be evaluated. Trigger of relocation of CAS into the pyrenoid as well as Ca^{2+} in response to changes in availability of CO_2 and light could be key regulatory factors for CO_2-sensing mechanisms in photosynthetic eukaryotes.

In LC-light conditions, the CAS protein is localized in the pyrenoid tubules (Fig. 29A and B) and exposed to the stromal side of the thylakoid membrane (Fig. 28D). Recent three-dimension structural analysis of the pyrenoid showed that multiple minitubules were bundled in each pyrenoid tubule (Engel et al., 2015), raising the possibility that CAS protein could be localized in these minitubules. However, the size of the complex containing CAS protein was predominantly 120 kDa or 240 kDa (Fig. 32), whose diameter was approximately 6 nm or 8 nm (Erickson, 2009). Considering that the diameter of the minitubule lumen is 3–4 nm by 8–15 nm, CAS is too big to be located inside the minitubules. This means that CAS could be localized in the thylakoid membrane and exposed to the pyrenoid matrix. To determine the detailed localization of CAS protein, an immunogold labelling using anti-CAS antibody should be conducted. In addition to CAS, hundreds of proteins, including, Rubisco, CAH3 and EPYC1, were also enriched in the pyrenoid in response to LC conditions (Mackinder et al., 2016). Further studies on the relocation of these proteins in the *CAS* mutant could be helpful to understand the relationships between CAS and proteins such as CAH3 and EPYC1. Additionally, a portion of Rubisco and CAH3 proteins were aggregated in pyrenoid even in dark conditions, after switching from HC to LC for 12 h (Mitchell et al., 2014). As a constitutive protein, some of CAS might also change its localization to pyrenoid in response to LC stress in dark conditions for 12 h, although further studies are required.

Retrograde signal generated by CAS protein in regulation of nuclear-encoded low-CO_2-induced genes

Taken with the fact that the accumulation of chloroplast-envelope-localized LCIA is required for the expression of *HLA3*, unknown retrograde signals from the chloroplast to nuclear genes have been suggested to support the CCM (Yamano et al., 2015). This study further revealed a new regulatory pathway associated with chloroplast-retrograde signaling from thylakoid- and/or pyrenoid-tubule-localized CAS to nuclear genes, because CAS was shown to be essential to maintain the expression of 13 genes possibly important for the operation of the CCM, including both *HLA3* and *LCIA*.

When chelating external Ca^{2+} by the application of BAPTA, the accumulation of HLA3 and LCIA was decreased, and the addition of $CaCl_2$ restored the accumulation (Fig. 34A). Because BAPTA cannot permeate the plasma membrane, it remains in the extracellular space (Polisensky and Braam, 1996) and prevents the elevation of both $[Ca^{2+}]_{cyt}$ and $[Ca^{2+}]_{stro}$ (Normura et al., 2012), suggesting that the elevation of intracellular Ca^{2+} is required for the accumulation of these two HCO_3^- transporters. In terrestrial plants, the fact that CO_2-induced changes in $[Ca^{2+}]_{cyt}$ and stomatal closing were attenuated by chelating or without adding external Ca^{2+} (Kim et al., 2010), raises a hypothesis for the participation of $[Ca^{2+}]_{cyt}$ in CO_2 signal transduction in guard cells. Considering that CAS also mediates transient elevation of $[Ca^{2+}]_{stro}$ and $[Ca^{2+}]_{cyt}$ (Nomura et al., 2008; Nomura et al., 2012), regulating the activity of nuclear transcription factor ABI4 through the phosphorylation by MAPK in *Arabidopsis* (Guo et al., 2016), the regulation of these HCO_3^- transporters by CAS could be through Ca^{2+} signals resulting from the influx of $[Ca^{2+}]_{ext}$ into the cytosol of *Chlamydomonas* cells. To test this hypothesis, the $[Ca^{2+}]_{cyt}$ in the *CAS* mutant when switching from HC to LC conditions should be compared with that of the WT strain by application of the a molecular Ca^{2+} indicator, such as cameleon and aequorin. The global transcriptional profile in LC-grown WT cells by RNA-seq analysis in the presence of BAPTA or W-7 should also be compared with those of CAS-dependent genes.

But, we could not rule out the possibility that other retrograde signals are involved in the CAS-mediated regulation of CCM. So far, several candidate signaling pathways and signaling molecules from chloroplast have been suggested to regulate nuclear gene expression in land plants, including reactive oxygen species (ROS) in high-light stress (Apel and Hirt, 2004), 3'-phosphoadenosine -5'-phosphate (PAP) in drought and high-light stresses (Estavillo et al., 2011), β-cyclocitral in high-light stress (Ramel et al., 2012), and tetrapyrroles (Strand et al., 2003; Woodson et al., 2011), chloroplast redox signal (Pfannschmidt et al., 2003), and abscisic acid in high-light stress (Wasilewska et al., 2008). In particular, chloroplast redox state in multiple physiological processes (Mochiji and Wakabayashi, 2012; Kabeya and Miyagishima, 2013), ROS production in multiple stresses (Stoiber et al., 2013; Zuo et al., 2014) and heme-derived linear tetrapyrroles in phototrophic growth (Duanmu et al., 2013) were focused on in *C. reinhardtii* as candidates of retrograde signals. Thus, the chloroplast redox states, ROS levels, and the amount of tetrapyrroles should be evaluated in H82 mutant during shifting from HC to LC conditions in future studies.

Possible roles of the N-terminus and C-terminus of the CAS protein

With the employment of a membrane-permeable Ca^{2+} indicator, free Ca^{2+} could be enriched in the pyrenoid, especially in LC-light conditions (Fig. 35A). Considering that the Ca^{2+}-binding sites of CAS appeared to be low affinity and high capacity (Han et al., 2003), the coexistence of CAS and enriched Ca^{2+} in the pyrenoid could be important to activate CAS function. Considering that the high levels of fluorescence signals in the pyrenoid were not affected by chelating the $[Ca^{2+}]_{ext}$ in the presence of BAPTA (Fig. 35B), the increased free Ca^{2+} in the pyrenoid in LC conditions could be released from the thylakoid lumen, which was regarded as a Ca^{2+} store (Hochmal et al., 2015), rather than from the entry of $[Ca^{2+}]_{ext}$. A rhodanese-like domain lacking the catalytic residue conserved in the C-terminal region of CAS is thought to exhibit a regulatory function rather than an enzymatic one (Bordo et al., 2002; Hochmal et al., 2015), might accounting for the consequent signal transduction followed by binding of Ca^{2+} at its N-terminus. Furthermore, considering that chloroplastic Ca^{2+} is important for the chloroplast metabolism and the function of the thylakoid (Hochmal et al., 2015), where the CAS protein is localized (Fig. 28B), it is possible that the absence of the calcium-binding protein CAS could cause damage to the thylakoid or pyrenoid structure in H82 cells in LC conditions. Of note, stronger fluorescent signals derived from the Ca^{2+} indicator in the pyrenoid in LC-light conditions were also observed in H82 cells (Fig. 35A), and this was not affected by the perturbation of intracellular Ca^{2+} homeostasis (Fig. 35B), suggesting that the change in Ca^{2+} concentration is not directly regulated by CAS protein. To further examine the function and property of each domain of the CAS protein, the effect of expressing modified CAS with truncated N-terminus, truncated C-terminus, truncated hydrophobic sequence, or specific mutations on the CO_2-requiring phenotype should be evaluated.

Regulation of LHCSR3 by CAS in response to low-CO_2 stress

LHCSR3 is a crucial component for the energy-dependent quenching (qE) in high-light conditions (Peer et al., 2009; Allorent et al., 2013). In addition to the high-light stress, LHCSR3 is also induced by LC stress (Yamano et al., 2008; Polukhina et al., 2016). Because LC stress induces a quenching by state transition (qT) rather than the LHCSR3-modulated qE in high-light conditions (Iwai et al., 2007), the function of accumulated LHCSR3 in LC conditions remains to be clarified. Considering that the artificial LC conditions is used to mimic the air conditions in present atmosphere containing 0.04% CO_2, it suggests that *Chlamydomonas* cells grown in nature environment always accumulate LHCSR3, leading to a rapid induction of qE in acclimation to the fluctuating light in nature.

Although it was proposed that CAS regulates the accumulation of LHCSR3 for qE in a long period in acclimation to high-light stress (Petroutsos et al., 2011), CAS only regulates LHCSR3 accumulation at an early stage of CCM in LC conditions (Fig. 26), suggesting that CAS regulates LHCSR3 to different extents in response to different stresses. Furthermore, because of the crosstalk between carbon supply and photoacclimation in *C. reinhardtii* (Polukhina et al., 2016), CAS could be involved in the different strategies of the acclimation to high-light stress in different CO_2 availability, or the acclimation to LC

stress in different light conditions. To examine the individual functions of CAS in response to high-light or LC stress, photosynthetic characteristics, including qT and qE, in H82 cells grown under high-light and HC, high-light and LC, low-light and HC, or low-light and LC conditions should be measured.

Regulation of the CO_2-concentrating mechanism by CAS is independent of cyclic electron flow

Because it was reported that CEF activity increases in LC conditions possibly for increased ATP demand for Ci uptake in the CCM (Lucker and Kramer, 2013), and that CAS is a component of the CEF complex formed in anaerobic conditions (Iwai et al., 2010; Terashima et al., 2012), it was possible that CAS-dependent CEF might contribute to the CCM. However, CEF activity was not affected by the lack of CAS protein in LC conditions at 120 μmol photons·m^{-2}·s^{-1} when the CCM is induced (Fig. 23). To some extent, this result coincided with the previous finding that down-regulation of CAS did not impair the CEF activity in aerobic conditions (Terashima et al., 2012). These results suggested that CEF is not involved in CAS-dependent regulation of the CCM. Additionally, CAS was proposed to interact with PGRL1 in the CEF complex with a size of 1,000 kDa in anaerobic conditions (Terashima et al., 2012), but in HC and LC conditions (regarded as typical aerobic conditions), CAS is part of a protein complex of 120 kDa or 240 kDa (Fig. 32). These results suggest that CAS functions in smaller complexes in aerobic conditions than that in anaerobic conditions. To determine that whether components other than CAS existed in these two protein complexes in aerobic conditions, the LC-MS/MS analysis of these two protein complexes should be further performed. Although both the *CAS* and *PGRL1* mutations caused an HC-requiring phenotype in normal light conditions, the *CAS* mutant was more sensitive to CO_2-limiting stress than the *pgrl1* mutant in dim light (Fig. 21). This suggested that the function of CAS might not totally overlap with that of PGRL1 in aerobic conditions.

Tentative model for the function of CAS in regulation of the CO_2-concentrating mechanism

Based on these results, a tentative model was proposed to illustrate a function of CAS in CO_2- and Ca^{2+}-mediated regulation of the CCM in *Chlamydomonas* cells (Fig. 36). In HC-light conditions, *Chlamydomonas* cells can obtain sufficient amounts of CO_2 for photosynthesis by the passive diffusion of extracellular CO_2 (Fig. 36A). In LC-light conditions, reduced extracellular Ci concentrations cause CO_2-limiting stress and a decrease in photosynthetic activity (Fig. 36B). To acclimate to this stress, CCM1/CIA5 rapidly induces the expression of CCM-related genes including *HLA3* and *LCIA* within 0.3 h (Fang et al., 2012). Besides, in response to LC stress in the light, Ca^{2+}-binding protein CAS changes its localization to the pyrenoid where enriched calcium could facilitate its Ca^{2+}-binding. This change in localization could be dependent on photosynthetic electron transfer because of inhibition by DCMU and DBMIB (Fig. 30A). Subsequently, CAS mediates a retrograde signal from the thylakoid membrane in chloroplast to the nucleus to maintain the expression of *HLA3* and *LCIA* (Table 6). It is possible that the rhodanese-like domain in the C-terminal region could be associated with regulatory signaling (Brodo et al., 2002; Hochmal et al., 2015). Considering that *Arabidopsis* CAS was proposed to mediate the transient

elevation of $[Ca^{2+}]_{cyt}$ and $[Ca^{2+}]_{stro}$ (Nomura et al., 2012; Gao et al., 2016) and that perturbation of intracellular Ca^{2+} homeostasis impaired the accumulation of HLA3 and LCIA (Fig. 33A and C), the internal Ca^{2+} signal could be mediated by CAS as a retrograde signal. This internal Ca^{2+} signal could be caused by the entry of $[Ca^{2+}]_{ext}$, because the accumulation of HLA3 and LCIA was defected by chelating $[Ca^{2+}]_{ext}$ (Fig. 34A). Finally, cells obtain concentrated Ci by transporter-mediated uptake of HCO_3^- and increase the CO_2 concentrations around Rubisco.

Regulation of the CO_2-concentrating mechanism in aquatic photosynthetic organisms

The regulation of the CCM has been studied in cyanobacteria (Omata et al., 2001; Wang et al., 2004; Klahn et al., 2015), *C. reinhardtii* (Xiang et al., 2001; Fukuzawa et al., 2001; Yoshioka et al., 2004), and diatoms (Harada et al., 2006; Tanaka et al., 2016). Three regulatory factors (CmpR, CcmR, and cyAbrB2) and two regulatory factors (CCM1 and LCR1) have been identified in cyanobacteria and *C. reinhardtii*, respectively, suggesting that protein-mediated regulation is involved in the regulatory network of the CCM. The identification of the novel regulatory factor CAS in this study helps to further understand the regulation of the CCM through retrograde signals from chloroplast, although CAS is specifically conserved in green eukaryotic photosynthetic organisms (Normura et al., 2008) rather than cyanobacteria and diatoms. In addition to the second messenger cAMP in diatoms (Harada et al., 2006; Tanaka et al., 2016), another second messenger, Ca^{2+} signaling was shown to regulate the *Chlamydomonas* CCM in this study. Considering that Ca^{2+} signaling is involved in the cellular responses to environmental changes in cyanobacteria, including the nitrogen starvation (Leganes et al., 2009) and heat stress (Tiwari et al., 2016), and in diatoms, such as photophobic response (Mclachlan et al., 2012), Ca^{2+} signaling could be also important for the CCM induction in these organisms. The CAS-mediated retrograde signal was already developed in the green algae lineage, throwing new light on understanding the crosstalk between Ca^{2+}- and CO_2-dependent signal transduction pathways in photosynthetic organisms in response to CO_2 and light.

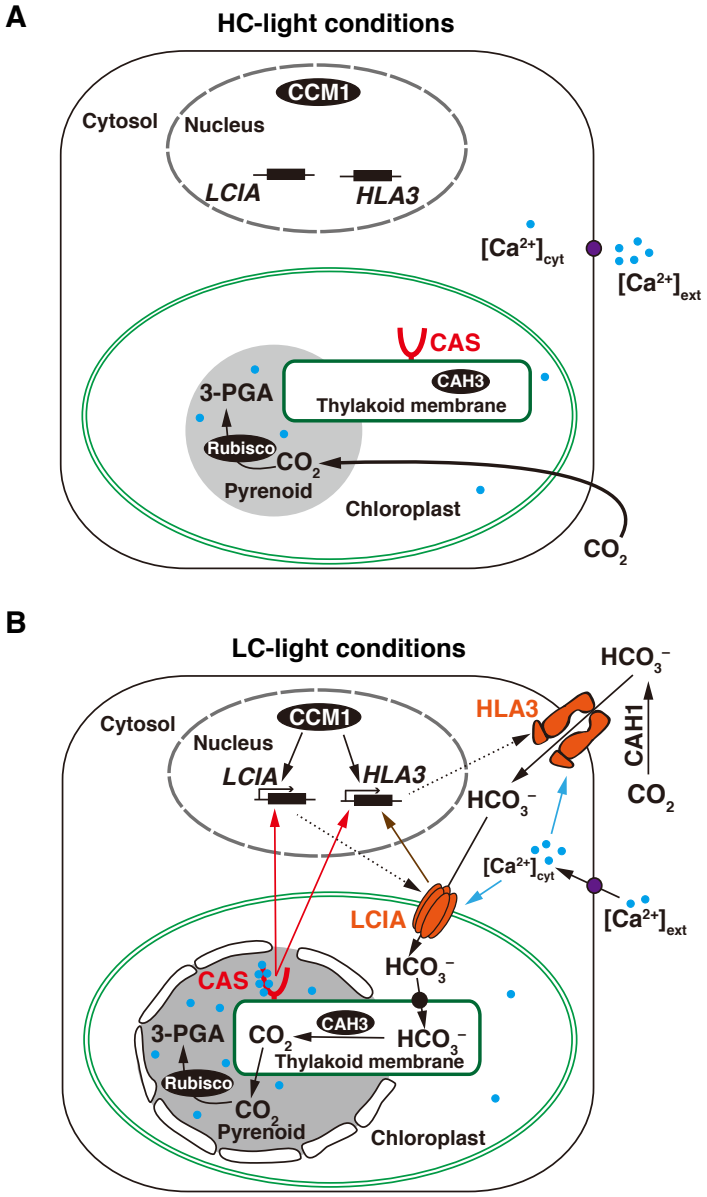

Figure 36. A tentative model illustrating how CAS protein and Ca^{2+} regulate the expression of *HLA3* and *LCIA* during CCM induction by switching from high-CO_2 (HC)-light (A) to low-CO_2 (LC)-light (B) conditions. The red structure indicates the CAS protein. The CAS-meditated pathways involved in regulating the expression of *HLA3* and *LCIA* are shown as red arrows. The purple dot indicates a putative plasma membrane-localized Ca^{2+} transporter. The Ca^{2+}-mediated pathways involved in regulating accumulation of HLA3 and LCIA are represented as blue arrows. Ca^{2+} ions are indicated as blue dots. The LCIA-mediated pathway involved in regulating expression of *HLA3* is indicated as brown arrows. PGA, phosphoglyceric acid; CAH, carbonic anhydrase.

Conclusion

In this study, by screening the DNA-tagged transformants, three HC-requiring mutants, including H24, H82, and P103 were isolated. In particular, an ortholog of Ca^{2+}-binding protein CAS, originally found in *A. thaliana*, was disrupted by the insertion of a hygromycin-resistance gene cassette in H82 cells. The thylakoid membrane-localized Ca^{2+}-binding protein CAS could control the expression of at least 44 nuclear-encoded genes including *HLA3* and *LCIA* by post-transcriptional regulation in a Ca^{2+}-dependent manner during induction of the CCM. Furthermore, CAS protein changed its localization from dispersed across the thylakoid membrane to being associated with tubule-like structures in the pyrenoid in response to LC stress in light. CCM1 and CAS could individually function in regulating the expression of *HLA3* and *LCIA* in response to CO_2 and light. These findings suggest that *Chlamydomonas* CAS regulates CCM and the expression of *HLA3* and *LCIA* through a Ca^{2+}-mediated retrograde signal from the thylakoid in the chloroplast to the nucleus in response to CO_2 and light.

References

Aizawa, K., Miyachi, S. (1986) Carbonic anhydrase and CO_2 concentrating mechanisms in microalgae and cyanobacteria. *FEMS Microb. Rev*. **39**, 215–233.

Allmer, J., Naumann, B., Markert, C., Zhang, M., Hippler, M. (2006) Mass spectrometric genomic data mining: Novel insights into bioenergetic pathways in *Chlamydomonas reinhardtii*. *Proteomics* **6**, 6207–6220.

Allorent, G., Tokutsu, R., Roach, T., Peers, G., Cardol, P., Girard-Bascou, J., Seigneurin-Berny, D., Petroutsos, D., Kuntz, M., Breyton, C., Franck, F., Wollman, F.A., Niyogi, K.K., Krieger-Liszkay, A., Minagawa, J., Finazzi, G. (2013) A dual strategy to cope with high light in *Chlamydomonas reinhardtii*. *Plant Cell* **25**, 545–557.

Alric, J., Lavergne, J., Rappaport, F. (2010) Redox and ATP control of photosynthetic cyclic electron flow in *Chlamydomonas reinhardtii* (I) aerobic conditions. *Biochim. Biophys. Acta.* **1797**, 44–51.

Apel, K., Hirt, H. (2004) Reactive oxygen species: metabolism, oxidative stress, and signal transduction. *Annu. Rev. Plant Biol.* **55**, 373–399.

Atkinson, N., Feike, D., Mackinder, L.C.M., Meyer, M.T., Griffiths, H., Jonikas, M.C., Smith, A.M., McCormick, A.J. (2016) Introducing an algal carbon-concentrating mechanism into higher plants: location and incorporation of key components. *Plant Biotechnol. J*. **14**, 1302–1315.

Badger, M.R., Kaplan, A., Berry, J.A. (1980) Internal inorganic carbon pool of *Chlamydomonas reinhardtii*-evidence for a carbon-dioxide concentrating mechanism. *Plant Physiol.* **66**, 407–413.

Badger, M.R., Price, G.D. (1992) The CO_2 concentrating mechanism in cyanobacteria and microalgae. *Physiol. Plant.* **84**, 606–615.

Badger, M.R., Andrew, T.J., Whitney, S.M., Ludwig, M., Yellowlees, D.C., Leggat, W., Price, G.D. (1998) The diversity and coevolution of Rubisco, plastids, pyrenoid, and chloroplast-based CO_2-concentrating mechanisms in algae. *Can. J. Bot.* **76**, 1052–1071.

Badger, M.R., Hanson, D., Price, G.D. (2002) Evolution and diversity of CO_2 concentrating mechanisms in cyanobacteria. *Funct. Plant Bio.* **29**, 161–173.

Badger, M.R., Price, G.D. (2003) CO_2 concentrating mechanism in cyanobacteria: molecular components, their diversity and evolution. *J. Exp. Bot*. **54**, 609–622.

Baek, K., Kim, D.H., Jeong, J., Sim, S.J., Melis, A., Kim, J.S., Jin, E., Bae, S. (2016) DNA-free two-gene knockout in *Chlamydomonas reinhardtii* via CRISPR-Cas9 ribonucleoproteins. *Sci. Rep.* **doi**, 10.1038.

Benson, A.A., and Calvin, M. (1950) Carbon dioxide fixation by green plants. *Annu. Rev. Plant Physiol*. **1**, 25–42.

Berthold, P., Schmitt, R., Mages, W. (2002) An engineered *Streptomyces hygroscopicus aphVII* gene mediates dominant resistance against hygromycin B in *Chlamydomonas reinhardtii*. *Protist* **153**, 401–412.

Blanco-Rivero, A., Shutova, T., Roman, M.J., Villarejo, A., Martinez, F. (2012) Phosphorylation controls the localization and activation of the luminal carbonic anhydrase in *Chlamydomonas reinhardtii*. *PLoS One* **7**, e49063.

Bordo, D., Bork, P. (2002) The rhodanese/Cdc25 phosphatase superfamily. *EMBO Rep.* **3**, 741–746.

Brueggeman, A.J., Gangadharaiah, D.S., Cserhati, M.F., Casero, D., Weeks, D.P., Ladunga, I. (2012) Activation of the carbon concentrating mechanism by CO_2 deprivation coincides with massive transcriptional restructuring in *Chlamydomonas reinhardtii*. *Plant Cell* **24**, 3843.

Burkhardt, S., Amoroso, G., Riebesell, U., Sultemeyer, D. (2001) CO_2 and HCO_3^- uptake in marine diatoms acclimated to different CO_2 concentrations. *Limnol. Oceanogr.* **46**, 1378–1391.

Burnap, R.L., Nambudiri, R., Holland, S. (2013) Regulation of the carbon-concentrating mechanism in the cyanobacterium *Synechocystis* sp. PCC6803 in response to changing light intensity and inorganic carbon availability. *Photosynth. Res.* **118**, 115–124.

Burnap, R.L., Hagemann, M., Kaplan, A. (2015) Regulation of CO_2 concentrating mechanism in cyanobacteria. *Life* **5**,348–371.

Cameron, J.C., Wilson, S.C., Bernstein, S.L., Kerfeld, C.A. (2013) Biogenesis of a bacterial organelle: the carboxysome assembly pathway. *Cell* **155**, 1131–1140.

Cannon, G.C., Baker, S.H., Soyer, F., Johnson D.R., Bradburne, C.E., Mehlman, J.L., Davies, P.S., Jiang, Q.L., Heinhorst, S., Shively, J.M. (2003) Organization of carboxysome genes in the *Thiobacilli*. *Curr. Microbio.* **46**, 115–119.

Chuartzman, S.G., Nevo, R., Shimoni, E., Charuvi, D., Kiss, V., Brumfeld, V., Reich, Z. (2008) Thylakoid membrane remodeling during state transitions in *Arabidopsis*. *Plant Cell* **20**, 1029–1039.

Clapham, D.E. (2007) Calcium Signaling. *Cell* **131**, 1047–1058.

Coleman, J.R., Grossman, A.R. (1984) Biosynthesis of carbonic anhydrase in *Chlamydomonas reinhardtii* during adaptation to low CO_2. *Proc. Natl. Acad. Sci. USA* **81**, 6049–6053.

Cot, S.S.W., So, A.K.C., Espie, G.S. (2008) A multiprotein bicarbonate dehydration complex essential to carboxysome function in cyanobacteria. *J. Bacteriol.* **190**, 936–945.

Cummins, E.P., Selfridge, A.C., Sporn, P.H., Sznajder, J.I., Taylor, C.T. (2014) Carbon dioxide-sensing in organisms and its implications for human disease. *Cell Mol. Life Sci.* **71**, 813–845.

Daley, S.M., Kappell, A.D., Carrick, M.J., Burnap, R.L. (2012) Regulation of the cyanobacterial CO_2-concentrating mechanism involves internal sensing of $NADP^+$ and alpha-ketogutarate levels by transcription factor CcmR. *PLoS ONE* **7**, e41286.

Dang, K.V., Plet, J., Tolleter, D., Jokel, M., Cuine, S., Carrier, P., Auroy, P., Richaud, P., Johnson, X., Alric, J., Allahverdiyeva, Y., Peltier, G. (2014) Combined increases in mitochondrial cooperation and oxygen photoreduction compensate for deficiency in cyclic electron flow in *Chlamydomonas reinhardtii*. *Plant Cell* **26**, 3036–3050.

Dawson, R.J.P., Locher, K.P. (2006) Structure of a bacterial multidrug ABC transporter. *Nature* **443**, 180–185.

Dent, R.M., Haglund, D.M., Chin, B.L., Kobayashi, M.C., Niyogi, K.K. (2005) Functional genomics of eukaryotic photosynthesis using insertional mutagenesis of *Chlamydomonas reinhardtii*. *Plant Physiol*. **137**, 545–556.

Driever, S.M., and Kromdijk, J. (2013) Will C_3 crops enhanced with the C_4 CO_2-concentrating mechanism live up to their full potential (yield)? *J. Exp. Bot*. **64**, 3925–3935.

Duanmu, D., Wang, Y., Spalding, M.H. (2009a) Thylakoid lumen carbonic anhydrase (*CAH3*) mutation suppresses air-dier phenotype of LCIB mutant in *Chlamydomonas reinhardtii*. *Plant Physiol*. **149**, 929–937.

Duanmu, D., Miller, A.R., Horken, K.M., Weeks, D.P., Spalding, M.H. (2009b) Knockdown of limiting-CO_2-induced gene *HLA3* decreases HCO_3^- transport and photosynthetic Ci affinity in *Chlamydomonas reinhardtii*. *Proc. Natl. Acad. Sci. USA* **106**, 5990–5995.

Duanmu, D., Casero, D., Dent, R.M., Gallaher, S., Yang, W., Rockwell, N.C., Martin, S.S.,Pellegrini, M., Niyogi, K.K., Merchant, S.S., Grossman, A.R., Lagarias, J.C. (2013) Retrograde bilin signaling enables *Chlamydomonas* greening and phototrophic survival. *Proc. Natl. Acad. Sci. USA* **110**, 3621–3626.

Engel, B.D., Schaffer, M., Cuellar, L.K., Villa, E., Plitzko, J.M., Baumeister, W. (2015) Native architecture of the *Chlamydomonas* chloroplast revealed by in situ cryo-electron tomography. *Elife* **4,** e04889, and correction (2015) **4**, e11383.

Engineer, C.B., Ghassemian, M., Anderson, J.C., Peck, S.C., Hu, H., Schroeder, J.I. (2014) Carbonic anhydrases, EPF2 and a novel protease mediate CO_2 control of stomatal development. *Nature* **513**, 246–250.

Engineer, C.B., Hashimoto-Sugimoto, M., Negi, J., Israelsson-Nordstrom, M., Azoulay-Shemer, T., Rappel, W.J., Iba, K., Schroeder, J.I. (2016) CO_2 sensing and CO_2 regulation of stomata conductance: advances and open questions. *Trends Plant Sci.* **21**, 16–30.

Erickson, H.P. (2009) Size and shape of protein molecules at the nanometer level determined by sedimentation, gel filtration, and electron microscopy. *Bio. Proced. Online*. **11**, 32–51.

Espie, G.S., Kimber, M.S. (2011) Carboxysomes: cyanobacterial RubisCO comes in small packages. *Photosynth. Res*. **109**, 7–20.

Estavillo, G.M., Crisp, P.A., Pornsiriwong, W., Wirtz, M., Collinge, D., Carrie, C., Giraud, E., Whelan, J., David, P., Javot, H., Brearley, C., Hell, R., Martin, E., Pogson, B.J. (2011) Evidence for a SAL1-PAP chloroplast retrograde pathway that functions in drought and high light signaling in *Arabidopsis*. *Plant Cell* **23**, 3992–4012.

Falkowski, P.G., Katz, M.E., Knoll, A.H., Quigg, A., Raven J.A., Schofield, O., Taylor F.J.R. (2004) The evolution of modern eukaryotic phytoplankton. *Science* **305**, 354–360.

Fang, W., Si, Y.Q., Douglass, S., Casero, D., Merchant, S.S., Pellegrini, M., Ladunga, I., Liu, P., Spalding, M.H. (2012) Transcriptome-wide changes in *Chlamydomonas reinhardtii* gene expression regulated by carbon dioxide and the CO_2-concentrating mechanism regulator CIA5/CCM1. *Plant Cell* **24**, 1876–1893.

Fuchs, S., Grill, E., Meskiene, I., Schweighofer, A. (2013) Type 2C protein phosphatases in plants. *FEBS J.* **280**, 681–693.

Fujiwara, S., Fukuzawa, H., Tachiki, A., Miyachi, S. (1990) Structure and differential expression of two genes encoding carbonic anhydrase in *Chlamydomonas reinhardtii*. *Proc. Natl. Acad. Sci. USA* **87**, 9779–9783.

Fujiwara, T., Kanesaki, Y., Hirooka, S., Era, A., Sumiya, N., Yoshikawa, H., Tanaka, K., Miyagishima, S.Y. (2015) A nitrogen source-dependent inducible and repressible gene expression system in the red alga *Cyanidioschyzon merolae*. *Front Plant Sci.* **6**, 1–10.

Fukuzawa, H., Fujiwara, S., Yamamoyo, Y., Dionisio-Sese, M.L., Miyachi, S. (1990) cDNA clonging, sequence, and expression of carbonic anhydrase in *Chlamydomonas reinhardtii*: regulation by environmental CO_2 concentration. *Proc. Natl. Acad. Sci. USA* **87**, 4383–4387.

Fukuzawa, H., Suzuki, E., Komukai, Y., Miyachi, S. (1992) A gene homologous to chloroplast carbonic anhydrase (icfA) is essential to photosynthetic carbon dioxide fixation by *Synechococcus* PCC7942. *Proc. Natl. Acad. Sci. USA* **89**, 4437–4441.

Fukuzawa, H., Ishizaki, K., Miura, K., Matsueda, S., Kucho, K., Ohyama, K. (1998) Isolation and characterization of high-CO_2 requiring mutants from *Chlamydomonas reinhardtii* by gene tagging. *Can. J. Bot.* **76**, 1092–1097.

Fukuzawa, H., Miura, K., Ishizaki, K., Kucho, K.I., Saito, T., Kohinata, T., Ohyama, K. (2001) *Ccm1*, a regulatory gene controlling the induction of a carbon-concentrating mechanism in *Chlamydomonas reinhardtii* by sensing CO_2 availability. *Proc. Natl. Acad. Sci. USA* **98**, 5347–5352.

Fukuzawa, H., Ogawa, T., Kaplan, A. (2012) The uptake of CO_2 by cyanobacteria and microalgae. Plastid Biology, Energy Conversion and Carbon Assimilation, Ed. by Eaton-rye, J.J., Tripathy, B.C., and Sharkey, T.D. (Springer, Heidelberg), pp 625–650.

Gao, H., Wang, Y., Fei, X., Wright, D.A., Spalding, M.H. (2015) Expression activation and functional analysis of HLA3, a putative inorganic carbon transporter in *Chlamydomonas reinhardtii*. *Plant J.* **82**, 1–11.

Giordano, M., Beardall, J., Raven, J.A. (2005) CO_2 concentrating mechanisms in algae: mechanisms, environmental modulation, and evolution. *Annu. Rev. Plant Biol* **56**, 99–131.

Gunning, B.E.S., Schwartz, M. (1999) Confocal microscopy of thylakoid autofluorescence in relation to origin of grana and phylogeny in the green algae. *Aust. J. Plant Physiol.* **26**, 695–708.

Guo, H., Feng, P., Chi, W., Sun, X., Xu, X., Li, Y., Ren, D., Lu, C., Rochaix, J.D., Leister, D., Zhang, L. (2016) Plastid-nucleus communication involves calcium-modulated MAPK signaling. *Nat. Commun.* **7**, 12173.

Haimovich-Dayan, M., Lieman-Hurwitz, J., Orf, I., Hagemann, M., Kaplan, A. (2014) Does 2-phosphoglycolate serve as an internal signal molecule of inorganic carbon deprivation in the cyanobacterium *Synechocystis* Sp. PCC 6803? *Environ. Microbiol.* **17**, 1794–1804.

Han, S., Tang, R., Anderson, L.K., Woerner, T.E., Pei, Z.M. (2003) A cell surface receptor mediates extracellular Ca^{2+} sensing in guard cells. *Nature* **425**, 196–200.

Hanawa, Y., Watanabe, M., Karatsu, Y., Fukuzawa, H., Shiraiwa, Y. (2007) Induction of a high-CO_2-inducible, periplasmic protein, H43, and its application as a high-CO_2-responsive marker for study of the high-CO_2-sensing mechanism in *Chlamydomonas reinhardtii*. *Plant Cell Physiol.* **48**, 299–309.

Harada, H., Nakajima, K., Sakaue, K., Matsuda, Y. (2006) CO_2 sensing at ocean surface mediated by cAMP in a marine diatom. *Plant Physiol.* **142**, 1318–1328.

Harris, E.H. (1989) *The Chlamydomonas Sourcebook*. (Academic Press, Inc., San Diego.) pp **780**.

Hashimoto, M., Negi, J., Young, J., Israelsson, M., Schroeder, J.I., Iba, K. (2006) *Arabidopsis* HT1 kinase controls stomatal movements in response to CO_2. *Nat. Cell Bio.* **8**, 391–397.

Hashimoto-Sugimoto, M., Negi, J., Higaki, T., Isogai, Y., Nakano, T., Hasezawa, S., Iba, K. (2016) Dominant and recessive mutations in the Raf-like kinase *HT1* gene completely disrupt stomatal responses to CO_2 in *Arabidopsis*. *J. Exp. Bot*. **67**, 3251–3261.

Hewet-Emmett, D., Tashian, R.E. (1996) Functional diversity conservation, and convergence in the evolution of the α-, β-, and γ-carbonic anhydrase gene families. *Mol. Phylogenet. Evol.* **5**, 50–77.

Higgins, C.F., Linton, K.J. (2004) The ATP switch model for ABC transporters. *Nat. Struct. Mol. Boil.* **11**, 918–926.

Hihara, Y., Kamei, A., Kanehisa, M., Kaplan, A., Ikeuchi, M. (2001) DNA microarray analysis of cyanobacterial gene expression during acclimation to high light. *Plant Cell* **13**, 793–806.

Hochmal, A.K., Schulze, S., Trompelt, K., Hippler, M. (2015) Calcium-dependent regulation of photosynthesis. *Biochim. Biophys. Acta.* **1847**, 993–1003.

Hochmal, A.K., Zinzius, K., Charoenwattanasatien, T., Gabelein, P., Mutoh, T., Tanaka, H., Schulze, S., Liu, G., Scholz, M., Nordhues, A., Offenborn, J.N., Petroutsos, D., Finazzi, G., Fufezan, C., Huang, K., Kurisu, G., Hippler, M. (2016) Calredoxin represents a novel type of calcium-dependent sensor-responder connected to redox regulation in the chloroplast. *Nat. Commun.* **7**, 11847.

Hogetsu, D., Miyachi, S. (1979) Role of carbonic anhydrase in photosynthetic CO_2 fixation in *Chlorella*. *Plant Cell Physiol.* **20**, 747–756.

Hollenstein, K., Frei, D.C., Locher, K.P. (2007) Structure of an ABC transporter in complex with its binding protein. *Nature* **446**, 213–216.

Hopkinson, B.M., Dupont, C.L., Matsuda, Y. (2016) The physiology and genetics of CO_2 concentrating mechanisms in model diatoms. *Curr. Opin. Plant Biol.* **31**, 51–57.

Hu, H.H., Boisson-Dernier, A., Israelsson-Nordstrom, M., Bohmer, M., Xue, S., Ries, A., Godoski, J., Kuhn, J.M., Schroeder, J.I. (2009) Carbonic anhydrases are upstream regulators of CO_2-controlled stomatal movements in guard cells. *Nat. Cell Bio.* **12**, 87–93.

Im, C.S., Grossman, A.R. (2001) Identification and regulation of high light-induced genes in *Chlamydomonas reinhardtii*. *Plant J.* **30**, 301–313.

Im, C.S., Zhang, Z., Shrager, J., Chang, C.-W., Grossman A.R. (2003) Analysis of light and CO_2 regulation in *Chlamydomonas reinhardtii* using genome-wide approaches. *Photosynth. Res.* **75**, 111–125.

Iwai, M., Kato, N., Minagawa, J. (2007) Distinct physiological response to a high light and low CO_2 environment revealed by fluorescence quenching in photoautotrophically grown *Chlamydomonas reinhardtii*. *Photosynth. Res.* **94**, 307–314.

Iwai, M., Takizawa, K., Tokutsu, R., Okamuro, A., Takahashi, Y., Minagawa, J. (2010) Isolation of the elusive supercomplex that drives cyclic electron flow in photosynthesis. *Nature* **464**, 1210–1213.

Jiang, W., Brueggeman, A.J., Horken, K.M., Plucinak, T.M., Weeks, D.P. (2014) Successful transient expression of Cas9 and single guide RNA genes in *Chlamydomonas reinhardtii*. *Eukaryot. Cell* **13**, 1465–1469.

Jin, M.S., Oldham, M.L., Zhang, Q., Chen, J. (2012) Crystal structure of the multidrug transporter P-glycoprotein from *Caenorhabditis elegans*. *Nature* **490**, 566–569.

Jones, H.G. (1992) Plants and microclimate: *A quantitative approach to environmental plant physiology* (Cambridge University Press Cambridge UK), **2nd** Ed.

Johnston, A.M., Raven, J.A. (1996) Inorganic carbon accumulation by the marine diatom *Pheodactylum tricornutum*. *Eur. J. Phycol.* **3**, 285–290.

Kabeya, Y., Miyagishima, S.Y. (2013) Chloroplast DNA replication is regulated by the redox state independently of chloroplast division in *Chlamydomonas reinhardtii*. *Plant Physiol.* **161**, 2102–2112.

Kaplan, A., Badger, M.R., Berry, J.A. (1980) Photosynthesis and intracellular inorganic carbon pool in the blue-green algae *Anabaena variabilis*: response to external CO_2 concentration. *Planta* **149**, 219–226.

Karlsson, J., Clarke, A.K., Chen, Z.Y., Hugghins, S.Y., Park, Y.I., Husic, H.D., Moroney, J.V., Samuelsson, G. (1998) A novel alpha-type carbonic anhydrase associated with the thylakoid membrane in *Chlamydomonas reinhardtii* is required for growth at ambient CO_2. *EMBO J.* **17**, 1208–1216.

Kikutani, S., Nakajima, K., Nagasato, C., Tsuji, Y., Miyatake, A., Matsuda, Y. (2016) Thylakoid luminal θ-carbonic anhydrase critical for growth and photosynthesis in the marine diatom *Phaeodactylum tricornutum*. *Proc. Natl. Acad. Sci. USA* **113**, 9828–9833.

Kim, T.H., Bohmer, M., Hu, H., Nishimura, N., Schroeder, J.I. (2010) Guard cell signal transduction network: advances in understanding abscisic acid, CO_2, and Ca^{2+} signaling. *Annu. Rev. Plant Biol.* **61**, 561-91.

Klahn, S., Orf, I., Schwarz, D., Matthiessen, J.K.F., Kopka, J., Hess, W.R., Hagemann, M. (2015) Integrated transcriptomic and metabolomics characterization of the low-carbon response using an *ndhR* mutant of *Synechocystis* sp. PCC 6803. *Plant Physiol.* **169**, 1540–1556.

Kobayashi, H., Odani, S., Shiraiwa, Y. (1997) A high-CO_2-inducible, periplasmic polypeptide in an unicellular green alga *Chlamydomonas reinhardtii*. *Plant Physiol.* **114**, S112.

Kohinata, T., Nishino, H., Fukuzawa, H. (2008) Significance of zinc in a regulatory protein, CCM1, which regulates the carbon-concentrating mechanism in *Chlamydomonas reinhardtii*. *Plant Cell Physiol.* **49**, 273–283.

Kroth, P., Chiovitti, A., Gruber, A., Martin-Jezequel, V., Mock, T., Parker, M., Stanley, M., Kaplan, A., Caron, L., Weber, T., Maheswari, U., Armbrust, E.V., Bowler, C. (2008) A model for carbohydrate metabolism in the diatom *Phaeodactylum tricornutum* deduced from comparative whole genome analysis. *PLoS ONE* **3**, e1426.

Kudla, J., Batistic, O., Hashimoto, K. (2010) Calcium signals: The lead currency of plant information processing. *Plant Cell* **22**, 541–563.

Kustka, A.B., Milligan, A.J., Zheng, H.Y., New, A.M., Gates, C., Bidle, K.D., Reinfelder, J.R. (2014) Low CO_2 results in a rearrangement of carbon metabolism to support C_4 photosynthetic carbon assimilation in *Thalassiosira pseudonana*. *New Phytol.* **204**, 507–520.

Lam, C.M., Yeung, P.K., Wong, J.T. (2005) Monitoring cytosolic calcium in the dinoflagellate *Crypthecodinium cohnii* with Calcium Orange-AM. *Plant Cell Physiol.* **46**, 1021–1027.

Langdale, J.A. (2011) C_4 cycles: past, present, and Future research on C_4 photosynthesis. *Plant Cell*. **23**, 3879–3892.

Lauersen, K.J., Kruse, O., Mussgnug, J.H. (2015) Targeted expression of nuclear transgenes in *Chlamydomonas reinhardtii* with a versatile, modular vector toolkit. *Appl. Microbiol. Biotechnol.* **99**, 3491–3503.

Leganes, F., Forchhammer, K., Fernandez-Pinas, F. (2009) Role of calcium in acclimation of the cyanobacterium *Synechococcus elongatus* PCC 7942 to nitrogen starvation. *Microbiology* **155**, 25–34.

Lieman-Hurwitz, J., Haimovich, M., Shalev-Malul, G., Ishii, A., Hihara, Y., Gaathon, A., Lebendiker, M., Kaplan, A. (2009) A cyanobacterial AbrB-like protein affects the apparent photosynthetic affinity for CO_2 by modulating low-CO_2-induced gene expression. *Environ. Microbiol.* **11**, 927–936.

Liu, Y.G., Whittier, R.F. (1995a) Thermal asymmetric interlaced PCR: automatable amplification and sequencing of insert end fragments from P1 and YAC clones for chromosome walking. *Genomics* **25**, 674–681.

Liu, Y.G., Mitsukawa, N., Oosumi, T., Whittier, R.F. (1995b) Efficient isolation and mapping of *Arabidopsis thaliana* T-DNA insert junctions by thermal asymmetric interlaced PCR. *Plant J.* **8**, 457–463.

Li, X., Zhang, R., Patena, W., Gang, S.S., Blum, S.R., Ivanova, N., Yue, R., Robertson, J.M., Lefebvre, P., Fitz-Gibbon, S.T., Grossman, A.R., Jonikas, M.C. (2016) An indexed, mapped mutant library enables reverse genetics studies of biological processes in *Chlamydomonas reinhardtii*. *Plant Cell.* **28**, 367–387.

Lin, M.T., Occhialini, A., Andralojc, P.J., Parry, M.A.J., Hanson, M.R. (2014) A faster Rubisco with potential to increase photosynthesis in crops. *Nature* **513**, 547–550.

Lodha, M., Schulz-Raffelt, M., Schroda, M. (2008) A new assay for promoter analysis in *Chlamydomonas* reveals roles for heat shock elements and the TATA box in *HSP70A* promoter-mediated activation of transgene expression. *Eukaryot. Cell* **7**, 172–176.

Lu, W., Schwarzer, N.J., Du, J., Gerbig-Smentek, E., Andrade, S.L.A., Oliver, E. (2012) Structural and functional characterization of the nitrite channel NirC from *Salmonella typhimurium*. *Proc. Natl. Acad. Sci. USA* **109**, 18395–18400.

Lucker, B., Kramer, D.M. (2013) Regulation of cyclic electron flow in *Chlamydomonas reinhardtii* under fluctuating carbon availability. *Photosynth. Res.* **117**, 449–459.

Ma, Y., Pollock, S.V., Xiao, Y., Cunnusamy, K., Moroney, J.V. (2011) Identification of a novel gene, *CIA6*, required for normal pyrenoid formation in *Chlamydomonas reinhardtii*. *Plant Physiol.* **156**, 884–896.

Mackinder, L.C.M., Meyer, M., Mettler-Altmann, T., Chen, V.K., Mitchell, M.C., Caspari, O., Rosenzweig, E.S.F., Pallesen, L., Reeves, G., Itakura, A., Roth, R., Sommer, F., Geimer, S., Muhlhaus, T., Schroda, M., Goodenough, U., Stitt, M., Griffiths, H., Jonikas, M. (2016) A repeat protein links Rubisco to form the eukaryotic carbon-concentrating organelle. *Proc. Natl. Acad. Sci. USA* **113**, 5958–5963.

Mangan, N.M., Brenner, M.P. (2013) Systems analysis of the CO_2 concentrating mechanism in cyanobacteria. *eLife* **3**, e02043.

Mariscal, V., Moulin, P., Orsel, M., Miller, A.J., Fernandez, E., Galvan, A. (2006) Differential regulation of the *Chlamydomonas Nar1* gene family by carbon and nitrogen. *Protist* **157**, 421–433.

Maruyama, K., Mikawa, T., Ebashi, S. (1984) Detection of calcium binding proteins by ^{45}Ca autoradiography on nitrocellulose membrane after sodium dodecyl sulfate gel electrophoresis. *J. Biochem.* **95**, 511–519.

Maruyama, S., Tokutsu, R., Minagawa, J. (2014) Transcriptional regulation of the stress-responsive light harvesting complex genes in *Chlamydomonas reinhardtii*. *Plant Cell Physiol.* **55**, 1304–1310.

Mason, C.B., Bricker, T., Moroney, J.V. (2006) A rapid method for chloroplast isolation from the green alga *Chlamydomonas reinhardtii*. *Nat. Protoc.* **1**, 2227–2230.

Matrosova, A., Bogireddi, H., Mateo-Penas, A., Hashimoto-Sugimoto, M., Iba, K., Schroeder, J.I., Israelsson-Nordstrom, M. (2015) The HT1 protein kinase is essential for red light-induced stomatal opening and genetically interacts with OST1 in red light and CO_2-induced stomatal movement responses. *New Phytol.* **208**,1126–1137.

Matsuda, Y., Hara, T., Colman, B. (2001) Regulation of the induction of bicarbonate uptake by dissolved CO_2 in the marine diatom, *Phaeodactylum tricornutum*. *Plant Cell Environ.* **24**, 611–620.

McGrath, J.M., and Long, S.P. (2014) Can the cyanobacterial carbon-concentrating mechanism increase photosynthesis in crop species? A theoretical analysis. *Plant Physiol*. **164**, 2247–2261.

McLachlan, D.H., Underwood, G.J.C., Taylor A.R., Brownlee, C. (2012) Calcium release from intracellular stores is necessary for the photophobic response in the benthic diatom *Navicula Perminuta*. *J. Phycol.* **48**, 675–681.

Meldrum, N.N., Roughton, F.J. (1933) Carbonic anhydrase: its preparation and properties. *Nature* **80**, 113–142.

Merchant, S.S., Prochnik, S.E., Vallon, O., Harris, E.H., Karpowicz, S.J., Witman, G.B., Terry, A., Salamov, A., Fritz-Laylin, L.K., Maréchal-Drouard, L., Marshall, W.F., Qu, L.H., Nelson, D.R., Sanderfoot, A.A., Spalding, M.H., Kapitonov, V.V., Ren, Q., Ferris, P., Lindquist, E., Shapiro, H., Lucas, S.M., Grimwood, J., Schmutz, J., Cardol, P., Cerutti, H., Chanfreau, G., Chen, C.L., Cognat, V., Croft, M.T., Dent, R., Dutcher, S., Fernández, E., Fukuzawa, H., González-Ballester, D., González-Halphen, D., Hallmann, A., Hanikenne, M., Hippler, M., Inwood, W., Jabbari, K., Kalanon, M., Kuras, R., Lefebvre, P.A., Lemaire, S.D., Lobanov, A.V., Lohr, M., Manuell, A., Meier, I., Mets, L., Mittag, M., Mittelmeier, T., Moroney, J.V., Moseley, J., Napoli, C., Nedelcu, A.M., Niyogi, K., Novoselov, S.V., Paulsen, I.T., Pazour, G., Purton, S., Ral, J.P., Riaño-Pachón, D.M., Riekhof, W., Rymarquis, L., Schroda, M., Stern, D., Umen, J., Willows, R., Wilson, N., Zimmer, S.L., Allmer, J., Balk, J., Bisova, K., Chen, C.J., Elias, M., Gendler, K., Hauser, C., Lamb, M.R., Ledford, H., Long, J.C., Minagawa, J., Page, M.D., Pan, J., Pootakham, W., Roje, S., Rose, A., Stahlberg, E., Terauchi, A.M., Yang, P., Ball, S., Bowler, C., Dieckmann, C.L., Gladyshev, V.N., Green, P., Jorgensen, R., Mayfield, S., Mueller-Roeber, B., Rajamani, S., Sayre, R.T., Brokstein, P., Dubchak, I., Goodstein, D., Hornick, L., Huang, Y.W., Jhaveri, J., Luo, Y., Martínez, D., Ngau, W.C., Otillar, B., Poliakov, A., Porter, A., Szajkowski, L., Werner, G., Zhou, K., Grigoriev, I.V., Rokhsar, D.S., Grossman, A.R. (2007) The *Chlamydomonas* genome reveals the evolution of key animal and plant functions. *Science*. **318**, 245–250.

Meyer, S., Mumm, P., Imes, D., Endler, A., Weder, B., Al-Rasheid, K.A.S., Geiger, D., Marten, I., Martinoia, E., Hedrich, R. (2010) AtALMT12 represents an R-type anion channel required for stomata movement in *Arabidopsis* guard cells. *Plant J.* **63**, 1054–1062.

Meyer, M.T., Genkov, T., Skepper, J.N., Jouhet, J., Mitchell, M.C., Spreitzer, R.J., Griffiths, H. (2012) Rubisco small-subunit α-helices control pyrenoid formation in *Chlamydomonas*. *Proc. Natl. Acad. Sci. USA* **109**, 19474–19479.

Meyer, M., Griffiths, H. (2015) The internal plumbing of algal chloroplasts. *Elife* **4**, e05983.

Mitchell, M., Meyer, M.T., Griffiths, H. (2014) Dynamics of carbon concentrating mechanism induction and protein relocalization during the dark-to-light transition in synchronized *Chlamydomonas reinhardtii*. *Plant Physiol*. **166**, 1073–1082.

Miura, K., Yamano, T., Yoshioka, S., Kohinata, T., Inoue, Y., Taniguchi, F., Asamizu, E., Nakamura, Y., Tabata, S., Yamato, K.T., Ohyama K., Fukuzawa, H. (2004) Expression profiling-based identification of CO_2-responsive genes regulated by CCM1 controlling a carbon-concentrating mechanism in *Chlamydomonas reinhardtii*. *Plant Physiol.* **135**, 1595–1607.

Mochiji, S., Wakabayashi, K. (2012) Redox regulation of phototactic migration in the green alga *Chlamydomonas reinhardtii* and its possible application. *Commun. Integr. Biol*. **5**, 196–198.

Morita, E., Kuroiwa, H., Kuroiwa, T., Nozaki, H. (1997) High localization of ribulose-1,5-bisphosphate carboxylase/oxygenase in the pyrenoids of *Chlamydomonas reinhardtii* (*Chlorophyta*), as revealed by cryofixation and immunogold electron microscopy. *J. Phycol.* **33**, 68–72.

Morita, E., Abe, T., Tsuzuki, M., Fujiwara, S., Sato, N., Hirata, A., Sonoike, K., Nozaki, H. (1998) Presence of the CO_2-concentrating mechanism in some species of the pyrenoid-less free-living algal genus *Chloromonas* (*Volvocales*, *Chlorophyta*). *Planta* **204**, 269–276.

Moroney, J.V., Wilson, B.J., Tolbert, N.E. (1986a) Glycolate metabolism and excretion by *Chlamydomonas reinhardtii*. *Plant Physiol.* **82**, 821–826.

Moroney, J.V., Tolbert, N.E., Sears, B.B. (1986b) Complementation analysis of the inorganic carbon concentrating mechanism of *Chlamydomonas reinhardtii*. *Mol. Gen. Genet.* **204**, 199–203.

Moroney, J.V., Somanchi, A. (1999) How do algae concentrate CO_2 to increase the efficiency of photosynthetic carbon fixation? *Plant Physiol*. **119**, 9–16.

Moroney, J.V., Bartlett, S.G., Samuelsson, G. (2001) Carbonic anhydrases in plants and algae. *Plant Cell Environ.* **24**, 141–153.

Moroney, J.M., and Ynalvez, R.A. (2007) Proposed carbon dioxide concentrating mechanism in *Chlamydomonas reinhardtii*. *Eukaryot. Cell* **6**, 1251–1259.

Nakajima, K., Tanaka, A., Matsuda, Y. (2013) SLC4 family transporters in a marine diatom directly pump bicarbonate from seawater. *Proc. Natl. Acad. Sci. USA* **110**, 1767–1772.

Nakazawa, Y., Hiraki, M., Kamiya, R., Hirono, M. (2007) SAS-6 is a cartwheel protein that establishes the 9-fold symmetry of the centriole, *Curr. Biol.* **17**, 2169–2174.

Negi, J., Matsuda, O., Nagasawa, T., Oba, Y., Takahashi, H., Kawai-Yamada, M., Uchimiya, H., Hashimoto, M., Iba, K. (2008) CO_2 regulator SLAC1 and its homologues are essential for anion homeostasis in plant cells. *Nature* **452**, 483–486.

Nomura, H., Komori, T., Kobori, M., Nakahira, Y., Shiina, T. (2008) Evidence for chloroplast control of external Ca^{2+}-induced cytosolic Ca^{2+} transients and stomata closure. *Plant J.* **53**, 988–998.

Nomura, H., Komori, T., Uemura, S., Kanda, Y., Shimotani, K., Nakai, K., Furuichi, T., Takebayashi, K., Sugimoto, T., Sano, S., Suwastika, I.N., Fukusaki, E., Yoshioka, H., Nakahira, Y., Shiina, T. (2012) Chloroplast-mediated activation of plant immune signaling in *Arabidopsis*. *Nat. Commun.* **3**, 926.

Ogawa, T. (1991) A gene homologous to the subunit-2 gene of NADH dehydrogenase is essential to inorganic carbon transport of *Synechocystis* PCC6803. *Proc. Natl. Acad. Sci. USA* **88**, 4275–4279.

Ohad, I., Siekevitz, P., Palade, G.E. (1967) Biogenesis of chloroplast membranes. I. Plastid dedifferentiation in a dark-grown algal mutant (*Chlamydomonas reinhardtii*). *J. Cell Bio.* **35**, 521–552.

Ohkawa, H., Pakrasi, H.B., Ogawa, T. (2000) Two types of functionally distinct NADH dehydrogenase in *Synechocystis* sp. Strain PCC6803. *J. Biol. Chem.* **275**, 31630–31634.

Ohnishi, N., Mukherjee, B., Tsujikawa, T., Yanase, M., Nakano, H., Moroney, J.V., Fukuzawa, H. (2010) Expression of low CO_2-inducible protein, LCI1, increase inorganic carbon uptake in the green alga *Chlamydomonas reinhardtii*. *Plant Cell* **22**, 3105–3117.

Omata, T., Price, D.G., Badger, M.R., Okamura, M., Gohta, S., Ogawa, T. (1999) Identification of an ATP-binding cassette transporter involved in bicarbonate uptake in the cyanobacterium *Synechococcus* sp. Strain PCC 7942. *Proc. Natl. Acad. Sci. USA* **96**, 13571–13576.

Omata, T., Gohta, S., Takahashi, Y., Harano, Y., Maeda, S. (2001) Involvement of a CbbR homolog in low CO_2-induced activation of the bicarbonate transporter operon in cyanobacteria. *J. Bacteriol.* **183**, 1891–1898.

Peers, G., Truong, T.B., Ostendorf, E., Busch, A., Elrad, D., Grossman, A.R., Hippler, M., Niyogi, K.K. (2009) An ancient light-harvesting protein is critical for the regulation of algal photosynthesis. *Nature* **462**, 518–521.

Pena, K.L., Castel, S.E., de Araujo, C., Espie, G.S., Kimer, M.S. (2010) Structural basis of the oxidative activation of the carboxysomal gamma-carbonic anhydrase, CcmM. *Proc. Natl. Acad. Sci. USA* **107**, 2455–2460.

Petroutsos, D., Busch, A., Janssen, I., Trompelt, K., Bergner, S.V., Weinl, S., Holtkamp, M., Karst, U., Kudla, J., Hippler, M. (2011) The chloroplast calcium sensor CAS is required for photoacclimation in *Chlamydomonas reinhardtii*. *Plant Cell* **23**, 2950–2963.

Pfannschmidt, T. (2003) Chloroplast redox signals: how photosynthesis controls its own genes. *Trends Plant Sci.* **8**, 33–41.

Price, G.D., Woodger, F.J., Badger, M.R., Howitt, S.M., Tucker, L. (2004) Identification of a SulP-type bicarbonate transporter in marine cyanobacteria. *Proc. Natl. Acad. Sci. USA* **101**, 18228–18233.

Polisensky, D.H., Braam, J. (1996) Cold-shock regulation of the *Arabidopsis TCH* genes and the effects of modulating the intracellular calcium levels. *Plant Physiol.* **111**, 1271–1279.

Pollock, S.V., Prout, D.L., Godfrey, A.C., Lemaire, S.D., Moroney, J.V. (2004) The *Chlamydomonas reinhardtii* proteins Ccp1 and Ccp2 are required for long-term growth, but are not necessary for efficient photosynthesis, in a low-CO_2 environment. *Plant Mol. Biol.* **56**, 125–132.

Polukhina, I., Fristedt, R., Dinc, E., Cardol, P., Croce, R. (2016) Carbon supply and photoacclimation crosstalk in the green alga *Chlamydomonas reinhardtii*. *Plant Physiol*. **doi**.org/10.1104/pp.16.01310.

Ramel, F., Birtic, S., Ginies, C., Soubigou-Taconnat, L., Triantaphylides, C., Havaux, M. (2012) Carotenoid oxidation products are stress signals that mediate gene responses to singlet oxygen in plants. *Proc. Natl. Acad. Sci. USA* **109**, 5535–5540.

Reinfelder, J.R., Kraepiel, A.M.L., Morel F.M.M. (2000) Unicellular C_4 photosynthesis in a marine diatom. *Nature* **407**, 996–999.

Robert, K., Granum, E., Leegood, R.C., Raven, J.A. (2007) Carbon acquisition by diatoms. *Photosynth. Res.* **93**, 79–88.

Rolland, N., Dorne, A.J., Amoroso, G., Sultemeyer, D.F., Joyard, J., Rochaix, J.-D. (1997) Disruption of the plastid *ycf10* open reading frame affects uptake of inorganic carbon in the chloroplast of *Chlamydomonas*. *EMBO J.* **16**, 6713–6726.

Rudenko, N.N., Ignatova, L.K., Fedorchuk, T.P., Ivanov, B.N. (2015) Carbonic anhydrases in photosynthetic cells of higher plants. *Biochemistry* **80**, 674–687.

Schmitz, F. (1882) Die chromatophoren der algen. *Verh. D. Naturhist, Verh. D. Preuss., Rheinl. U. Westf.* **40**, 1-180.

Schwartz, A., Ilan, N., Grantz, D.A. (1988) Calcium effects on stomatal movement in *Commelina communis L. Plant Physiol.* **87**, 583–587.

Shibata, M., Ohkawa, H., Kaneko, T., Fukuzawa, H., Tabata, S., Kaplan, A., Ogawa, T. (2001) Distinct constitutive and low-CO_2-induced CO_2 uptake systems in cyanobacteria: Genes involved and their phylogenetic relationship with homologous genes in other organisms. *Proc. Natl. Acad. Sci. USA* **98**, 11789–11794.

Shibata, M., Katoh, H., Sonoda, M., Ohkawa, H., Shimoyama, M., Fukuzawa, H., Kaplan, A., Ogawa, T. (2002) Genes essential to sodium-dependent bicarbonate transport in cyanobacteria: function and phylogenetic analysis. *J. Biol. Chem.* **277**, 18658–18664.

Shin, S.E., Lim, J.M., Koh, H.G., Kim, E.K., Kang, N.K., Jeon, S., Shin, W.S., Lee, B., Hwangbo, K., Kim, J., Ye, S.H., Yun, J.Y., Seo, H., Oh, H.M., Kim K.J., Kim, J.S., Jeong, W.J., Chang, Y.K., Jeong, B. (2016) CRISPR/Cas9-induced knockout and knock-in mutations in *Chlamydomonas reinhardtii*. *Sci. Rep*. **6**, 27810.

Shiraiwa, Y., Miyachi, S. (1979) Enhancement of ribulose 1,5-bisphosphate carboxylation reaction by carbonic anhydrase. *FEBS Letters* **106**, 243–246.

Shutova, T., Kenneweg, H., Buchta, J., Nikitina, J., Terentyev, V., Chernyshov, S., Allakhverdiev, S.I., Klimov, V.V., Dau, H., Samuelsson, G. (2008) The photosystem II-associated Cah3 in *Chlamydomonas* enhance the O_2 evolution rate by proton removal. *EMBO J.* **27**, 782–791.

Sinetova, M.A., Kupriyanova, E.V., Markelova, A.G., Allakhverdiev, S.I., Pronina, N.A. (2012) Identification and functional role of the carbonic anhydrase Cah3 in thylakoid membranes of pyrenoid of *Chlamydomonas reinhardtii*. *Biochim. Biophys. Acta*. **1817**, 1248–1255.

Somanchi, A., Handley, E.R., Moroney, J.V. (1996) *Chlamydomonas reinhardtii* cDNAs upregulated in low-CO_2 conditions: expression and analyses. *Can. J. Bot.* **76**, 6.

Soupene, E., King, N., Feild, E., Liu, P., Niyogi, K.K., Huang, C.H., Kustu, S. (2002) Rhesus expression in a green alga is regulated by CO_2. *Proc. Natl. Acad. Sci. USA* **99**, 7769–7773.

Soupene, E., Inwood, W., Kustu, S. (2004) Lack of the Rhesus protein Rh1 impairs growth of the green alga *Chlamydomonas reinhardtii* at high CO_2. *Proc. Natl. Acad. Sci. USA* **101**, 7787–7792.

Spalding, M.H. (2009) The CO_2 concentrating mechanism and carbon assimilation. In The *Chlamydomonas* Sourcebook: Organellar and Metabolic Processer (Oxford: Academic), 2, 2nd Ed. pp 257–290.

Stoiber, T.L., Shafer, M.M., Armstrong, D.E. (2013) Induction of reactive oxygen species in *Chlamydomonas reinhardtii* in response to contrasting trace metal exposures. *Environ. Toxicol.* **28**, 526–523.

Strand, A., Asami, T., Alonso, J., Ecker, J.R., Chory, J. (2003) Chloroplast to nucleus communication triggered by accumulation of Mg-protoporphyrinlX. *Nature* **421**, 79–83.

Sun, Y., Casella, S., Fang, Y., Huang, F., Faulkner, M., Barrett, S., Liu, L. (2016) Light modulates the biosynthesis and organization of cyanobacterial carbon fixation machinery through photosynthetic electron flow. *Plant Physiol.* **171**, 530–541.

Tanaka, A., Ohno, N., Nakajima, K., Matsuda, Y. (2016) Light and CO_2/cAMP signal cross talk on the promoter elements of chloroplastic β-carbonic anhydrase genes in the marine diatom *Phaeodactylum tricornutum*. *Plant Physiol.* **170**, 1105–1116.

Terashima, M., Specht, M., Naumann, B., Hippler, M. (2010) Characterizing the anaerobic response of *Chlamydomonas reinhardtii* by quantitative proteomics. *Mol. Cell Proteomics* **9**, 1514–1532.

Terashima, M., Petroutsos, D., Hudig, M., Tolstygina, I., Trompelt, K., Gabelein, P., Fufezan, C., Kudla, J., Weinl, S., Finazzi, G., Hippler, M. (2012) Calcium-dependent regulation of cyclic photosynthetic electron transfer by a CAS, ANR1, and PGRL1 complex. *Proc. Natl. Acad. Sci. USA* **109**, 17717–17722.

Tian, W., Hou, C., Ren, Z., Pan, Y., Jia, J., Zhang, H., Bai, F., Zhang, P., Zhu, H., He, Y., Luo, S., Li, L., Luan, S. (2015) A molecular pathway for CO_2 response in *Arabidopsis* guard cells. *Nat. Commun.* **6**, 6057.

Tiwari, A., Singh, P., Asthana, R.K. (2016) Role of calcium in the mitigation of heat stress in the cyanobacterium *Anabaena* PCC7120. *J. Plant Physiol.* **199**, 67–75.

Tolleter, D., Ghysel, B., Alric, J., Petroutsos, D., Tolstygina, I., Krawietz, D., Happe, T., Auroy, P., Adriano, J.M., Beyly, A., Cuine, S., Plet, J., Reiter, I.M., Genty, B., Cournac, L., Hippler, M., Peltier, G. (2011) Control of hydrogen photoproduction by the proton gradient generated by cyclic electron flow in *Chlamydomonas reinhardtii*. *Plant Cell* **23**, 2619–2630.

Trapnell, C., Roberts, A., Goff, L., Pertea, G., Kim, D., Kelley, D.R., Pimentel, H., Salzberg, S., Rinn, J.L., Pachter, L. (2012) Differential gene and transcript expression analysis of RNA-seq experiments with TopHat and Cufflinks. *Nat. Protoc.* **7**, 562–578.

Trimborn, S., Lundholm, N., Thoms, S., Richter, K.U., Krock, B., Hansen, P.J., Rost, B. (2008) Inorganic carbon acquisition in potentially toxic and non-toxic diatom: the effect of pH-induced changes in seawater carbonate chemistry. *Physiol. Plant* **133**, 92–105.

Triumani, S., Kokkanti, M., Chaudhari, V., Shukla, M., Rao, B.J. (2014) Regulation of CCM genes in *Chlamydomonas reinhardtii* during conditions of light-dark cycles in synchronous cultures. *Plant Miol. Biol.* **85**, 277–286.

Tsuzuki, M., Miyachi, S. (1979) Effects of CO_2 concentration during growth and of ethoxyzolamide on CO_2 compensation point in *Chlorella*. *FEBS Letters* **103**, 221–223.

Turkina, M.V., Blanco-Rivero, A., Vainonen, J.P., Vener, A.V., Villarejo, A. (2006) CO_2 limitation induces specific redox-dependent protein phosphorylation in *Chlamydomonas reinhardtii*. *Proteomics* **6**, 2693–2674.

Vainonen, J.P., Sakuragi, Y., Stael, S., Tikkanen, M., Allahverdiyeva, Y., Paakkarinen, V., Aro, E., Suorsa, M., Scheller, H.V., Vener, A.V., Aro, E.M. (2008) Light regulation of CaS, a novel phosphoprotein in the thylakoid membrane of *Arabidopsis thaliana*. *FEBS J.* **275**, 1767–1777.

Vahisalu, T., Kollist, H., Wang, Y.F., Nishimura, N., Chan, W.Y., Valerio, G., Lamminmaki, A., Brosche, M., Moldau, H., Desikan, R., Schroeder, J.I., Kangasjarvi, J. (2008) SLAC1 is required for plant guard cell S-type anion channel function in stomata signaling. *Nature* **452**, 487–491.

Van, K., Spalding, M.H. (1999) Periplasmic carbonic anhydrase (*Cah1*) structural gene mutant in *Chlamydomonas reinhardtii*. *Plant Physiol.* **120**, 757–764.

Vance, P., Spalding, M.H. (2005) Growth, photosynthesis, and gene expression in *Chlamydomonas* over a range of CO_2 concentrations and CO_2/O_2 ratios: CO_2 regulates multiple acclimation states. *Can. J. Bot.* **83**, 796–809.

Villand, P., Eriksson, M., Samuelsson, G. (1997) Carbon dioxide and light regulation of promoters controlling the expression of mitochondrial carbonic anhydrase in *Chlamydomonas reinhardtii*. *Biochem. J.* **327**, 51–57.

Villarejo, A., Shutova, T., Moskvin, O., Forssen, M., Klimov, V.V., Samuelsson, G. (2002) A photosystem II-associated carbonic anhydrase regulates the efficiency of photosynthetic oxygen evolution. *EMBO J.* **21**, 1930–1938.

Wang, H.L., Poster, B.L., Burnap, R.L. (2004) Alterations in global patterns of gene expression in *Synechocystis* sp. PCC 6803 in response to inorganic carbon limitation and the inactivation of *ndhR*, a LysR family regulator. *J. Biol. Chem.* **279**, 5739–5751.

Wang, Y., Spalding, M.H. (2006) An inorganic carbon transport system responsible for acclimation specific to air levels of CO_2 in *Chlamydomonas reinhardtii*. *Proc. Natl. Acad. Sci. USA* **103**, 10110–10115.

Wang, Y., Huang, Y., Wang, J., Cheng, C., Huang, W., Lu, P., Xu, Y.-N., Wang, P., Yan, N., Shi, Y. (2009) Structure of the formate transporter FocA reveals a pentameric aquaporin-like channel. *Nature* **462**, 467–472.

Wang, Y., Spalding, M.H. (2014a) Acclimation to very low CO_2: Contribution of limiting CO_2 inducible proteins, LCIB and LCIA, to inorganic carbon uptake in *Chlamydomonas reinhardtii*. *Plant Physiol.* **166**, 2040–2050.

Wang, Y., Spalding, M.H. (2014b) LCIB in the *Chlamydomonas* CO_2-concentrating mechanism. *Plant Physiol.* **121**, 185–192.

Wang, H., Gau, B., Slade, W.O., Juergens, M., Li, P., Hicks, L.M. (2014c) The global phosphoproteome of *Chlamydomonas reinhardtii* reveals complex organellar phosphorylation in the flagella and thylakoid membrane. *Mol. Cell Proteomics* **13**, 2337–2353.

Wang, Y.J., Stessman, D.J., Spalding, M.H. (2015) The CO_2 concentrating mechanism and photosynthetic carbon assimilation in limiting CO_2: how *Chlamydomonas* works against the gradient. *Plant J.* **82**, 429–448.

Wasilewska, A., Vlad, F., Sirichandra, C., Redko, Y., Jammes, F., Valon, C., Frei Dit Frey, N., Leung, J. (2008) An update on abscisic acid signaling in plants and more. *Mol. Plant* **1**, 198–217.

Webb, A.A.R., McAinsh, M.R., Mansfield, T.A., Hetherington, A.M. (1996) Carbon dioxide induces increases in guard cell cytosolic free calcium. *Plant J.* **9**, 297–304.

Weinl, S., Held, l., Schlucking, K., Steinhorst, L., Kuhlgert, S., Hippler, M., Kudla, J. (2008) A plastid protein crucial for Ca^{2+}-regulated stomata responses. *New Phytol.* **179**, 675–686.

Wilkens, S. (2015) Structure and mechanism of ABC transporters. *F1000Prime Rep.* **7**, 7–14.

Woodson, J.D., Perez-Ruiz, J.M., Chory, J. (2011) Heme synthesis by plastid ferrochelatase I regulates nuclear gene expression in plants. *Curr. Biol.* **21**, 897–903.

Xiang, Y., Zhang, J., Weeks, D.P. (2001) The *Cia5* gene controls formation of the carbon concentrating mechanism in *Chlamydomonas reinhardtii*. *Proc. Natl. Acad. Sci. USA* **98**, 5341–5346.

Xu, Y., Feng, L., Jeffrey, P., Shi, Y., Morel, F. (2008) Structure and metal exchange in the cadmium carbonic anhydrase of marine diatoms. *Nature* **452**, 56–61.

Xue, S., Hu, H., Ries, A., Merilo, E., Kollist, H., Schroeder, J.I. (2011) Central functions of bicarbonate in S-type anion channel activation and OST1 protein kinase in CO_2 signal transduction in guard cell. *EMBO J.* **30**, 1645–1658.

Yamano, T., Miura, K., Fukuzawa, H. (2008) Expression analysis of genes associated with the induction of the carbon-concentrating mechanism in *Chlamydomonas reinhardtii*. *Plant Physiol.* **147**, 340–354.

Yamano, T., Tsujikawa, T., Hatano, K., Ozawa, S., Takahashi, Y., Fukuzawa, H. (2010) Light and low-CO_2-dependent LCIB-LCIC complex localization in the chloroplast supports the carbon-concentrating mechanism in *Chlamydomonas reinhardtii*. *Plant Cell Physiol.* **51**, 1453–1468.

Yamano, T., Iguchi, H., Fukuzawa, H. (2013) Rapid transformation of *Chlamydomonas reinhardtii* without cell-wall removal. *J. Biosci. Bioeng.* **115**, 691–694.

Yamano, T., Asada, A., Sato, E., Fukuzawa, H. (2014) Isolation and characterization of mutants defective in the localization of LCIB, an essential factor for the carbon-concentrating mechanism in *Chlamydomonas reinhardtii*. *Photosynth. Res.* **121**, 193–200.

Yamano, T., Sato, E., Iguchi, H., Fukuda, Y., Fukuzawa, H. (2015) Characterization of the cooperative bicarbonate uptake into chloroplast stroma in the green alga *Chlamydomonas reinhardtii. Proc. Natl. Acad. Sci. USA* **112**, 7315–7320.

Yoshihara, C., Inoue, K., Schichnes, D., Ruzin, S., Inwood, W., Kustu, S. (2008) An Rh1-GFP fusion protein is in the cytoplasmic membrane of a white mutant strain of *Chlamydomonas reinhardtii*. *Mol. Plant* **1**, 1007–1020.

Yoshioka, S., Taniguchi, F., Miura, K., Inoue, T., Yamano, T., Fukuzawa, H. (2004) The novel Myb transcription factor LCR1 regulates the CO_2-responsive gene Cah1, encoding a periplasmic carbonic anhydrase in *Chlamydomons reinhardtii*. *Plant Cell* **16**, 1466–1477.

Young, J.J., Mehta, S., Israelsson, M., Godoski, J., Grill, E., Schroeder, J.I. (2006) CO_2 signaling in guard cells: Calcium sensitivity response modulation, a Ca^{2+}-independent phase, and CO_2 insensitivity of the *gca2* mutant. *Proc. Natl. Acad. Sci. USA* **103**, 7506–7511.

Zaffagnini, M., Bedhomme, M., Groni, H., Marchand, C.H., Puppo, C., Gontero, B., Cassier-Chauvat, C., Decottignies, P., Lemaire, S.D. (2012) Glutathionylation in the photosynthetic model organism *Chlamydomonas reinhardtii*: a proteomic survey. *Mol. Cell Proteomics.* **11**, M111.014142.

Zhang, P., Battchikova, N., Jansen, T., Appel, J., Ogawa, T., Aro, E.-M. (2004) Expression and functional roles of the two distinct NDH-1 complexes and carbon acquisition complex NdhD3/NdhF3/CupA/Sll1735 in *Synechocystis* sp PCC 6803. *Plant Cell.* **16**, 3326–3340.

Zuo, Z., Peng, K., Shi, M., Chen, Z., Zhu, Y., Bai, Y., Gao, Y., Wang, Y. (2014) ROS production is associated with glycolate metabolism in *Chlamydomonas reinhardtii* (*Chlorophyceae*) under salt stress. *Phycologia* **53**, 502–507.

Acknowledgment

I would like to express my sincere gratitude to my major supervisor Professor Hideya Fukuzawa for offering me the opportunity to achieve significant growth academically. His patience, perseverance, and insightful thoughts have always inspired me. He directed the most beneficial study route in my research and his constructive guidance helped me a lot in my research. Without his effective supervision and kindness, this thesis would not have been possible in 4 years.

My sincere appreciation also goes to Dr. Takashi Yamano and Dr. Masataka Kajikawa, who educated me how to think about research experimentally and supported me with constructive suggestions. Dr. Takashi Yamano has always encouraged me in both my research and life throughout my years of study at the laboratory of Applied Molecular Microbiology in Kyoto University. His scientific talents have always enlightened me. I also would like to thank my sub-supervisors Professor Takayuki Kohchi and Dr. Taiho Kambe for constructive advice on my research, Professor Fuyuki Ishikawa and Mr. Yuzo Watanabe for LC-MS/MS assay, and Professor James Hejna for the scientific English education, Ms. Emiko Nishimoto for her assistance in dealing with the administrative matters.

I also deeply appreciate the contributions from following members to my two academic papers, Professor Yuichiro Takahashi (Okayama University) and Dr. Shin-ichiro Ozawa (Okayama University) for the measurement of P_{700} kinetics, Professor Jun Minagawa (National Institute for Basic Biology) and Dr. Ryutaro Tokutsu (National Institute for Basic Biology) for measurement of NPQ, Professor Hirofumi Yoshikawa (Tokyo University of Agriculture) and Dr. Yu Kanesaki (Tokyo University of Agriculture) for RNA-seq analysis, and Professor Masafumi Hirono (Hosei University) for tetrad analysis, Professor Gilles Peltier (Commissariat à l'Energie Atomique et aux Energies Alternatives) and Dr. Xenie Johnson (Commissariat à l'Energie Atomique et aux Energies Alternatives) for providing the *pgrl1* mutant and its complemented strain, Professor Göran Samuelsson (Umeå University) for providing the anti-CAH3 antibody, and Professor Michael Hippler (University of Münster) for providing the anti-LHCSR3 antibody.

I would like to thank the lab members, Mr. Shunsuke Takane, Ms. Hiro Iguchi, Ms. Hatsue Mizuhara, Mr. Yuki Niikawa, Ms. Chihana Toyokawa, Ms. Haruka Shinkawa, Ms. Tomoko Akiyama, Ms. Noriko Nagamine, and Mr. Kosuke Tsuda.

Finally, thanks to my family and my friends for their encouragement and support during these years.

This doctoral thesis is based on material contained in the following scholarly paper:

Wang L., Yamano T., Kajikawa M., Hirono M., Fukuzawa H. (2014) Isolation and characterization of novel high-CO_2-requiring mutants of *Chlamydomonas reinhardtii*. ***Photosynth. Res.*** **121**, 175–184. **Wang L.,** Yamano T., Takane S., Niikawa Y., Toyokawa C., Ozawa S., Tokutsu R., Takahashi Y., Minagawa J., Kanesaki Y., Yoshikawa H., Fukuzawa H. (2016) Chloroplast-mediated regulation of CO_2-concentrating mechanism by Ca^{2+}-binding protein CAS in the green alga *Chlamydomonas reinhardtii*. ***Proc. Natl. Acad. Sci. USA*** **113**, 12586–12591.

Applicant Name: WANG, Lianyong Signature: _____